A Comparative Study of the Performance of Overhead Crane System Swing Angle Control

Eyerusalem Paulos Bogale

A Thesis Submitted to the Department of Electrical Power and Control Engineering

School of Electrical Engineering and Computing

Presented in Partial Fulfillment of the Requirement for the Degree of Master of Science in Electrical Power and Control Engineering

(Control Engineering)

Office of Graduate Studies

Adama Science and Technology University

June, 2022

Adama, Ethiopia

A Comparative Study of the Performance of Overhead Crane System Swing Angle Control

Eyerusalem Paulos Bogale

Advisor: **Dr. Endalew Ayenew**

A Thesis Submitted to the Department of Electrical Power and Control Engineering

School of Electrical Engineering and Computing

Presented in Partial Fulfillment of the Requirement for the Degree of Master of Science in Electrical Power and Control Engineering

(Control Engineering)

Office of Graduate Studies

Adama Science and Technology University (ASTU)

June, 2022

Adama, Ethiopia

DECLARATION

I hereby declare that this Master Thesis entitled *"A Comparative Study of the Performance of Overhead Crane System Swing Angle Control"* is my original work. That is, it has not been submitted for the award of any academic degree, diploma or certificate in any other university. All sources of materials that are used for this thesis have duly acknowledged through citation.

______________________________	______________________	___________________
Name of Student	Signature	Date

RECOMMENDATION

I, the advisor/supervisor of this thesis, hereby certify that I have read the revised version of the thesis entitled *"A Comparative Study of the Performance of Overhead Crane System Swing Angle Control"* prepared under my guidance by **Eyerusalem Paulos Bogale** submitted in partial fulfillment of the requirements for the degree of Master of Science in Control Engineering. Therefore, I recommend the submission of the revised version of the thesis to the department following the applicable procedures.

Dr. Endalew Ayenew		01-07-2022
Major Advisor	Signature	Date

APPROVAL PAGE

I, the advisor of the thesis entitled *"A Comparative Study of the Performance of Overhead Crane System Swing Angle Control"* and developed by **Eyerusalem Paulos Bogale**, hereby certify that the recommendation and suggestions made by the board of examiners are appropriately incorporated into the final version of the thesis.

Dr. Endalew Ayenew		01-07-2022
Major Advisor	Signature	Date

We, the undersigned, members of the Board of Reviewers of the thesis by **Eyerusalem Paulos Bogale** have read and evaluated the thesis entitled *"A Comparative Study of the Performance of Overhead Crane System Swing Angle Control"* and examined the candidate during open defense. This is, therefore, to certify that the thesis is accepted for partial fulfillment of the requirement of the degree of **Master of Science in Control Engineering**.

Mr. Mesfin Megra (M.Sc)		01-07-2022
Chairperson	Signature	Date
Prof. Gang Gyoo Jin		23-06-2022
Internal Examiner	Signature	Date
Dr. Beteley Teka		20-06-2022
External Examiner	Signature	Date

Finally, approval and acceptance of the thesis is contingent upon submission of its final copy to the Office of Postgraduate Studies (OPGS) through the Department Graduate Council (DGC) and School Graduate Committee (SGC).

Department Head	Signature	Date
School Dean	Signature	Date
Office of Postgraduate Studies, Dean	Signature	Date

ACKNOWLEDGEMENT

First and foremost, glory be to the **Almighty God**, a one who was with me all the way through, who comfort and sustain, for the grace He gave, and for all thing He allowed to be in my life. For all thing comes from Him, and for His glory.

Then, my heartfelt gratitude goes to **Dr. Endalew Ayenew**, my supervisor, for his very friendly attitude, and many valuable insights according to the existing theories and a real-time application. Thank you for assisting me to always take a step back and properly investigate the problems again since formulating the title, until the end of thesis. Your diligence is always inspiring and you are highly appreciated!

Next, I would like to express my great respect to **Mr. Mesfin Megra (M.Sc)**, EPCE Department Head, and **Dr. Milkias Berhanu**, The Department Postgraduate Coordinator, for their initiation, coordination, and encouragement to accomplish the thesis in scheduled time.

Moreover, I would like to thank the former EPCE Department Head, **Mr. Hinsermu Alemayehu** for his humbleness, and making a very friendly environment for communication and information in the application and registration time.

Furthermore, I would really like to offer my sincere gratitude to my entire family for their encouragement and love. Especially, my deepest gratitude goes to my heroine mother, **W/ro Ufaissie Bergene**, for her prayers and unceasing follow-up. Mom, and all my siblings, words are inadequate to express how grateful I am to have you! Beloveds, thank you for inspiring me to face challenges and overcome difficult situations.

Finally, I would like to express my heartfelt gratitude to all my instructors in ASTU, and whoever that made sacrifices on my behalf. In particular, I would like to thank **Mr. Hise Teferi**, for his supportive ideas and motivation in my thesis.

Eyerusalem Paulos Bogale

DEDICATION

In loving memory of my brave father, **Ato Paulos Bogale.**

(A genuine model of goodness)

CONTENTS

LIST OF TABLES

LIST OF FIGURES

LIST OF ACRONYMS AND INITIALISMS

AC	Alternating Current
ACO	Ant Colony Optimization
ANFIS	Adaptive Neuro-Fuzzy Inference System
ASTU	Adama Science and Technology University
BLDC	Brushless Direct Current
BLDCM	Brushless Direct Current Motor
CLTF	Closed Loop Transfer Function
CMAA	Crane Manufacturer Association of America
CoG	Center of Gravity
DC	Direct Current
DE	Differential Evolution
DIN	Deutsches Institut für Normung (or) German institute for standardization
DOI	Digital Object Identifier
Emf	Electromotive Force
EPCE	Electrical Power and Control Engineering
FEM	Fédération Européenne dela Manutention (or) European Materials Handling Federation
FIS	Fuzzy Inference System
FL	Fuzzy Logic
FOPID	Fractional Order Proportional Integral Derivative
FPID	Fuzzy Proportional Integral Derivative
GA	Genetic Algorithm

GUI	Graphical User Interface
IEEE	Institute of Electrical and Electronics Engineers
ISO	International Organization for Standardization
MATLAB	Matrix Laboratory
MRC	Maximum Rated Capacity
OCS	Overhead Crane System
OLTF	Open Loop Transfer Function
PD	Proportional Derivative
PI	Proportional Integral
PID	Proportional Integral Derivative
PSO	Particle Swarm Optimization

LIST OF ABBREVIATIONS

Ckt	Circuit
cm	Centimeter
Ex.	Example
et al.	et alia (and others)
kg	Kilogram
m	Meter
Max.	Maximum
Min.	Minimum
rad	Radian
Vs.	Versus

LIST OF SYMBOLS (PARAMETERS)

α	The payload swing angle relative to the vertical position of the trolley (degree($\circ$) or rad)
F	Overall force on the trolley (N)
F_m	Force that produces the torque developed by the motor (N)
m_t	The mass of the trolley (Kg)
m_l	The mass of payload (Kg)
r	The length of rope(m)
x	Horizontal position of the trolley (m)
$\dot{x}$	Velocity of the trolley (m/s)
$\ddot{x}$	Acceleration of the trolley (m/s^2)
$\dot{\alpha}$	Angular velocity of the load swing angle (rad/s)
$\ddot{\alpha}$	Angular acceleration of the load swing angle (rad/sec^2)
v	The load velocity (m/s)
g	Gravitational acceleration (m/s^2)
B_r	Viscous damping constant (Kg/s)
B_t	Trolley viscous damping (Kg/s)
M	Moment of inertia ($Kg - m^2$)
V_a	Motor armature voltage (V)
i_a	Armature current of the motor (A)
R_a	Motor armature resistance (Ω)
L_a	Motor armature inductance (H)
$e_a = E$	Motor armature emf (V)

r_d	Radius of the drum/pulley (m)
T	Developed torque of the motor (Nm)
J	Motor inertia ($Nmsec/rad$)
θ	Motor shaft angle(rad)
w_m	Motor angular speed (rad/sec), $w_m = \frac{\dot{x}}{r_p}$
b	Rotor viscous friction ($Nmsec/rad$)
k_t	Torque constant (Nm/A)
k_e	Electric constant ($vsec/rad$)

ABSTRACT

An overhead crane is a type of heavy machinery capable of efficiently transporting extremely heavy loads. Due to their simple and compact structure, easy and flexible operation, fast delivery and convenient installation, reasonable design, and different slings for lifting to suit various situations, overhead cranes can raise, lower, and transport a large cargo through the overhead surface in a facility. However, due to the payload continuous oscillations caused by the low damping ratio during movement, manual control is difficult, reducing the accuracy and delaying overall positioning time. As being non-linear and under-actuated, the overhead crane system has two degree of freedom and one control input. The main target is to control the overhead crane system, and to improve the performance by eliminating the swing angle and reducing positioning error in order to increase productivity and reduce the safety hazard related to the presence of oscillatory heavy loads. To study and improve the overall performance of entire system, the model of the overall system is derived by considering the actuator, which is a Brushless DC Motor (BLDCM) in this thesis. In this regard, the performance characteristics of BLDCM for overhead cranes are studied. The control designs in this study to control and improve the performance of an overhead crane system are: A conventional Proportional Integral Derivative (PID) controller by using analytical pole placement technique, with a reasonable control theory; from self-adaptive PID control strategies, Fuzzy-PID (FPID) and Particle Swarm Optimization based PID (PSO-PID) control designs successfully performed the aim; and lastly, PI-Regulator which has a state variable to design PI-Regulator as a state feedback is designed and successfully achieved the goal. The performance and robustness evaluations for each of designed controllers were done under different conditions using the MATLAB/ Simulink software tool for implementation. Therefore, the time domain performance measures of controllers at the worst case, which means, when the maximum swing of the load is $10^\circ = 0.175\ rad$ *, and with a disturbance added to the system, PID had a rise time,* t_r*, of 0.3822 sec, a settling time,* t_s*, of 5.3449 sec, and with a maximum overshoot,* M_p*, of 17.7099%; FPID with* t_r *of 0.3800 sec,* t_s *of 6.4918 sec, and* M_p*, 15.1083%; PSO-PID with* t_r *of 0.2527 sec,* t_s *of 2.1372 sec, and* M_p *of 5.2489%; Finally, PI-Regulator had* t_r *of 2.4134 sec,* t_s *of 4.6637 sec, and* M_p *0% respectively. In general, the performance and robustness of each of the designed controllers for the system is evaluated, and compared under disturbance and parameter uncertainty. Based on the time domain performance measures of controllers, the performance of overhead crane system is improved by reducing the swing angle, and maintaining an accurate positioning. In this thesis, PSO-PID control of overhead crane system had a best performance.*

Keywords: *MATLAB/Simulink, Overhead crane, PID controller, PI-Regulator, Self-adaptive PID controller, Swing angle, Trolley position.*

CHAPTER ONE

INTRODUCTION

1.1 Background of the Study

Different forms of crane system technology have emerged as a result of rapidly evolving technology in industries, depots, warehouses, heavy industrial workshops, constructions, and other facilities that carry hazardous materials and heavy loads from one position to another. Since its invention in ancient Greece, the crane has been an integral component of the working landscape, and it remained so for heavy lifting operations of all kinds. As shown in Figure 1.1 (*What is Overhead Bridge Crane — Dongqi overhead crane*, 2016), an overhead crane is equipped with cables and pulleys, and it can lift and lower loads far beyond the capacity of humans using fundamental mechanical principles. Crane design has evolved to fulfill the demands of a wide range of industrial purposes, and modern cranes typically coordinate basic systems to do complicated lifting operations, sometimes in hazardous situations for workers.

A crane that uses a hoist mounted in a stationary mechanical housing and a high overhead gantry to lift and manoeuvre extremely heavy loads is known as an overhead crane. These cranes are commonly employed in factories, shipyards, and many other commercial areas to carry hanging loads.

Every type of crane must follow the laws of physics in order to keep its crucial stability and perform efficiently. The deepest concern in this regard is that, the crane must not carry weights greater than its maximum rated capacity (MRC), and that any stressful motions occurring outside of each machine's specified plane of operation should be avoided as much as possible. A crane can lift objects because the weight is balanced by counterweights, which allow the crane to lift and transfer its cargo. Steam was once used to power some cranes. The majority of crane types, on the other hand, are driven by electric motors, hydraulic power, or an internal combustion engine (*7 TYPES OF CRANES USED IN CONSTRUCTION WORKS*, 2017). The earliest overhead cranes, for example, were steam-powered and invented by Germans in the 1830s. The first electric overhead cranes, however, did not exist until 1876, when they were manufactured in England (*Overhead crane*, 2022). The crane componentry, such as the hoist, end trucks, and controls, is largely decided by the application for which the cranes are being utilized, as well as the capacity of the overhead crane system required.

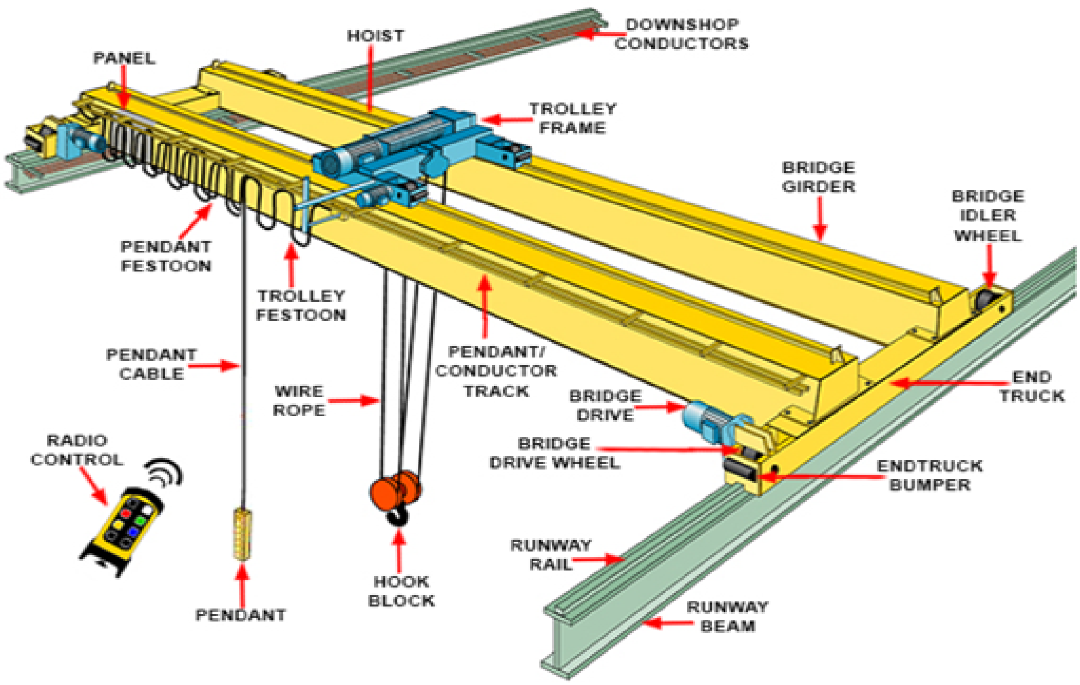

Figure 1.1: The physical diagram of overhead crane.(*What is Overhead Bridge Crane — Dongqi overhead crane*, 2016)

Users in industrial practice are distrustful of adaptive digital controllers based on the optimal theory of automatic control, due to the fact that understanding the algorithms involved needs a thorough comprehension of the theory of automatic control. Since its birth in the mid-twentieth century, adaptive control application has been a very persuasive trend in emerging technologies. Consider non-linear servomechanism control (R. Garrido & Soria, 2005), chemical reactor control (Dostál, Kubalčík, Bobál, & Vojtěšek, 2011), turbulence control for drug reduction, and even control of the human glucose-regulatory system. Because the processes in these systems are nonlinear, a good adaptive controller design is crucial for improving reliability and efficiency.

The first thing to consider is controller performance, and if the needs are minimal, a controller with constant parameters and conservative tuning can be chosen. If the process dynamics are constant, a controller with constant parameters should be implemented, with the controller variables obtained by auto-tuning. It is useful to adjust for changes in the process dynamics or the type of the disturbances by modifying the controller. PID controllers are the most used controller design in all industries because they have various significant properties such as feedback, integral, and derivative action. PID type controllers are also user-friendly because they are straightforward, well-known, and simple to apply. However, because it is linear, it is in general unsuitable for nonlinear systems. Fuzzy control is viewed as a modern alternative to PID control. The major advantage of fuzzy control is that non-linearities, input, and logic signals are simple to handle. As a result, fuzzy systems can also be utilized to identify non-linear systems. Changing the rules and membership functions of fuzzy systems allows them to be well-tuned. Therefore, combining these and other methodologies, more suitable controller designs for overhead crane system are developed.

This thesis aim is to improve the performance of overhead crane system on the development of self-adaptive controller, and PI-Regulator with a robust performance, for the swing angle and position control of overhead crane. Considering the input of the overhead crane system is the input armature voltage and the outputs of the system are the horizontal position of the crane (motion of the trolley) and the swing angle of the hanging mass (swing of the payload), the input-output transfer function is modelled and the performance and robustness of designed controllers are verified based on their responses, with disturbances and uncertain initial conditions.

1.2 Statement of the Problem

Overhead cranes are widely employed in transportation and assembly processes for a variety of applications and in various locations due to their primary benefits of high load capacity, remarkable resource and energy saving ability, low investment, and flexible operation. The swing of the load, however, cannot be regulated directly and effectively by the operator because to the under-actuation characteristics. Anti-swing control is difficult since the operator can only manipulate the trolley to hold down the load swing. This makes anti-swing control difficult. As a result, the overhead crane control must minimize or completely avoid the load swinging angle, as well as properly and swiftly reach the trolley prescribed position. As a result, it is critical and particularly essential to implement an efficient and effective overhead crane control system.

The operation of overhead cranes is always associated with two major issues. One is an unwanted load swing, which is typically experienced by load hoisting, which is caused by the crane acceleration required for motion. The other is low operational efficiency, which is caused by the swing, and this can sometimes not only reduce efficiency but also cause load damage and additional safety problems.

The strong state coupling between the motion of the trolley and the swing of the payload makes designing efficient and effective control systems for under actuated cranes complicated. The primary aim to design controller is to assure the best and fastest transition possible to maintain the target displacement at predefined position and basically, to transport the load safely, in the minimum time and without swing, and to save cost and time in controlling overhead crane.

Working with overhead cranes, whenever there is sudden stop of the movement either from the operator command or the power failure, high oscillation to the payload happens. Which in turn means there is swinging angle; And it results in the **juggling torque**. In most of industries, this type of torque happens if the operators are not expert to work with the overhead crane and this torque in turn increases the swing angle, further more accidents for humans, and damages for materials.

The proposed control will ensure an accurate control of swing angle and trolley position by taking into account the lifting capacity and range, as well as the weight and dimension of the payload of the overhead crane, in order to improve the capability and performance of the overhead crane system and reduce the swing angle of the payload.

1.3 Objectives of the Thesis

1.3.1 General Objective

The main goal of this thesis is to design controllers for overhead crane which perform efficiently under different conditions, and a comparative study of the performance of the system.

1.3.2 Specific Objectives

Specific objectives of this thesis are to:

1. Develop the mathematical model of an overhead crane system for control design.

2. Set the appropriate parameters for the control and overall performance of overhead crane system.
3. Design controllers using PID technique, self-adaptive PID approaches and PI-Regulator technique.
4. Simulate the overall system using MATLAB/Simulink.
5. Compare and analyze the performance of overall control system.

1.4 Research Questions

In this thesis, the following basic research questions are illustrated to be answered:

i. How to design the mathematical model of overhead crane system for control design by considering the actuator?

ii. What are the unique characteristics of overhead crane and what are the performance parameters of overhead crane?

iii. What are the disturbances of the overhead crane system?

1.5 Significance of the Study

As the crane is under actuated system, anti-swing and positioning accuracy are two basic requirements, which are highly correlated in the operation of crane. In this thesis, taking conventional control technique with intelligent and (or) adaptive control method and designing PI-Regulator, the swing angle and position control with improved performance is done. This mechanism is very important for efficiency and performance improvement and ability, as well as to avoid the damages due to the oscillations.

1.6 Delimitations and Limitations of the Study

This thesis is limited to show the performance and robustness of the designed controllers for the overhead crane system using MATLAB/Simulink. The implementation of a real system is limited due to time and cost. The effectiveness of proposed technique is evaluated with simultaneous hoisting of the payload, also considering instant disturbances and uncertain initial conditions.

1.7 Thesis Organization

This thesis flow is grouped into six, as follows:

Chapter One: Introduces what is done and the background, the statement of problem. The general and specific objectives, the significance and limitation of thesis is covered.

Chapter Two: Includes the two basic parts of the literature review. Theoretical literature is presented in the first part and previous studies, their Contributions with the drawbacks each of mechanisms are studied in the second section.

Chapter Three: The materials used in the thesis and methods followed are discussed. The mathematical model of the system is designed and open loop responses are analyzed according to the control theory.

Chapter Four: Controller design and analysis is presented.

Chapter Five: The results of the designed controllers are presented and the performance and robustness of each of the controller is verified under different conditions.

Conclusion and Recommendation: Conclusion is made based on the result and further study is recommended in this section.

CHAPTER TWO

LITERATURE REVIEW

2.1 Overview of the Chapter

In this chapter, two basic revisions are made. Review of general and basic theories of cranes in the former sections; previous research findings of the overhead crane system, their contributions, and drawbacks in the latter sections. More specifically, the features, types, and applications of overhead cranes and the existing controlling techniques of overhead crane systems are seen to a broad extent.

2.2 Features and Capabilities of Different Types of Cranes

Some of the most common features of cranes, and more specifically, basic features to be considered in controlling overhead cranes, are the following:

1. **Lifting Capacity -** What is the maximum lifting capacity of the crane?
2. **Lifting Capacity -** What is the maximum lifting capacity of the crane?
3. **Lifting Range -** Where to lift to?
4. **Lift Angle -** How much angle to lift?
5. **Working Radius -** What is the span of the crane?
6. **Mobility -** How much area for the crane to work?
7. **Weight and dimensions -** How much does a crane lift?(*7 TYPES OF CRANES USED IN CONSTRUCTION WORKS*, 2017)

2.3 Types of Cranes and Their Applications

There are different standards that classifies cranes on service class. Different crane manufacturer associations like ISO (International) (*Cranes — Monitoring for crane design working period*, 2014), FEM (Europe) (*FEM classification*, 2016), DIN (Germany) (*FEM/DIN standard double girder overhead crane*, 2016), CMAA (America) (*Types of cranes and classifications*, 2016), give different classifications according to average load intensities and number of cycles. Cranes among several varieties are applied in many applications. For example: Although mobile cranes are usually installed on wheeled vehicles, cranes used in railway work are specially designed to travel on train tracks. On urban construction sites, a tower crane is a type of balance crane. It is attached to the ground and provides the optimal platform of height and lifting capacity for erecting multi-story city constructions. A telescopic crane is a crane that is powered by hydraulics and has a set of concentric tubular steel booms that can be readily expanded and retracted to change the working height of the crane. A strong, steel-braced central tower on which is attached a powerful double-cantilever beam is known as a Giant Cantilever crane, sometimes known as a Hammerhead crane. The major function of this type of crane is to lift and transfer weights via rotational movement of the entire cantilevered cross beam. The crane hook of a level-luffing crane is designed to keep at a constant level due to a particular mechanism. As a result, jib arm up and down movements will only move the hook towards or away from the base of the crane. Crawler cranes are a particular form of mobile crane equipped with caterpillar tracks that can operate on rough and wet ground where wheeled vehicles are unable to operate. Because they are part of an aircraft, aerial cranes/flying cranes have the broadest range of any crane type. They are connected to a helicopter by a lifting mechanism that is typically used to carry containers, prefabricated constructions, and timber. Overhead cranes use a strong overhead gantry to lift and handle extremely high industrial loads (*Types of cranes and classifications*, 2016). They use a hoist mounted in a fixed machinery housing or otherwise able to slide along a rail framework. The mechanism for reducing swing angle varies depending on the application region of the crane, and the amount and type of load the crane is expected to lift and or lower and move from one position to another.

There are various types of overhead cranes. So, before deciding on the type of overhead crane, it is necessary to determine the type and size of overhead crane required. It will be straightforward to limit down the search once the type of overhead crane is determined. Table 2.1 shows the various types of overhead cranes available, ranging from simple to complex (*FEM/DIN Double Girder Overhead Crane*, 2022), (*OVERHEAD CRANE TYPES - Different types of overhead cranes*, 2022).

Table 2.1: Types of overhead cranes.(*OVERHEAD CRANE TYPES - Different types of overhead cranes*, 2022)

No.	Types of Overhead Cranes	Features and Applications
1.	The Bridge Crane	* It has two overhead runways and a bridge that rides on them, as well as a hoist and a side-to-side trolley. * This thesis work is on this type of overhead crane.
2.	Gantry Crane	* It's similar to bridge cranes, except that instead of being suspended in the air, it has legs and rides on ground. * This crane is versatile and can be employed in a variety of environments, including outdoor settings, shipyards, and rail yards with a high duty cycle. * They are used to avoid overhead barriers in interior applications.
3.	Monorail Crane	* In assembly lines, this type of overhead crane equipment is employed to execute without any side motion. * The trolley is placed on the bottom of the beam and enables for load transfer. * It can move cargoes from one rail to another via a track switch.
4.	Jib Crane	* They are commonly utilized when the overhead rail system of the crane is not available. * They can be wall-mounted or floor-mounted, depending on the service they provide. * It also has the ability to rotate 180 degrees or 360 degrees.
5.	Workstation Cranes	* These cranes are used by an individual person. * It can be freestanding or hung in a coiling configuration.

2.3.1 The Basic Components of Overhead Bridge Cranes

The basic components of overhead crane system is a component that is involved in the working movement of overhead crane system and shown in the Table 2.2.

Table 2.2: Basic components of overhead bridge cranes. (*What is Overhead Bridge Crane — Dongqi overhead crane*, 2016)

No.	Components of Overhead crane	Functions
1.	Hook	It's used to connect the payload to the crane. As a result, it can be moved and raised.
2.	Hoist	It's what allows the hook to travel up and down.
3.	Trolley	It's what propels the hoist across the bridge from side to side.
4.	Bridge	Is the load-bearing beam upon which the trolley travels. It can be a top- or bottom-running design.
5.	Runway Beam	Is responsible for allowing the bridge to travel from one end to the other.
6.	End Trucks	Are what drive the bridge down the runway physically. They are propelled by wheels and engines (like a car).

2.4 The Block Diagram of Overhead Crane Control and Its Description

2.4.1 The Working Principle of Overhead Crane System

Overhead bridge cranes can be applied in a variety of settings, including industries, warehouses, and construction. And all the application working movement is based on the following basic principles:

i. Crane hook up and down lifting.
ii. Trolley lateral movement. And,
iii. Crane long travelling longitudinal motion (*OVERHEAD CRANE TYPES - Different types of overhead cranes*, 2022).

In industries, a push-button pendant controller is commonly used to operate overhead crane systems. A control system supports the operator by determining where a crane will stop when a payload significantly lags behind their control inputs supplied by a human operator. Figure 2.1 (Ramli, Mohamed, Abdullahi, Jaafar, & Lazim, 2017) shows a block diagram of an overhead crane system with a human operator. Even if the operator messes up with the pendent/joystick manipulation, the system will automatically avoid the obstacle.

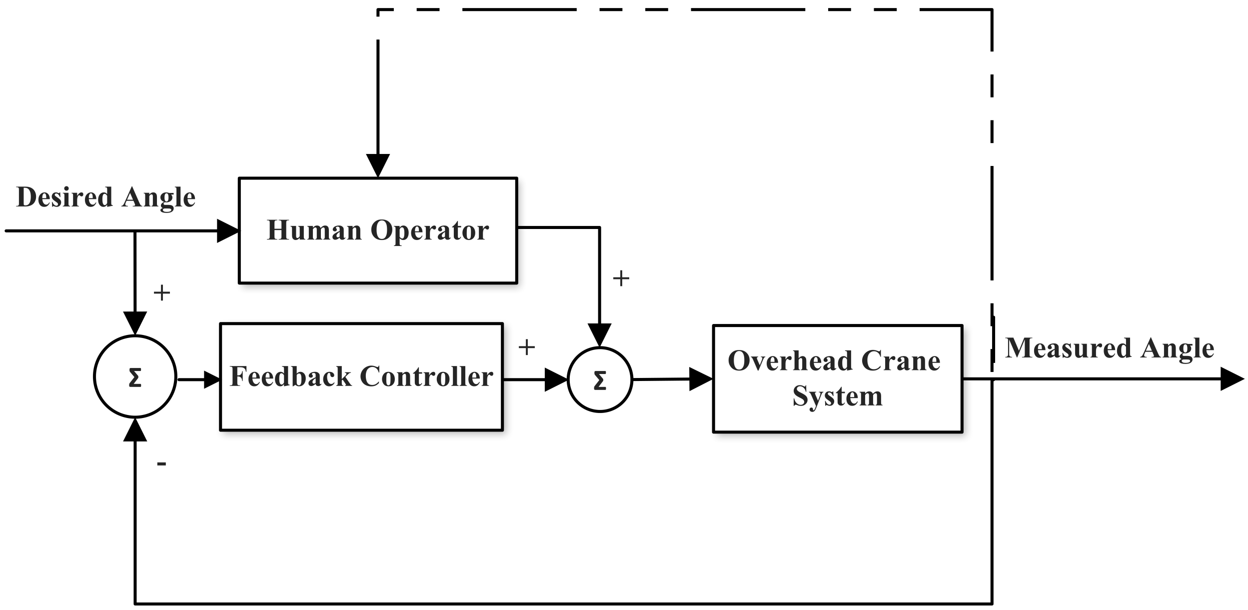

Figure 2.1: The block diagram of overhead crane system with human operator. (Ramli et al., 2017)

2.5 Related Works on the Control Strategy of Overhead Crane System

Overhead cranes are used to transport heavy cargoes in factories, warehouses, marine industries, and building sites all over the world. However, it suffer from an extreme swing as a result of a human operator inability to handle it, as well as the presence of sudden and unexpected interruptions. The swing, twisting, and bouncing were also caused by the payload being hoisted. As a result, it is critical to build efficient and effective controllers that can prevent the excessive swing caused by the aforementioned parameters in order to achieve a quick operation, avoid damage, and maintain a safe working environment. As presented in many literatures (Ramli et al., 2017), (Z. Wang, Shi, & Li, 2018), (Z. Sun et al., 2019), (Z. Sun et al., 2021), (Liu et al., 2019) the actuating force is the input to the overhead crane system, and the outputs are the position of the trolley and the swing angle of the load mass, resulting in the system being underactuated. Many scholars have investigated the anti-swing and trolley position control of underactuated overhead crane systems utilizing various types of controllers and mechanisms at various times. A great significance is made on the efficiency and performance of overhead crane system in designing an intelligent control method (Z. Sun et al., 2019), (Moon et al., 1996), (Li et al., 2005). Also, these controllers merged with conventional PID controller get the advantages of both that result very impressive performance (Solihin et al., 2007), (H. I. Jaafar & Mohamed, 2017).

Overhead cranes are controlled in a variety of ways depending on the industrial sectors. To address the control challenges of overhead crane systems, a number of researchers investigated various control approaches. The techniques are divided into three groups after a comprehensive review of the prior control schemes. As shown in Figure 2.2 (Ramli et al., 2017), open-loop control, closed-loop control, and hybrid (a combination of both open-loop and closed-loop) control techniques exist.

Open-loop control strategy is studied to the control of payload swing angle (Chandran, Vivek, & Amritha, 2017). In this scheme, there is no feedback, that is easily implemented and no need to additional sensors to measure the swing angle, and which in turn means it saves cost. However, the major limitation of this scheme is that, being sensitive to external disturbances and initial uncertainties, which means, in an open-loop scheme, the input doesn't account for the changes of control system. The major open-loop schemes revised in this thesis are input shaping (S. Garrido, Abderrahim, Gimenez, Diez, & Balaguer, 2008), command smoothing (Lu, Fang, & Sun, 2015), and filter (Ahmad, Ismail, Ramli, & Hambali, 2010) control strategies.

The optimal control strategy was first proposed as an open-loop strategy for determining the most effective control sequence. The motion trajectories are optimal in terms of actual goals, such as steady-state error or transportation time (Moon et al., 1996) and (Piazzi & Visioli, 2002), while also meeting practical and physical constraints. And input shaping is a command generating approach that aims to reduce residual swing (Piazzi & Visioli, 2002), and it is done in real time by convolving the command signal with an impulse sequence (Singhose, Porter, Kenison, & Kriikku, 2000). However, because neither optimum control nor input shaping control have closed-loop processes, they are not suited for some applications with considerable system uncertainties and external disturbances.

Closed-loop control strategy has been commonly and widely studied for overhead crane system (Khan, Chatterjee, & Dey, 2016), (N. Sun, Fang, Zhang, & Yuan, 2012),(Ma & Bao, 2018),(Wu, Xia, & Zhu, 2015),(X. Wang, Liu, Lai, Xu, & Jiang, 2017), and (Lu, Fang, & Sun, 2018). It includes the feedback loop, which means, based on the desired output, the overhead crane system can adjust its performance. To get an accurate position and to minimize the oscillations, the estimation and measurement of the system is done in this control scheme. Closed-loop control or feedback control scheme requires sensors to determine the payload position and the sway angle. The limitations of this type of control scheme on overhead crane systems are issues of stability and noise, and the slow response because of input delay with the feedback loop. On the other hand, the feedback control strategy can be tracking (trajectories are designed to maximize operation efficiency) or non-tracking (to the regulation of control performance in real-time), which divides the fold of feedback control strategy into two.

The trajectories that are designed to maximize the operating efficiency under particular physical restrictions are used in the tracking strategy (N. Sun et al., 2012), and then feedback control is used to track the planned trajectories in the presence of disturbances and uncertainties (Fang et al., 2011), (Park et al., 2008), (Masoud & Nayfeh, 2003). Even though the optimum designed trajectories are expected to minimize residual swing, more residual swing will be caused throughout the tracking process in the tracking strategy. In order to regulate control performance in real time, non-tracking solutions have been developed (Lee*, 2005),(N. Sun & Fang, 2012), (Tuan, Lee, et al., 2013), (Yang & Yang, 2007). Even if the process of trajectory planning is missed in this method, positioning precision and stabilization are still attained. But, due to a lack of planning tools, optimizing operational efficiency for this type of feedback strategy is difficult. From literatures on the closed-loop control scheme (Yang & Yang, 2007), (Z. Sun et al., 2015), (Fang et al., 2003), (Ngo & Hong, 2010), (Tuan, Moon, et al., 2013), (Park et al., 2014), (Mahfouf et al., 2000) of overhead crane systems, linear control, adaptive control, intelligent control, optimal control, sliding mode control and other feedback control types are revised in this thesis.

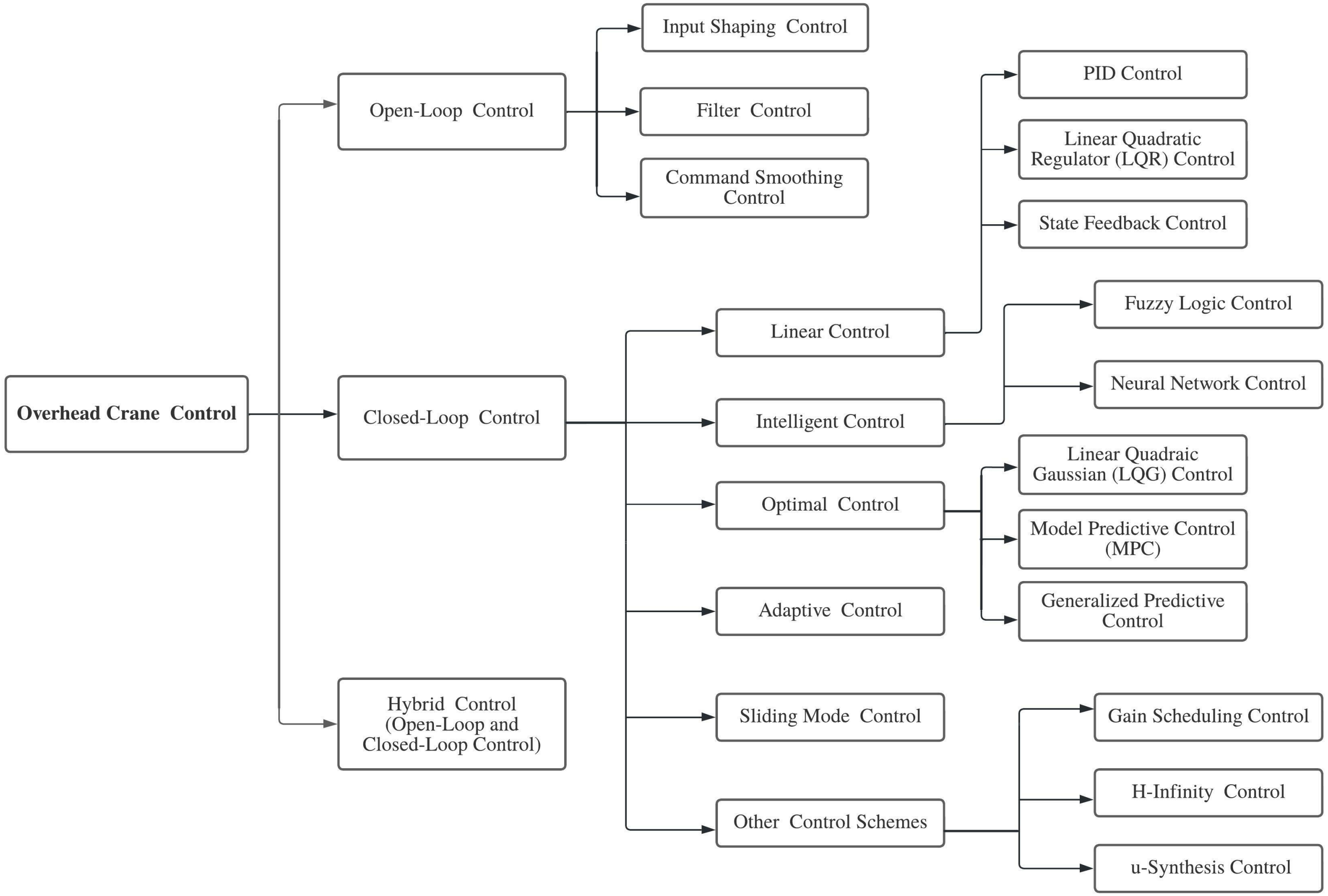

Figure 2.2: Overhead crane control strategies. (Ramli et al., 2017)

The three forms of hybrid control schemes, which blend open-loop and closed-loop control techniques, are as follows: First, a payload position feedback control scheme; second, a payload position feedback technique that can detect and reject disturbances; and third, input shaping and feedback control to prevent payload oscillation and limit the effect of disturbances such as wind. A feedback and command shaping control was given by Huang et al. (Huang et al., 2013) to eliminate the payload oscillation and reduce the effects of wind. Both feed-forward and feedback controllers are used in a hybrid control strategy. The proposed controllers were robust and reduced the various combinations of wind disturbances and driving motions, according to the simulation results.

The authors investigated the design of a sliding-mode controller for anti-swing control of overhead cranes in a paper mentioned in the literature (Shyu et al., 2005). They developed an anti-swing control scheme based on sliding-mode control to meet the strict swing angle requirement as well as an accurate trolley position control in the presence of load mass uncertainty. The authors, on the other hand, only focused at the stability of sliding surfaces. Also, in the literature (X. Wang et al., 2017), because of overhead crane is an under-actuated system (system input element is smaller than system output element variables), the controller is also unable to control the payload swing directly and must instead depend on the control of the trolley to restrain the payload sway. However, nonlinear characteristics and unforeseen conditions cannot be omitted in this literature. As a result, several assumptions about the payload mass, the rope mass between the crane and the cargoes, and other factors need to be considered.

In the literature (Mahfouf et al., 2000), and (Xie et al., 2018), (Zhai et al., 2017), Fuzzy logic control is used to effectively incorporate operational experience and solve shortcomings caused by system model parameter variation. In order to improve the controller parameter's performance, Genetic algorithms (GAs) (Gao et al., 2016), particle swarm optimization (PSO) (Chiou et al., 2012), differential evolution algorithm (DE) (Z. Sun et al., 2020), Ant colony optimization (ACO) (Waikoonvet et al., 2021), are emerged to get effective parameters.

These and other investigations have been performed to develop effective and efficient control mechanisms for under-actuated cranes that guarantee safety. (Ramli et al., 2017), (Lu et al., 2018), (H. Jaafar et al., 2018), (Chen et al., 2017), (Guo et al., 2020),

(Z. Wang et al., 2011), (Hu et al., 2021), (Wei-feng & Shan, 2019), (M. Zhang et al., 2016), (A. P. Singh et al., 2017), (A. Singh & Agrawal, 2018), (N. Sun et al., 2016), (Shao et al., 2019), (Önen & Çakan, 2017). Many previous studies have looked into how to improve overhead crane regulation performance.

Almost all studies indicate that the difficulty of control arises from the high state coupling between payload swing and the trolley motion. This swing not only affects operational efficiency, but also creates a serious of destroying the payload or surrounding objects. As a result, studying such kinematic coupling behavior is the first task in crane control.

2.5.1 Summary of Related Works

To summarize the related works, recent works in the past four consecutive years have been selected, and their contributions and weaknesses are seen in this study. First, in the literature (M. Zhang et al., 2018), an adaptive proportional derivative sliding mode control (PD-SMC) is applied with the objective of achieving efficient positioning and rapid payload swing elimination. Despite the fact that they outperformed the LQR and enhanced coupling controllers, their study is limited to transient responses. Also, in the literature (Z. Sun et al., 2019), the authors' objective is to control the movement of the load and eliminate the oscillations of the payload by using a method of designing and applying fuzzy PID control for overhead crane systems. In this study, the dynamic control of a crane was achieved under different conditions. But the system has a higher overshoot and settling time. Furthermore, in the literature (Ramli et al., 2020), the NNUMZV-APIDLNN (Neural Network Unity Magnitude Zero Vibration-Adaptive PID like Neural Network) algorithm is applied with the objective of Overhead crane swing control is subjected to simultaneous hoisting and external disturbances. In this literature, when compared to the NNUMZV-PIDPSO controller, it is possible to handle both constraints at the same time and achieve considerable reductions in overall and residual swings. However, the input shaper used is an open-loop control, which lacks a feedback loop. Finally, in the literature (Z. Sun et al., 2021), a method of designing fuzzy adaptive PID control is attained with the objective of improving anti-swing control. In this literature, the objective is achieved under different conditions. But, the system with the proposed method has a higher overshoot and settling time.

CHAPTER THREE

MATERIALS AND METHODS

3.1 Introduction

In the previous chapter, the review of literature is seen to a broad extent. The theoretical parts and the previous research are the general categories discussed. The drawbacks and the gap in studies of the previous research are also covered.

This chapter deals with the materials and methods in the general classification. The materials used are presented in the former section, and the methods with their respective sub-classes are discussed in the latter section. The methodology of this thesis adopts an engineering research method. Then, the analysis of the overhead crane system dynamics is discussed in detail, and finally, the mathematical modeling of the overall overhead crane system is designed by modeling the overall movement and modeling the actuator. Finally, based on these, the open-loop response without any controller is obtained and discussed based on the control theory.

3.2 Materials

Software materials used in this thesis are Microsoft Office 2021, Lucid Chart, Concept Draw Office, Math Type 2022, MATLAB R2021a, and TeXstudio. Microsoft Office is used to write and edit the progress of the study from the very beginning up to the result and final discussion; for documentation and progress presentations. Lucid Chart and Concept Draw Office are used to draw blocks, diagrams, flowcharts, and figures online and manually, respectively. Math Type is a graphical editor for mathematical equations, which is used to write the mathematical equations, interfacing with Microsoft Office when modeling the system and designing the controller. MATLAB R2021a, which is a computing software that consists of Simulink and technical toolboxes, is used to design and implement the entire system. TeXstudio is an integrated writing environment for creating LaTeX documents, and it is used for writing this thesis document in an attractive and comfortable form.

3.3 Methods

Figure 3.1 (*Engineering Design Process*, 2022), (Kothari, 2004), depicts the methods used in this thesis to meet requirements and obtain the desired result, which is an engineering research method.

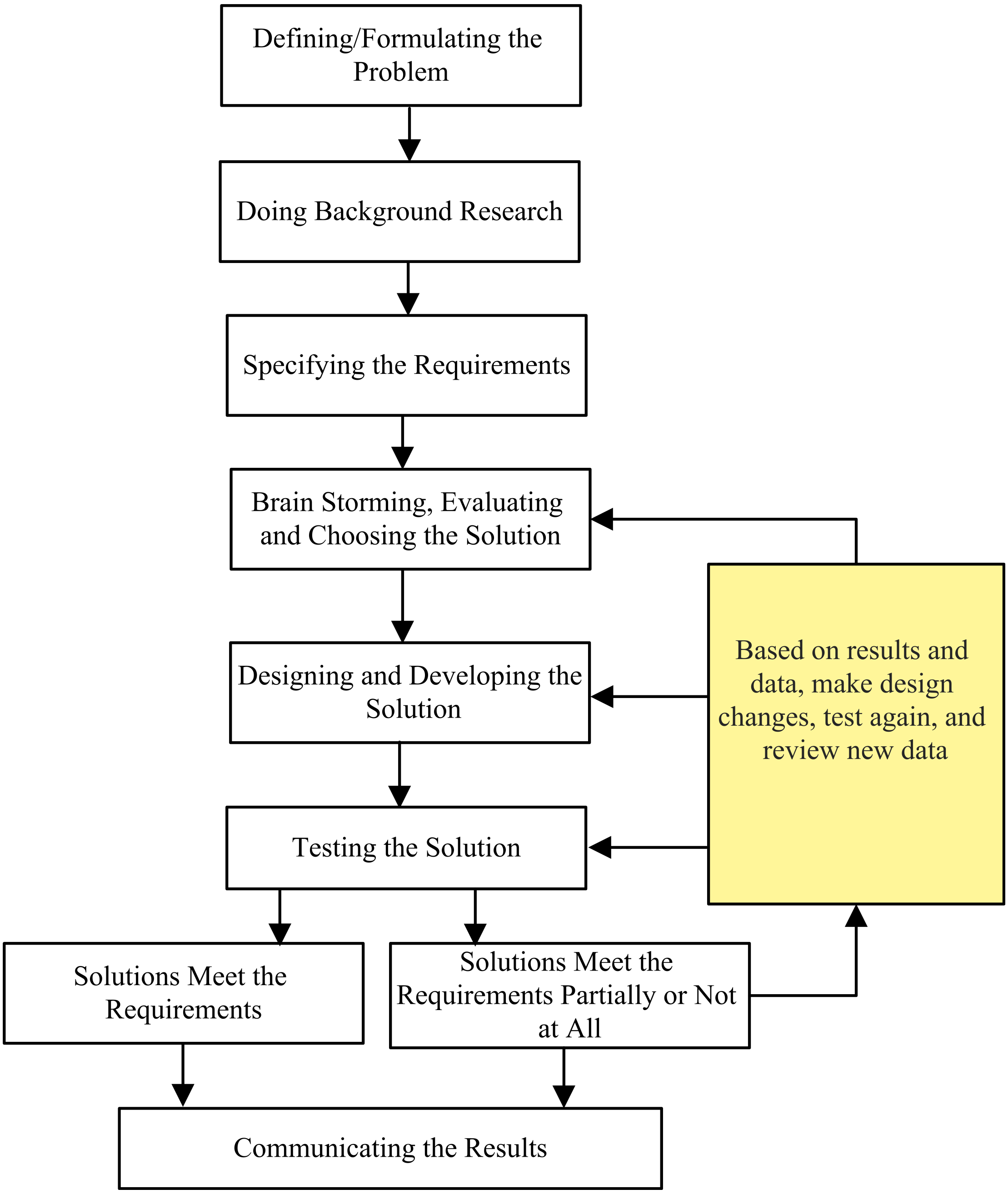

Figure 3.1: Block diagram of the research methodology.(*Engineering Design Process*, 2022)

In the first step, the problem is known and defined, which is defined in the statement of the problem. Second, closely related and latest research works are reviewed, as per

ASTU guidelines. Third, the requirements are specified regarding both the system and the actuator (or) the DC motor, the necessary data used throughout the study are collected and analyzed. Fourth, based on the collected and analyzed data, the solution is designed, developed, evaluated, and chosen.

Then, the solution performance is tested by different initial conditions and considering disturbances. And finally, after testing the solution with system performance, the pre-specified requirements are matched with the output response, and results are communicated until the best performance is obtained.

3.4 Analysis of Overhead Crane System Dynamics

An overhead crane is a type of crane that uses cables and pulleys to lift, lower, and move big and bulky objects beyond the capability of humans. It works by applying fundamental mechanical principles to lift, lower, and move heavy objects from one location to another. It utilizes a strong overhead gantry to lift and handle extremely heavy industrial loads using a hoist mounted in a fixed machinery enclosure or able to travel along a rail framework. The hoist, end trucks, and type of controls used in cranes are the essential components. The capacity of the overhead crane system required is defined by the application in which the cranes are employed.

3.4.1 The Power and Driving Force of Overhead Crane System

A crane can lift materials because the weight of the load is balanced by counterweights, which allow the crane to lift and move its cargo. Most cranes are powered by electric motors, hydraulic power, or an internal combustion engine. While some cranes were once powered by steam, This thesis considers the types of cranes powered by electric motors, specifically brushless DC motors, because they have advantages of cleaner, faster, more efficient, and quieter operation and a longer maintenance-free life than other motors. And it has a linear speed/torque curve with speed proportional to voltage and torque proportional to current (ignoring iron losses). Also, using input voltage as a speed command makes it simple to adjust speed and position.

3.4.2 Specifications of Overhead Crane System

This study considers 2-D overhead crane system. An overhead crane system and its actuator parameter specifications are according to experimental data obtained from previous study (Solihin et al., 2007). The features and capabilities of overhead crane systems like the lifting capacity, lifting height, and work span, are considered accordingly.

3.5 Mathematical Modelling of Overhead Crane System

In the development of modelling the overall system, the modelling of the overall movement of the overhead crane system and the modelling of the crane actuator (brushless DC motor) are presented to benchmark with the overall system modelling dynamics. Finally, the simulation results of the designed performance improvement controller are discussed

The overhead crane structure is illustrated in Figure 3.2 below. Where, x, α, *and* F are the trolley's position relative to the vertical axis, the payload swing angle, and overall force on the trolley. The payload is connected with constant rope length,r, and the trolley move on the horizontal bridge.

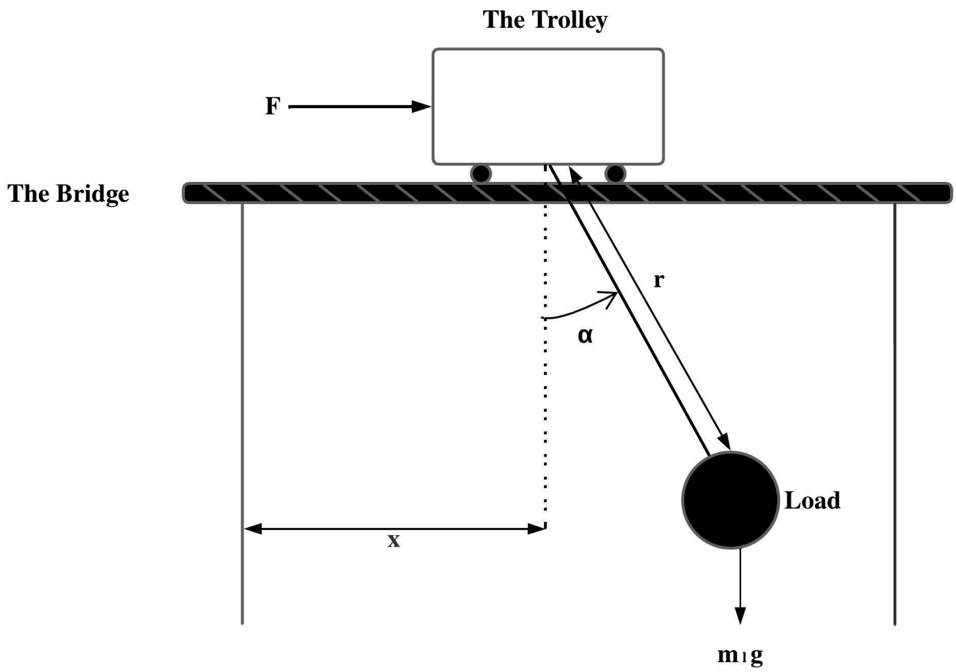

Figure 3.2: The schematic diagram of the overhead crane system.

3.5.1 Mathematical Modelling of Overhead Crane Overall Movement

Considering the crane is rigid, the trolley runs on a frictionless rail, the trolley and the load are point masses, the rope is smooth by flexible suspension rope with length r and the load and trolley are assumed to move the x-y plane, the equations that connect force and acceleration in kinematic characteristics are obtained by balancing the horizontal forces and the moment about the pivot point of the load. The rope is assumed to be massless and then, the gravitational influence and the moment of inertia that may contribute to the effect of the rigid body can be ignored. The resulting equations derived which connect the force and acceleration are:

A) Balancing the horizontal forces by applying Newton's laws of motion:

1. Trolley force in the horizontal direction:

$$m_t \frac{d^2x}{dt^2} = F + m_l g \sin\alpha \tag{3.1}$$

2. Load mass in the horizontal direction:

$$m_l \frac{d^2(x + r\sin\alpha)}{dt^2} = -m_l g \sin\alpha \tag{3.2}$$

F is the overall input force. Substituting Equation (3.2) into Equation (3.1) and re-arranging, the horizontal force equation becomes:

$$(m_t + m_l)\ddot{x} - m_l r \sin\alpha\dot{\alpha}^2 + m_l r\ddot{\alpha}cos\alpha = F \tag{3.3}$$

B) Balancing the Torque or Moment about the center of gravity by and applying Newton's second law of motion:

$$\sum M = 0$$

$$m_l r^2\ddot{\alpha} + m_l r cos\alpha\ddot{x} + m_l g r \sin\alpha = 0 \tag{3.4}$$

This Equation relates the trolley and the load position. Where the acronyms of the overall movement of the overhead crane system are depicted in the preliminary page, in the list of symbols.

3.5.2 Mathematical Modeling of Overhead Crane Actuator

The actuator of the overhead crane in this thesis is Brushless DC (BLDC) Motor, for it has a linear torque and speed curve (neglecting iron losses), with torque proportional to current and speed proportional to voltage and this produces a predictable speed regulation. BLDC requires less maintenance, which means it has a longer life than both brushed DC and Induction motors.

BLDC motors operate more quietly than brushed motors having many advantages compared to brushed DC motors and AC induction motors. The comparison of BLDC with both a brushed DC motor and an AC induction motor is summarized in the Table 3.1 (D P Kothari, 2010).

Table 3.1: Comparison between BLDC motor, Brushed DC motor and AC induction motor. (D P Kothari, 2010)

Features	**BLDC Motor**	**Brushed DC Motor**	**AC Induction Motor**
Speed/Torque characteristics	Flat - Enables operation at all speeds with rated load.	Moderately flat - Brush friction increases, thus reducing torque.	Nonlinear - Lower torque at lower speeds.
Efficiency	High – Due to the absence of friction of brushes.	Moderate.	Low - Due to the creation of electromagnets.
Output Power/ Frame size	Low - Better dynamic characteristics.	High- Reduced size due to superior thermal characteristics. Better heat dissipation.	Moderate/Low- Increasing the temperature in the air gap.
Rotor Inertia	Low rotor inertia. Improving the dynamic response and better dynamic characteristics.	Higher rotor inertia limits the dynamic characteristics.	High rotor inertia - Poor dynamic characteristics.

Thus, the equivalent circuit of the actuator, a separately excited DC motor (D P Kothari, 2010), more specifically field control with fixed armature current type, where the field winding is physically and electrically separate from the armature winding and for its simple but high-performance control, is shown in Figure 3.3 (Åström & Wittenmark, 2013). The dynamic model parameters of separately excited DC motor are listed in the preliminary section of list of special symbols.

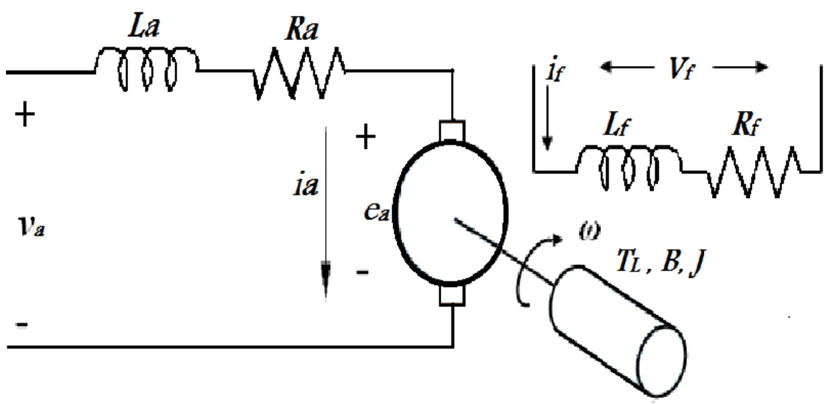

Figure 3.3: DC Motor equivalent circuit. (Åström & Wittenmark, 2013)

The trolley is driven by a DC Motor (Lu et al., 2018), (Haq & Okumus, 2016), (Chaudhary, Khatoon, & Singh, 2016) and the dynamic equation of DC motor is:

$$V_a = R_a i_a + L_a \dot{i}_a + K_e \dot{\theta}, \quad i_a = \frac{T}{k_t} \tag{3.5}$$

$$T = k_t i_a \tag{3.6}$$

$$T = J\ddot{\theta} + b\dot{\theta} + F_m r_d \tag{3.7}$$

Now, the force, F_m, that produces the torque developed by the motor, is written as:

$$F_m = m_t \ddot{x} + B_t \dot{x} + F \tag{3.8}$$

Where the total force, F is substituted from the Equation (3.3) and re-arranged, it becomes:

$$F_m = (2m_t + m_t)\ddot{x} + B_t \dot{x} + m_l r(\cos\alpha\ddot{\alpha} - \sin\alpha\dot{\alpha}^2) \tag{3.9}$$

$$\ddot{\theta} = \frac{\ddot{x}}{r_d} = \dot{w}_m \tag{3.10}$$

$$\dot{\theta} = \frac{\dot{x}}{r_d} = w_m \tag{3.11}$$

Substituting Equations (3.9), (3.10), and (3.11) into Equation (3.7), it becomes:

$$T = J\ddot{\theta} + b\dot{\theta} + r_d * F_m$$

$$T = J\frac{\ddot{x}}{r_d} + b\frac{\dot{x}}{r_d} + r_d((2m_t + m_l)\ddot{x} + B_t\dot{x} + m_l r(\cos\alpha\ddot{\alpha} - \sin\alpha\dot{\alpha^2})) \tag{3.12}$$

To simplify and linearize the mathematical Equation using simple mathematics describing a given dynamic system assuming that the normal operating position is when the load is at the downward position, the load-displacement, α, is very small. So that the following approximations are valid for the small angle.

$$\sin\alpha \cong 0 \tag{3.13a}$$

$$\cos\alpha \cong 1 \tag{3.13b}$$

Now, the simplified torque Equation becomes:-

$$T = J\frac{\ddot{x}}{r_d} + b\frac{\dot{x}}{r_d} + r_d((2m_t + m_l)\ddot{x} + B_t\dot{x} + m_l r\ddot{\alpha}) \tag{3.14}$$

Re-arranging Equation (3.5), it becomes:-

$$V_a = K_e\dot{\theta} + \frac{L_a}{k_t}\frac{dT}{dt} + \frac{R_a}{k_T}T \tag{3.15}$$

Substituting Equation (3.11) and Equation (3.14) into Equation (3.15), doing the derivation and re-arranging, it becomes:

$$\begin{aligned} V_a = \frac{L_a}{k_t}\left[\frac{J}{r_d} + r_d(2m_t + m_l)\right]\dddot{x} \\ + \left[\frac{L_a}{k_t}\left(\frac{b}{r_d} + r_d B_t\right) + \frac{R_a}{k_t}\left(\frac{J}{r_d} + r_d(2m_t + m_l)\right)\right]\ddot{x} \\ + \left[\frac{R_a}{k_t}\left(\frac{b}{r_d} + r_d B_t\right) + \frac{k_e}{r_d}\right]\dot{x} + \frac{L_a}{k_t}(r_d m_l r)\dddot{\alpha} + \frac{R_a}{k_t}(r_d m_l r)\ddot{\alpha} \end{aligned} \tag{3.16}$$

To have a simplified equation, the following terms are used:

$$
\begin{aligned}
a_1 &= \frac{L_a}{k_t}\left[\frac{J}{r_d} + r_d(2m_t + m_l)\right] && \text{(3.17a)}\\
a_2 &= \frac{L_a}{k_t}\left(\frac{b}{r_d} + r_d B_t\right) + \frac{R_a}{k_t}\left(\frac{J}{r_d} + r_d(2m_t + m_l)\right) && \text{(3.17b)}\\
a_3 &= \frac{R_a}{k_t}\left(\frac{b}{r_d} + r_d B_t\right) + \frac{k_e}{r_d} && \text{(3.17c)}\\
b_1 &= \frac{L_a}{k_t}(r_d m_l r) && \text{(3.17d)}\\
b_2 &= \frac{R_a}{k_t}(r_d m_l r) && \text{(3.17e)}
\end{aligned}
$$

Therefore, the Equation (3.16) is re-written as:-

$$V_a = a_1 \dddot{x} + a_2 \ddot{x} + a_3 \dot{x} + b_1 \dddot{\alpha} + b_2 \ddot{\alpha} \tag{3.18}$$

The Laplace transform of Equation (3.18) by taking all the initial conditions zero:-

i.e.,

$$
\begin{aligned}
s^2 x(0^-) = s x(0^-) = x(0^-) = 0\\
s^2 \alpha(0^-) = s\alpha(0^-) = \alpha(0^-) = 0
\end{aligned} \tag{3.19}
$$

$$V_a(s) = (a_1 s^3 + a_2 s^2 + a_3 s)x(s) + (b_1 s^3 + b_2 s^2)\alpha(s) \tag{3.20}$$

From Equation (3.4), taking the approximation for small angle as shown in Equation (3.13a) and Equation (3.13b), it becomes:-

$$m_l r^2 \ddot{\alpha} + m_l r \ddot{x} = 0 \tag{3.21}$$

Taking the Laplace transform by making all the initial conditions zero, as described in Equation (3.19) and solving in terms of the trolley position:-

$$x(s) = -r * \alpha(s) \tag{3.22}$$

Substituting Equation (3.22) into Equation (3.20) and re-arranging, the equation that relates the load swing angle to the input armature voltage is obtained as: -

$$\frac{\alpha(s)}{v_a(s)} = \frac{1}{s\left[(b_1 - ra_1)s^2 + (b_2 - ra_2)s - ra_3\right]} \tag{3.23}$$

Now, from Equation (3.22), solving for $\alpha(s)$,

$$\alpha(s) = \frac{-1}{r}x(s) \tag{3.24}$$

Substituting Equation (3.24) into (3.23), the overall equation that relates the trolley position to the input armature voltage is obtained as: -

$$\frac{x(s)}{v_a(s)} = \frac{-r}{s\left[(b_1 - ra_1)s^2 + (b_2 - ra_2)s - ra_3\right]} \tag{3.25}$$

Both Equations, Equation (3.23) and Equation (3.25) are the required equations that include all the parameters in the overall movement of the overhead crane system and its actuator, which is a DC motor. Before going to the controller design, the plant-model final transfer function is obtained by substituting the experimental data from Table 3.2 (Solihin et al., 2007) and after getting the numerical value of the transfer function, the open-loop responses are interpreted by control theory.

Table 3.2: Parameters for the overhead crane system and its actuator. (Solihin et al., 2007)

Parameter	Description	Values
m_l	Mass of the load	6 kg
m_t	Mass of the trolley	5 kg
r	Length of the rod	2 m
r_d	The radius of the drum	0.02 m
R_a	Armature resistance	5.5 Ω
L_a	Armature inductance	0.0025 H
B_t	Trolley viscous damping	0.002 Nsec/m
k_t	Torque constant	0.03 Nm/A
k_e	Electric constant	0.03 v-s
J	Motor inertia	$2 \times 10^{-5} Nmsec/rad$
b	Rotor viscous friction	$5 \times 10^{-5} Nmsec/rad$

Substituting the parameters for each term in Equation (3.17a) to Equation (3.17e), and solving for the Equation (3.22) to Equation (3.25), the following values are obtained for the swing angle and trolley position to the input armature voltage respectively.

$$\frac{\alpha(s)}{v_a(s)} = \frac{-1}{0.0335s^3 + 73.7s^2 + 3.9314s} \tag{3.26}$$

$$\frac{x(s)}{v_a(s)} = \frac{2}{0.0335s^3 + 73.7s^2 + 3.9314s} \tag{3.27}$$

3.6 The Behavior of System without Controller (Open-Loop Responses)

From Equations (3.26) and (3.27), it is noted that the model of input voltage-to-position is multiplied by a constant value of -2. Now, the following are the open-loop responses, the pole-zero graphs, and the unity feedback closed-loop responses.

As seen from the Figure 3.4, the responses of open-loop and uncontrolled closed loop, both define that the system is unstable. And the open-loop response has almost similar time responses as the closed-loop uncontrolled response.

As noted from the Figure 3.5 below, the responses resemble to the responses of swing angle-to-input voltage responses shown in Figure 3.4. Because, the Equation of one is a multiple of another. The difference here is that, even if the responses of bode-plot is stable for the open-loop system for position of the trolley-to-input voltage, it is stable for only the given time and beyond the given values, uncertain initial conditions and disturbances, it must be checked with a controller design.

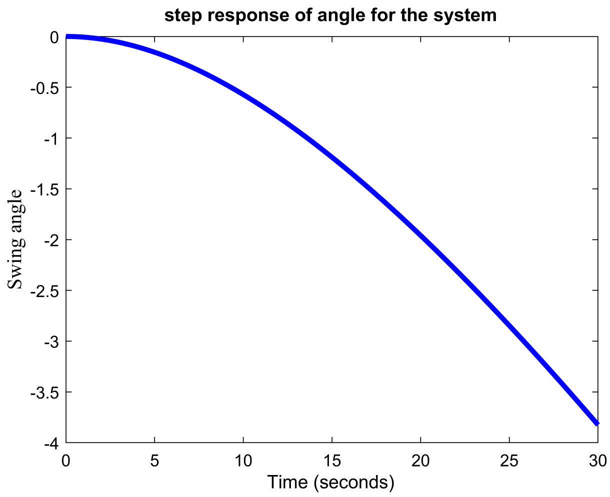

(a) Swing angle step response of the system.

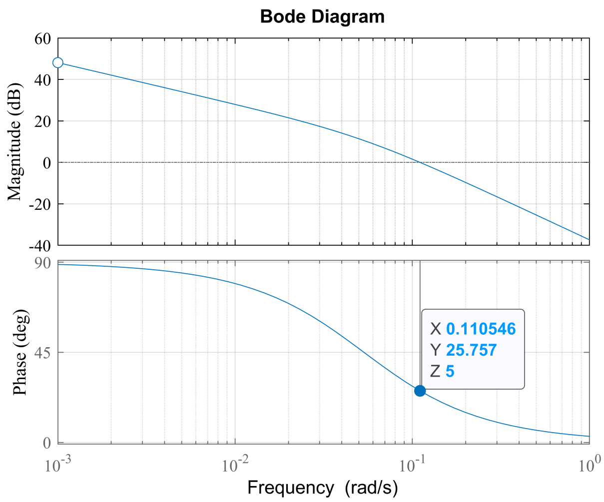

(b) Bode plot diagram of the system.

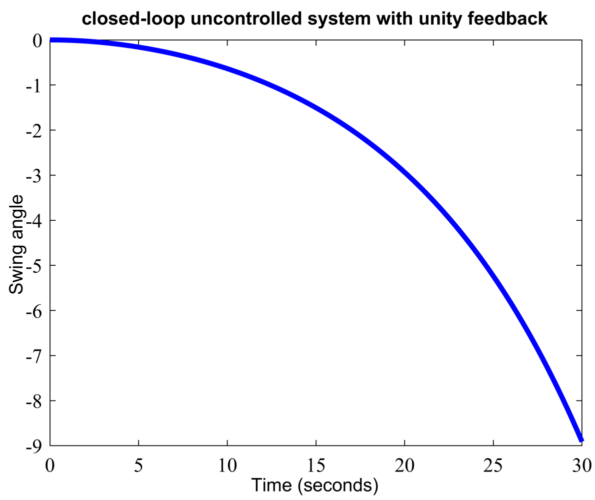

(c) Closed − loop uncontrolled system behaviour with unity feedback.

Figure 3.4: System behaviour of uncontrolled swing angle.

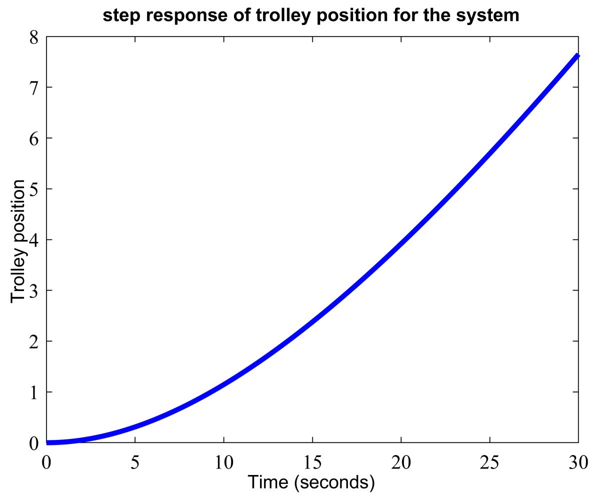

(a) *Trolley position step response of the system.*

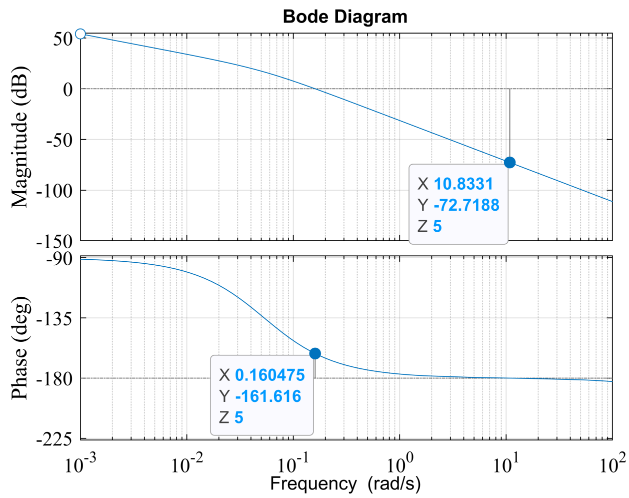

(b) *Bode plot diagram of the system.*

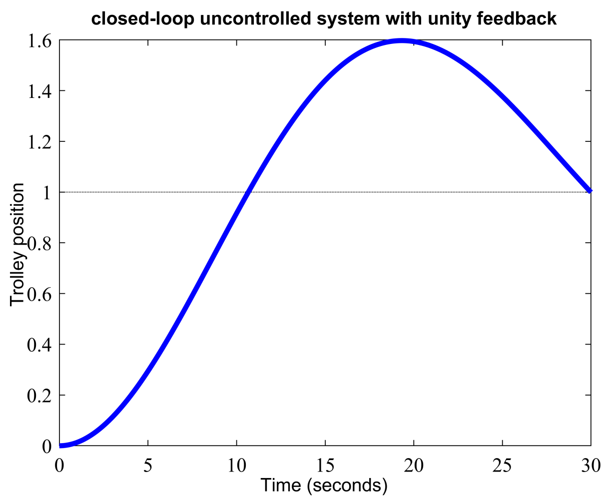

(c) *Closed − loop uncontrolled system behaviour with unity feedback.*

Figure 3.5: System behaviour of uncontrolled trolley position.

CHAPTER FOUR

CONTROLLER DESIGNS

4.1 Introduction

In the previous chapter, the mathematical model of the overall system of overhead crane was formulated. The responses of uncontrolled unity feedback closed-loop system showed the behavior of the system. In this chapter, different types of controller designs are presented. The designed controller's performance for overhead crane system is shown and compared with each other; the responses of each is analyzed, in the next chapter.

The general block diagram of overhead crane system control is described in Figure 4.1. Where, the input to the system is the armature voltage and the output is the swing angle of the load. And, this measured swing angle is fed back, the control error, which is the difference between the actual (measured) swing angle and the desired (reference) swing angle is an input to the controller. Then, the controller adjusts the required variables. In this case, the primary thing to be controlled is the swing angle of the payload. Also, according to the relation of the swing angle to the trolley position described in Equation (3.22), the position of the trolley is also controlled by controlling the swing angle of the payload. Figure 4.1 summarizes the relation between the swing angle of the payload and the position of the trolley in a single block diagram.

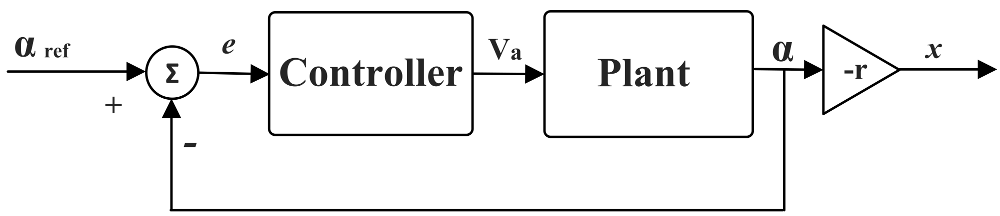

Figure 4.1: The general block diagram of control design of overhead crane system

The types of controllers designed for overhead crane system in this chapter are: Conventional Proportional Integral Derivative (PID) controller, Fuzzy PID (FPID) controller, Particle Swarm Optimization based PID (PSO-PID), and PI-Regulator respectively. Simulink block diagram and the design parameters of each is seen in detail in the following sections.

4.2 PID Controller Design and Its Performance Criteria

A proportional-integral-derivative controller (PID controller) is also called a **three-term controller**. It is historically the oldest but currently still the most used one, and it is used in industrial processes in the near and far future because of the increase of the number of PID tunning mechanisms (Ogata et al., 2010). To generate a difference equation using the present, past and the future values of the control error made a remarkably simple ability of the PID controller and it forecast it to a long-term perspective.

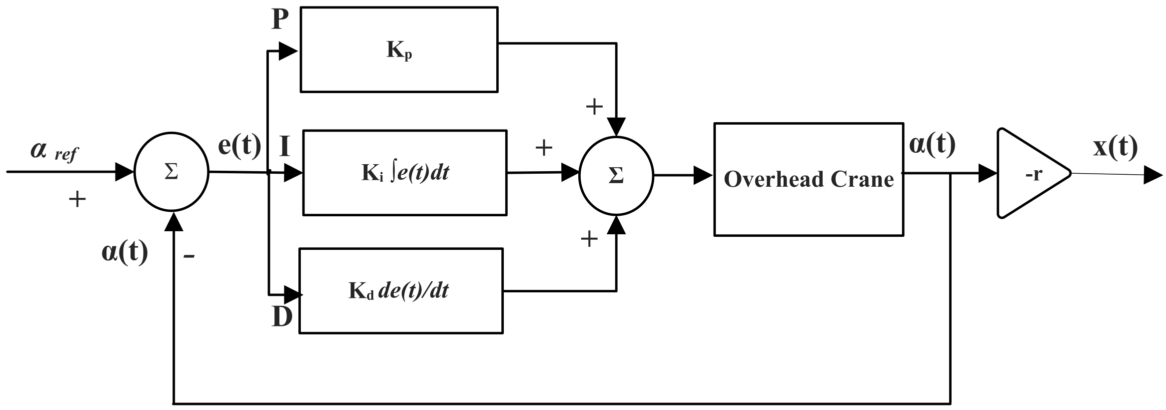

Figure 4.2: The block diagram of a PID feedback loop.(Ogata et al., 2010)

PID controller is a type of controller that continuously calculates an error value e(t) as the difference between a desired set point or a reference value and the measured process variable and applies a correction based on the proportional (P), integral (I), and derivative (D) terms, respectively. Coming to the practical terms, a PID controller automatically applies responsive and accurate correction to a control function. The PID controller algorithm restores the measured output to the desired output with a minimal overshoot and delay, by increasing the output of the plant in a controlled manner. The ability to use three control terms of proportional, integral and derivative influence on the controller output to apply accurate and optimal control is a distinguishing feature of the P-I-D controller. The block diagram of PID controller is shown in the Figure 4.2, α_{ref} is the desired swing angle or the set point, and $\alpha(t)$ is the measured angle value.

As shown in Figure 4.2, PID controller continuously calculates an error value α_{ref} as a difference between a desired swing angle and a measured angle value,$\alpha(t)$ and applies a

correction based on the proportional, integral, and derivative terms. By the adjustment of a control variable, the PID controller attempts to minimize the error over time.
In the PID control model:

- **P** term is proportional to the current value of error $e(t)$. If the error is large and also positive, the control output will be proportionally large and positive, while taking into account. The proportional control alone, by itself will generally result in an error between the set point and the actual process value because it requires an error value to generate the proportional response. Which means, the controller cannot adjust the system unless there is an error.

- **I** term is for past value of error and integrates them over time to produce the integral term, **I** Which means, if there is a residual $\alpha_{ref} - \alpha(t)$ error after the application of the proportional control, an integral term seeks to eliminate the residual error by adding a control effect due to the past cumulative value of the error. So, when the error is eliminated, the integral term will stop to grow. Which in turn result in the proportional effect reducing as the error decreases, but it is compensated for by the increasing integral effect.

- **D** term is used for estimating of the future $\alpha_{ref} - \alpha(t)$ error, which is based on the current rate of change of error. Sometimes it is called *"anticipatory control"*, for it effectively seek to reduce the effect of the $\alpha_{ref} - \alpha(t)$ error by exerting a control influence generated by the rate of error change, that means the more rapid the change, the greater the damping effect or the higher the controlling.

Therefore, PID controllers are important parts of distributed control systems, predictive control structures, because of their coefficients are adapted by means of fuzzy and neural control and set by the intelligent algorithms. This and other advantages made the PID controllers preferable for over 83 years, for their outstanding ability of diverse tuning methods, which are a good prerequisite for achieving a satisfactory performance in simple and demanding industrial applications (Ogata et al., 2010).
From the block diagram of the PID controller, the PID controller can be described as:

$$C(s) = K_p + \frac{K_i}{s} + K_d s \tag{4.1}$$

Recalling the plant or overhead crane system model as obtained in Equation (3.27):-

$$G(s) = \frac{-1}{0.0335s^3 + 73.7s^2 + 3.9314s}$$

From the two functions, the closed loop transfer function (CLTF) is obtained as:

$$\frac{\alpha(s)}{V_a(s)} = \frac{C(s)G(s)}{1 + C(s)G(s)} \tag{4.2}$$

By substituting the values, the final closed-loop transfer function is:

$$\frac{\alpha(s)}{V_a(s)} = \frac{-(K_d s^2 + K_p s + K_1)}{0.0335s^4 + 73.7s^3 + (3.9314 - K_d)s^2 - K_p s - K_i} \tag{4.3}$$

From the characteristic Equations of (4.2) and (4.3), according to Routh Hurwitz stability criteria, the system is stable if and only if the characteristic equation coefficients are greater than zero and the bounds of the gains of the PID controller are satisfied as follows:

$$3.9314 - K_d > 0, K_d < 3.9314 \tag{4.4a}$$

$$-K_p > 0, K_p < 0 \tag{4.4b}$$

$$K_i > 0, K_i < 0 \tag{4.4c}$$

To obtain the values of the gains and to tune the PID controller, the above bounds must be obeyed and the values of the gains obtained must keep the system stable.

In this thesis, the gains of PID controller are obtained by pole-placement technique, which is from analytical tunning mechanism.

4.2.1 Analytical (Pole-Placement) Tunning Method of PID Controller

Pole placement method is a controller design method which is used to determine the places of the closed-loop system poles in the complex plane by setting a controller gain, K (K_p, K_i, K_d) Where, the poles describe the behavior of linear dynamical systems. So, through the use of feedback attempting, it is possible to change that the behavior in a way that is more favorable for the specific system. Thus, it is possible to decide where the closed loop poles should be, then force them to be there by designing a feedback control system via pole-placement method where that places the poles on their desired locations.

From the control theory, it is known that for a higher order system ($n > 2$), that have a complicated transient response, the desired poles are based on second order approximation. That means, two dominant poles from desired transient response and the remaining poles at least five times farther from the imaginary axis. Therefore, the order of overhead crane system now is 4 and the dominant and non-dominant poles are carefully selected accordingly.

From the transient response characteristics, choosing the maximum overshoot, ($M_p = 0.2765\%$) and the settling time, ($T_s = 5.5888\ sec$) and from the time domain performance parameters relation, the values of damping coefficient and natural frequency are obtained, which are used in pole placement as (SmarajitGhosh, n.d.):

$$T_s = \frac{4}{\zeta W_n} \tag{4.5}$$

$$M_p = e^{-\frac{\pi\zeta}{\sqrt{1-\zeta^2}}} \tag{4.6}$$

Based on the chosen values of the maximum overshoot and the settling time, and the Equations (4.5) and (4.6), zeta(ζ) and natural frequency,w_n values obtained are 0.846 and 0.846 rad/sec respectively.

Therefore,

$$\begin{aligned} P_{1,2} &= w_n(\zeta \pm j\sqrt{1 - w_n^2}) \\ P_{1,2} &= -0.71565 \pm j0.4511 \\ P_3 &= -2.1 \\ P_4 &= -2199.5 \end{aligned} \tag{4.7}$$

$$\Delta(S) = (s - P_1)(s - P_2)(s - P_3)(s - P_4) \tag{4.8}$$

Equation (4.8) is the characteristic polynomial for the pole placement method which include both the dominant and non-dominant poles that must be equal to the characteristic equation of the closed loop system. Here, the basic thing to consider is that, if the two characteristic equations do not match at any of the polynomial coefficients, the selection of poles must be checked again and corrected. Therefore, substituting Equations of (4.7) into the Equation (4.8), the characteristic polynomial is equalized as:

$$\Delta(S) = 0.0335s^4 + 73.7s^3 + 260.3325s^2 + 274.2536s + 110.7361 \tag{4.9}$$

$$\Delta(S) = 0.0335s^4 + 73.7s^3 + (3.9314 - K_d)s^2 - K_p s - K_i \tag{4.10}$$

Balancing Equations (4.9) and (4.10), the values of the PID gains are obtained as follows:

$$K_p = -274.2536 \tag{4.11}$$

$$K_i = -110.7361 \tag{4.12}$$

$$K_d = -256.3911 \tag{4.13}$$

Therefore, the results of the gains of PID controller matched with the given bound, as to be in the Equations (4.4a)-(4.4c). A reader can check the root locus diagram in appendix-1. And the closed-loop transfer function of PID controller becomes:

$$\frac{\alpha(s)}{V_a(s)} = \frac{256.3911s^2 + 274.2536s + 110.7361}{0.0335s^4 + 73.7s^3 + 260.3225s^2 + 274.2536s + 110.7361} \tag{4.14}$$

4.3 Adaptive Control Designs

4.3.1 Adaptive Control

Adaptive control is the capability of the system to modify its own operation to achieve the best possible mode of operation. Which means, adaptive control implies that an adaptive system must be capable of performing functions providing continuous information about the system. It is the control method used by the controller which must adapt to a controlled system with parameters which vary, or are initially uncertain.

Adaptive control is different from robust control in that it doesn't need a priori information about the bounds on these uncertain or time-varying parameters; robust control guarantees that if the changes are within given bounds the control law need not be changed, while adaptive control is concerned with control law changing itself.

In general, adaptive control is distinguished between feedforward adaptive control and feedback adaptive controls; As well as between direct methods, indirect methods and hybrid methods. Direct methods are ones wherein the estimated parameters are those directly used in the adaptive controller. Where as in contrast, indirect methods are those in which the estimated parameters are used to calculate required controller parameters. Hybrid methods rely on both estimation of parameters and direct modification of control law.

Adaptive control is based on feedback of signals in a controlled system for control adaptation to effectively handle system uncertainties. Feedback is crucial for performance guarantees in control systems, including adaptive control systems, which can be designed in either continuous or discrete time. Adaptive controller is a controller with adjustable parameters and a mechanism for adjusting the parameters. An adaptive control system can have two loops. One loop is normal feedback with the process and the controller. The other loop is the parameter adjustment loop and this loop is often slower than the normal feedback loop. A block diagram of an adaptive system is shown in the Figure 4.3 (Åström & Wittenmark, 2013).

In recent times, adaptive control has been merged with conventional and intelligent techniques to bring forth new concepts (Åström & Wittenmark, 2013) ,(Tao, 2003). In this thesis, fuzzy logic based PID (FPID) and particle swarm optimization based PID (PSO-PID) techniques are studied and designed for overhead crane system.

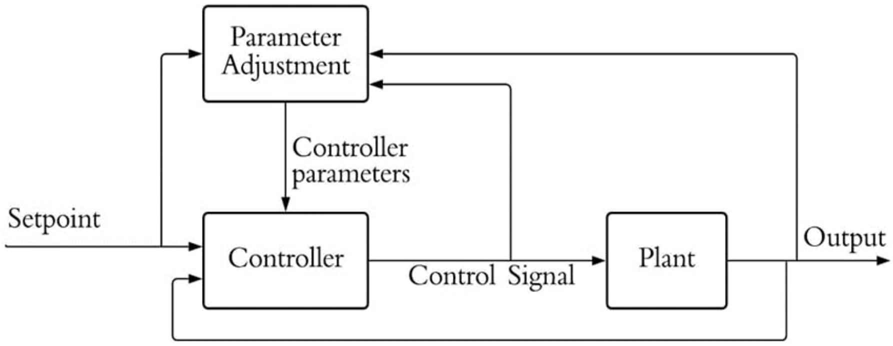

Figure 4.3: Block diagram of an adaptive control system.(Åström & Wittenmark, 2013)

4.3.2 Fuzzy Logic Based PID Controller Design

Fuzzy logic is a form of artificial intelligence with a recent application. Where, the concept was initially established in 1965 by a computer scientist named Lotfi Zadeh. It was described as a method of data processing that allowed partial set membership instead of crisp set membership or non-membership. He claimed that human thought is frequently fuzzy, imprecise, or vague in character, and thus cannot be described by yes (1) or no (0). The programmer can use fuzzy logic to deal with realistic, ”linguistic sets” of states, like extremely fast, fast, slow, and so on. Fuzzy logic is a basic method for reaching a certain conclusion based on unclear, inaccurate, noisy, or missing raw data. Its approach to problem-solving is similar to how a person could make the decisions, and it is significantly faster (Ross, 2005).

Fuzzy Logic Control (FLC) main concept is to use a human operator’s expert knowledge and experience to develop a controller or application process which the input output relationship is defined by a set of fuzzy control rules based on linguistic variables rather than a sophisticated dynamic model. The FLC converts crisp error and error change variables into fuzzy variables, which are subsequently mapped into linguistic labels. Each label has a membership function,which has two inputs and one or more outputs. The swing angle error and change in swing angle error are the inputs, and the outputs are the domains of PID controller ($K_p,\ K_i,\ and\ K_d$). Instead of attempting to model a system mathematically, the Fuzzy Inference System uses ”IF... THEN...” statements with ”OR” or ”AND” connectors in the rule statement to make the necessary decision to solve a control problem.

4.3.2.1 Design Process of FLC

First, the Fuzzy variables are identified as controller inputs and outputs. Where the inputs are the input error and change in error, and the outputs are the PID gains, Kp, Ki, and Kd, respectively. Second, the inputs and outputs are labeled and divided into different fuzzy sets based on the problem. As a result, in this study, the sets for both inputs and outputs are Negative (N), Zero (Z), and Positive (P). Third, a membership function (MF) is assigned or determined for each fuzzy set. Therefore, triangular MF is used for inputs and Sigmoid for outputs. The scaling factor for the input and output variables is then chosen to normalize them to the simplest interval range. The scaling factor assigned is -274.2536, and the ranges for $K_p,\ K_i,\ and\ K_d$ are 0.8 to 1.2, 0.2 to 0.6, and 0.6 to 1.0, respectively. The next step is to Fuzzify the inputs. As a result, similar fuzzy IF-THEN rules have been developed for PID gains. The next step is to choose an appropriate inference mechanism. For this study, the Mamdani Fuzzy Inference System (FIS), which employs fuzzy sets as a rule, is applied to an overhead crane system.

Finally, the fuzzy outputs of each rule are aggregated, and a suitable defuzzification method is selected. Center of gravity (CoG), the most popular defuzzification technique and the preferred choice in most applications, is chosen for defuzzification of fuzzy outputs due to its unique characteristics. In terms of accuracy, it outperforms other defuzzification methods and can track continuous changes in system inputs to provide smooth and continuous output values.

The fuzzy logic designer Graphical User Interface (GUI) is shown in the Figure 4.4 with entire inputs and outputs.

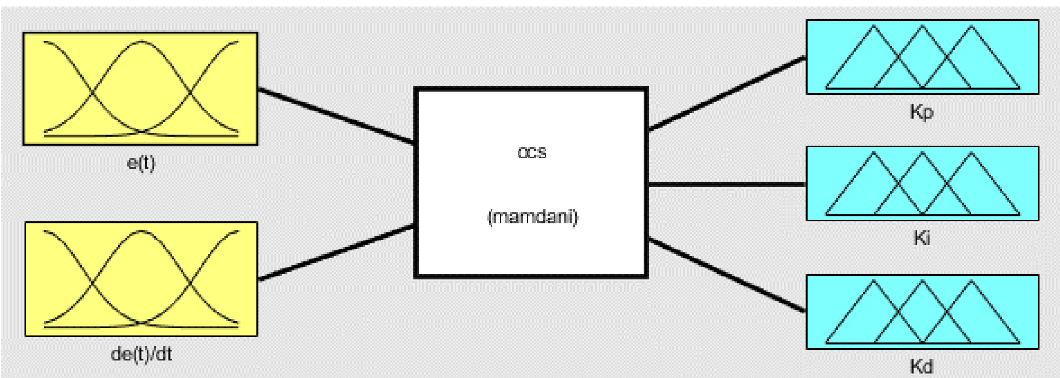

Figure 4.4: Fuzzy logic designer for overhead crane system.

A Fuzzy Logic Controller usually consists of:

I) Fuzzification

Fuzzification is a unit that converts crisp value measurement inputs into fuzzy linguistic values that a fuzzy reasoning process can employ. It's the process of making a precise number fuzzier. It converts the physical values of the error signal, rate of change of error, that are fed into the fuzzy logic controller into a fuzzy set that includes an interval for the range of input values and an associate membership function that describes the degrees of confidence that the input belongs to that range. A membership function performs the conversion process. The goal of this fuzzification stage is to make the actual input signal compatible with the controller's fuzzy control rule base.

II) Knowledge Base

The fuzzy logic knowledge base is a collection of expert control knowledge needed to meet the control objective. It has two parts: a data base and a rule base. The main function of a data base is to give the essential information for the fuzzification, rule base, and defuzzification units to function properly. This data comprises the following:

A. The linguistic meaning of the membership functions of the input variables and control output variables.

B. Physical domains with their normalized equivalents, as well as scaling, and normalization variables.

C. The fuzzy set membership functions.

For fuzzy logic controllers, the rule base is how expert knowledge is described. The primary purpose of rule base is to convey expert knowledge in the form of an if-then rule structure. The ability of fuzzy rule-based systems to produce "excellent" results with relatively simple mathematical operations is their strength.

III) Inference Mechanism

An inference engine, also known as a fuzzy reasoning mechanism, is a device that uses fuzzy logic to interpret the control action for given fuzzy inputs. We need a system that can produce an output from a collection of IF-THEN rules in order to derive inferences from a rule base. The computational rule of inference is used to do this.

The Inference Mechanism is responsible for referring to the rule base and firing the necessary rules. Mamdani's Max-Min and Max-Algebraic Product (or Max-Dot) composition are the two most widely utilized inference processes in FLC (Ross, 2005). In this thesis, the Max-Algebraic Product (Max-Dot) composition method is used. The error $e(t)$ and change in error $ce(t)$ are the inputs, while the gains of PID controllers, $K_p,\ K_i,\ and\ K_d$ are the outputs

Max-Dot (Max-Product) Composition:

In this composition, the maximum of individual products is chosen in a fuzzy relation. Consider a system with two antecedents and three consequences for each rule. A collection of n linguistic IF- THEN rules describes a fuzzy system with two non-interactive inputs (antecedents) and three outputs (consequents). There are two inputs and three outputs in this case, resulting in nine linguistic IF-THEN rules for each of the gains $(K_p,\ K_i,\ K_d)$ with fuzzy sets (linguistic labels) and rule bases of N (Negative), Z (Zero), and P (Positive).

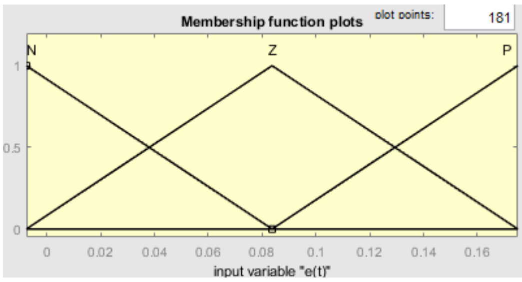

(a) Error - input to FLC.

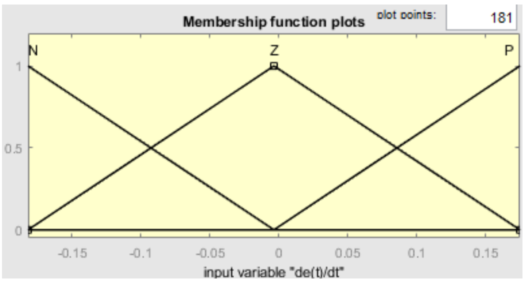

(b) Change in error - input to FLC.

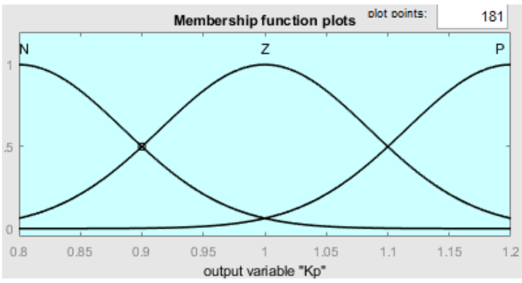

(c) Kp – Output of FLC.

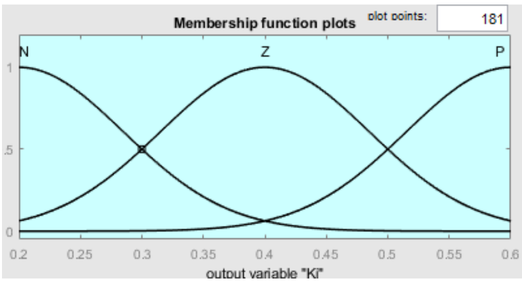

(d) Ki – Output of FLC.

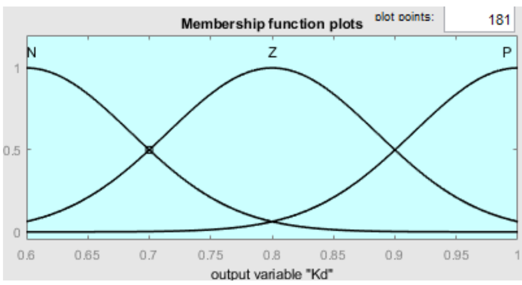

(e) Kd – Output of FLC.

Figure 4.5: Membership functions for input and output of FLC.

Fuzzy IF-THEN Rules are:

1. If ($e(t)$ is N) and ($de(t)/dt$ is N) then (K_p is Z)(K_i is Z)(K_d is Z)(1)
2. If ($e(t)$ is N) and ($de(t)/dt$ is Z) then (K_p is Z)(K_i is Z)(K_d is Z)(1)
3. If ($e(t)$ is N) and ($de(t)/dt$ is P) then (K_p is P)(K_i is P)(K_d is P)(1)
4. If ($e(t)$ is Z) and ($de(t)/dt$ is N) then (K_p is Z)(K_i is Z)(K_d is Z)(1)
5. If ($e(t)$ is Z) and ($de(t)/dt$ is Z) then (K_p is Z)(K_i is Z)(K_d is Z)(1)
6. If ($e(t)$ is Z) and ($de(t)/dt$ is P) then (K_p is P)(K_i is P)(K_d is P)(1)
7. If ($e(t)$ is P) and ($de(t)/dt$ is Z) then (K_p is P)(K_i is P)(K_d is P)(1)
8. If ($e(t)$ is P) and ($de(t)/dt$ is P) then (K_p is P)(K_i is P)(K_d is P)(1)

The rule base of the fuzzy logic controller is shown in the Table 4.1 where, the outputs are the gains of PID controller ($K_p,\ K_i,\ and\ K_d$).

Table 4.1: Rule-base for fuzzy logic controller.

e / ce	N	Z	P
N	Z	Z	P
Z	Z	Z	P
P	-	P	P

IV) Defuzzification

The defuzzification unit converts inferred fuzzy control actions into crisp control values that can be entered into the system process. The technique is the inverse of the fuzzification process in FLC. By transforming the fuzzy controller output fuzzy variables to a crisp actual signal, it changes a fuzzy quantity to a precise amount. Among the many strategies published in the literature in recent years for defuzzifying fuzzy output functions (membership functions), the centroid technique is presented here as one of many weighted average formulas in many forms.

The centroid method, also known as the center of area or center of gravity method (CoG), is the most frequent and simplest of all defuzzification techniques, and it can reflect overall inference information as illustrated in Figure 4.6. Where the algebraic expression is (Ross, 2005):

$$x^* = \frac{\sum \mu_x(x) * x}{\sum \mu_x(x)} \tag{4.15}$$

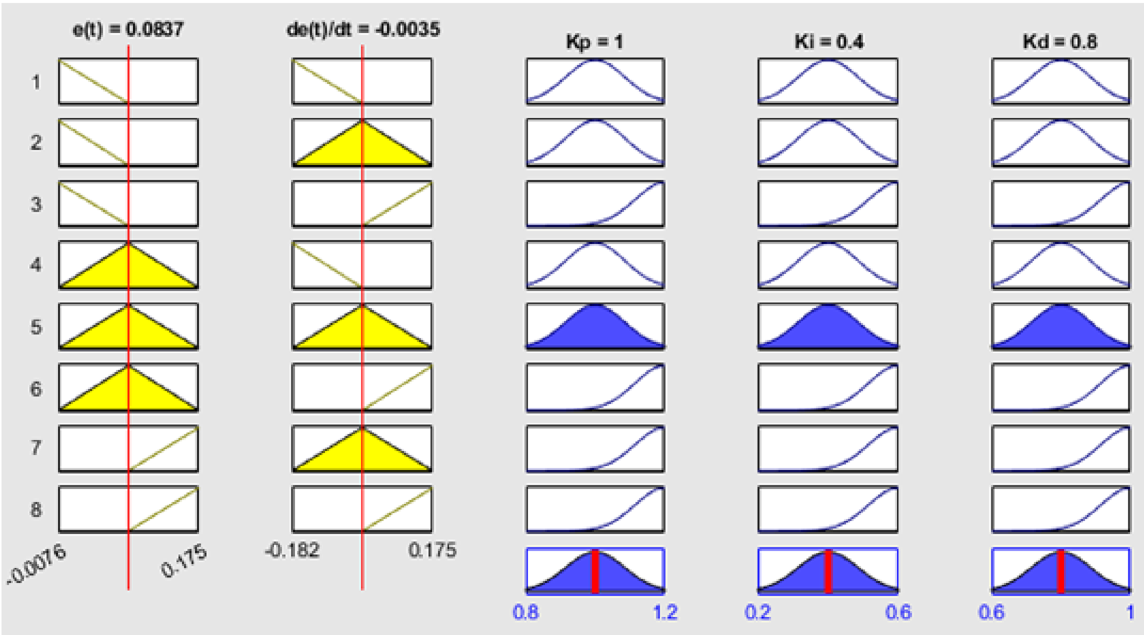

Figure 4.6: Output of fuzzy rule viewer.

Therefore, Figure 4.7 summarizes fuzzy logic process.

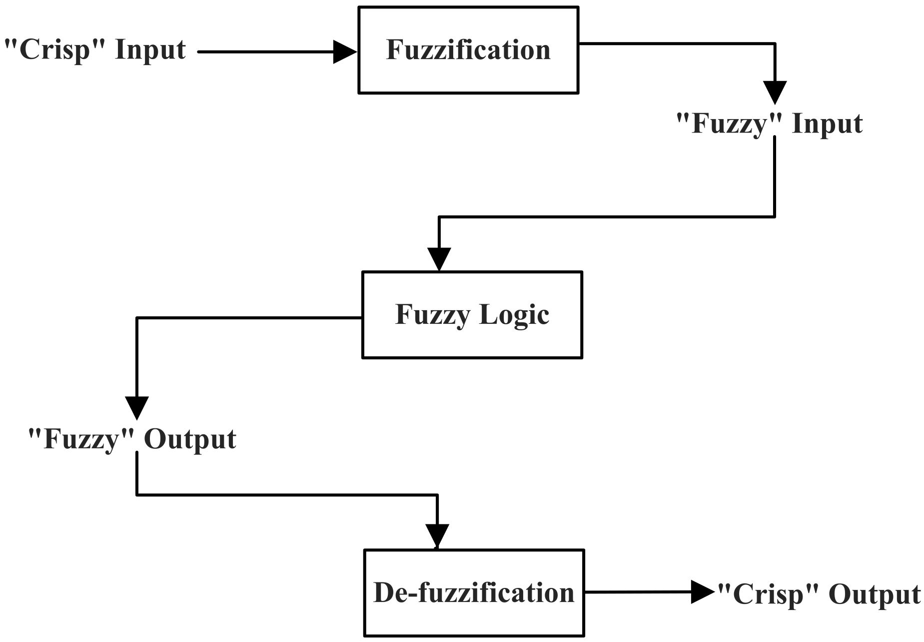

Figure 4.7: Fuzzy logic process.

The surface view of fuzzy rule of each of the output of FLC, which are the gains of

PID controller ($K_p,\ K_i,\ K_d$) are shown in the Appendix - 2, that is used to know how the output is changing based on the given input values.

The designed FPID control for the swing angle and position of the trolley is shown in the Figure 4.8.

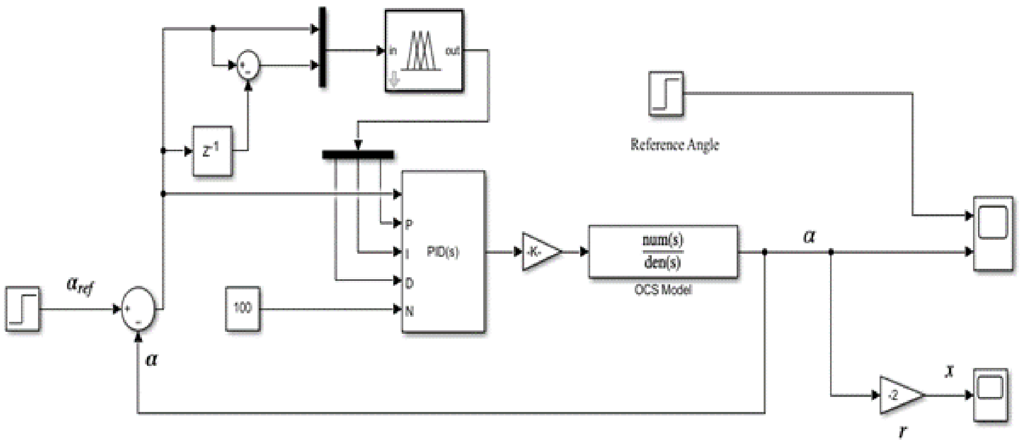

Figure 4.8: Simulink diagram of FPID controlled overhead crane system.

4.3.3 PSO Based PID Controller Design

Particle swarm optimization is one of optimization technique by Shi and Eberhart. They stated that the few parameters adjustment of PSO makes it widely used for optimizations. It was evaluated with a promising future application areas like product mix optimizations, human tremor analysis, and power system load stabilizations, since its introduction in 1995. It is developed and based on flock movement behavior of fish and bird and it is an optimization algorithm, a heuristic global optimization method. PSO is widely used for the requirement of few particles to be tuned and for its easy implementation.

With a new parameter called inertia weight, w, is added by Shi and Eberhart, this the modified version has become the commonly used PSO where the inertia weight decreases linearly with the iterations.

In PSO, each particle represents a potential solution to a problem in g- dimensional search space. The coordinate which linked to the best evaluation value of the particles has achieved so far is keep tracked and this value is called pbest. The other value which is being tracked is called gbest. gbest is the overall location and best value of any particle, obtained in the group.

Each of the particles in PSO adjusts its “flying” in the g-dimensional search space according to its own and companions “flying” experience with its own velocity. And at each time step (iteration), the particles update their location at every time step as they “fly” toward the pbest and gbest values (X. Zhang, Liu, & Tu, 2020).

The particles update their location at each particle toward its pbest and gbest locations at each iteration according to the following equations (Yusoff, Yahya, & Senawi, 2006), (Gopal, Sultani, & Bansal, 2020):

For PID controller parameter $K = [K_p, K_i, K_d]$ vector, the position vector is:

$$X_{ij}^{n+1} = [X_{1j}^{n+1} \;\; X_{2j}^{n+1} \;\; X_{3j}^{n+1}] = [K_{p,j}^{n+1} \;\; K_{ij}^{n+1} \;\; K_{dj}^{n+1}] \tag{4.16}$$

for i=1,2,3 is PID parameters

$j = j^{th}$ particle of N. Where, N is the total particles in i^{th} parameter.

$n = n^{th}$ iteration

Initial positions for $n + 1 = 0$ is:

$$X_{1j}^{0} = K_{p0}^{min} + (K_{p0}^{max} - K_{p0}^{min})^{*} r_{pj} \tag{4.17a}$$

$$X_{2j}^{0} = K_{i0}^{min} + (K_{i0}^{max} - K_{i0}^{min})^{*} r_{ij} \tag{4.17b}$$

$$X_{3j}^{0} = K_{d0}^{min} + (K_{d0}^{max} - K_{d0}^{min})^{*} r_{dj} \tag{4.17c}$$

For $K_p^{min} \leq K_p \leq K_p^{max},\; K_i^{min} \leq K_i \leq K_i^{max},\; and\;\; K_d^{min} \leq K_d \leq K_d^{max}$

$r_{pj},\; r_{ij},\; r_{dj}$ are random numbers for P,I,D parameters of PID controller to be generated.

$r_{pj},\; r_{ij},\; r_{dj}$ are on [0, 1].

$$X_j^0 = [X_{1,j}^0 \;\; X_{2,j}^0 \;\; X_{3,j}^0] \tag{4.18}$$

For j = 1,2,...,N iterations.

For example, at first iteration, j = 1,

$$X_1^0 = [X_{1,1}^0 \;\; X_{2,1}^0 \;\; X_{3,1}^0]$$

- **Vector Initialization:**

$$V_{1j}^{0} = x_{\frac{1j}{2}}^{0},\ \ V_{2j}^{0} = x_{\frac{2j}{2}}^{0},\ \ and\ \ V_{3j}^{0} = x_{\frac{3j}{2}}^{0} \tag{4.19}$$

- **Vector Update:**

$$V_j^{n+1} = V_{ij}^{n+1} = w^n v_{ij}^n + C_1^m r_1^n (p_{best\ ij}^n - x_{ij}^n) + c_2^m r_2^n ({G^n}_{ij} - x_{ij}^n) \tag{4.20}$$

For r_1 , r_2 are random on [0 1], and w_n = inertia weight $[W_{min}\ \ W_{max}] = [0.4\ \ 0.9]$.

$$X_{ij}^{n+1} = X_j^{n+1} = X_j^n + \Delta t V_j^n \tag{4.21}$$

i.e., $K_j^{n+1} = K_j^n + \Delta t V_j^n$

For Δt = time step, $C_1, C_2 = [1\ \ 2]$ which are cognitive and social factors.

Note: $W^n = (N - j)(W_{max} - Wmin) + W_{min}$ which means, at initial iteration,($j = 0$), $W^0 = 0.9$ and at $j = N, W^n = 0.4$.

The objective function to be optimized can be:

$$P(k) = \frac{1}{J(k)} \tag{4.22}$$

Where,

$$minJ(k) = min((1 - e^{-\beta})(M_p + e_{ss}) + e_{-\beta}(T_s - t_r) + IAE) \tag{4.23}$$

And,

$$IAE = \int_0^\infty |e(t)| dt \tag{4.24}$$

β = Wheighting factors and $\beta > 0.7$ to reduce M_p and E_{ss}, $\beta < 0.7$ to reduce T_s and T_r.

k = array control parameters $(K_p,\ K_i,\ K_d)$ for PID (Azmi, Yahya, Fu, & Yusoff, 2019). And, e_{ss} = Steady state error

M_p = overshoot

T_s = setting time

t_r = raise time

At j-particle, and iteration n+1, we have position of parameters:

$$\begin{bmatrix} K_{pj}^{n+1} \\ K_{ij}^{n+1} \\ K_{dj}^{n+1} \end{bmatrix} = \begin{bmatrix} K_{pj}^{n} \\ K_{ij}^{n} \\ K_{dj}^{n} \end{bmatrix} + \triangle t \begin{bmatrix} V_{pj}^{n+1} \\ V_{ij}^{n+1} \\ V_{dj}^{n+1} \end{bmatrix} \tag{4.25}$$

For the cost function evaluation:

$$\begin{bmatrix} V_{pj}^{n+1} \\ V_{ij}^{n+1} \\ V_{dj}^{n+1} \end{bmatrix} = \begin{bmatrix} V_{pj}^{n} & P_{bpj}^{n} - K_{pj}^{n} & G_{bpj}^{n} - K_{pj}^{n} \\ V_{ij}^{n} & P_{bij}^{n} - K_{ij}^{n} & G_{bij}^{n} - K_{ij}^{n} \\ V_{dj}^{n} & P_{bdj}^{n} - K_{dj}^{n} & G_{bdj}^{n} - K_{dj}^{n} \end{bmatrix} \begin{bmatrix} W^{n} \\ C_1^n r_1^n \\ C_2^n r_2^n \end{bmatrix} \tag{4.26}$$

And the output of the considered plant will be evaluated at each vector $(K_{pj}^n,\ K_{ij}^n,\ K_{dj}^n)$ and compared with the reference value to generate the error, which is the difference between the output (measured) and the reference (desired) value.

For instance, if we have 5 particles of populations on each individual parameter. i.e.,

$$\begin{aligned} K_p &= K_{p1}K_{p2}K_{p3}K_{p4}K_{p5} \\ K_i &= K_{i1}K_{i2}K_{i3}K_{i4}K_{i5} \\ K_d &= K_{d1}K_{d2}K_{d3}K_{d4}K_{d5} \end{aligned}$$

With velocity of each particles as:

$$\begin{aligned} V_p &= V_{p1}V_{p2}V_{p3}V_{p4}V_{p5} \\ V_i &= V_{i1}V_{i2}V_{i3}V_{i4}V_{i5} \\ V_d &= V_{d1}V_{d2}V_{d3}V_{d4}V_{d5} \end{aligned}$$

For 1^{st} iteration (j=1) with initials are known,

$$\begin{bmatrix} V_{p1}^1 \\ V_{i1}^1 \\ V_{d1}^1 \end{bmatrix} = \begin{bmatrix} V_{p1}^0 & P_{bp1}^0 - K_{p1}^0 & G_{bp1}^0 - K_{p0}^0 \\ V_{i1}^0 & P_{bi0}^0 - K_{i0}^0 & G_{bi0}^0 - K_{i0}^0 \\ V_{d1}^0 & P_{bd1}^0 - K_{d1}^0 & G_{bd1}^0 - K_{d1}^0 \end{bmatrix} \begin{bmatrix} W^n \\ C_1^0 r_1^0 \\ C_2^0 r_2^0 \end{bmatrix} \tag{4.27}$$

So that,

$$\begin{bmatrix} K_{pj}^1 \\ K_{ij}^1 \\ K_{dj}^1 \end{bmatrix} = \begin{bmatrix} K_{p1}^0 \\ K_{i1}^0 \\ K_{d1}^0 \end{bmatrix} + \triangle t \begin{bmatrix} V_{p1}^0 \\ V_{i1}^0 \\ V_{d1}^0 \end{bmatrix} \tag{4.28}$$

The cost function is evaluated using values of vector $[K_{p1}^1 \quad K_{i1}^1 \quad K_{d1}^1]$.

And all the position and velocity are evaluated for all particles and the iteration is repeated until the parameters/positions of each will be converged.

The flow-chart of PSO-PID is shown in the Figure 4.9 (Chiou et al., 2012). And the Control parameters for the PSO algorithm to tune the PID controller are presented in the Table 4.2

.

Table 4.2: Parameters of PSO-PID.

Parameter	Value
Population size	1000
Max. number of Iterations	100
Number of variables	3
w	[0.4 0.8]
C_1	0.2
C_2	0.6
Lower Bound	$[-280 - 30 - 500]$
Upper Bound	$[-250 - 5 - 200]$

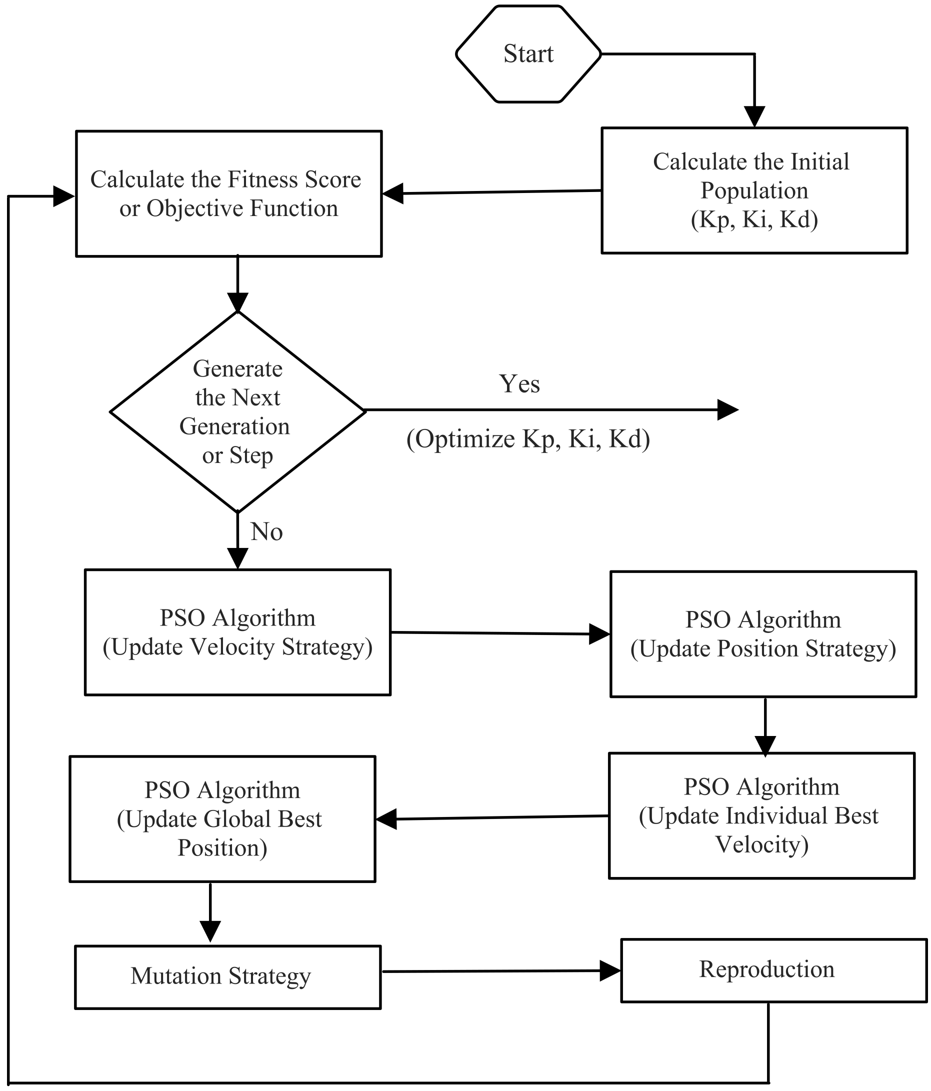

Figure 4.9: A flow-chart of PSO-PID strategy.(Chiou et al., 2012)

4.4 PI-Regulator Design

As its name indicates, PI-Controller is the combination of the proportional controller and the integral controller. Which in turn means, it controls the system to the desired value by reducing the error value as combination of the error signal and the integral of the error signal. With its characteristics, reducing the steady state error, without affecting the stability of the system. Where, PI-Regulator is designed for an overhead crane system for its unique characteristics to allow the system to quickly eliminate the effects of load or disturbance and to ensure that the output quickly matches the setpoint, in this case, the desired amount of swing angle.

A closed loop control system is a feedback control loop that calculates an error signal by taking the difference between the output of a system and the desired (reference) value, in this case it is the swing angle of the load of the overhead crane system, and the desired angle with required set points.

Referring to the Equation (3.23) which relates the swing angle $\alpha(s)$ to the DC motor input voltage $V_a(s)$ and, assuming the system is controllable and all state variables fed back:

$$\frac{\alpha(s)}{V_a(s)} = \frac{1}{(b_1 - ra_1)s^3 + (b_2 - ra_2)s^2 - ra_3 s}$$

Taking simple relations for simplicity:- i.e.,

$$r_1 = b_1 - ra_1 \tag{4.29a}$$

$$r_2 = b_2 - ra_2 \tag{4.29b}$$

$$r_3 = -ra_3 \tag{4.29c}$$

$$\frac{\alpha(s)}{V_a(s)} = \frac{1}{r_1 s^3 + r_2 s^2 + r_3 s} \tag{4.30}$$

Then, the PI- Regulator block diagram is described in the Figure 4.10. It has both forward path block and feedback path block. It includes the input, which is the reference angle; the summation block, which subtracts the feedback(output) value from the reference value, or the desired swing angle value; input voltage, that is armature input voltage applied to the system; the plant, which is the overall system, obtained in the Equation (4.30); disturbance (d), that is any variable that may affect the control system output and increase the system error; the controller (PI in this case), that adjusts the system to the expected performance; and the output of the system, that is fed back to compare until the reference angle is equal to the output angle.

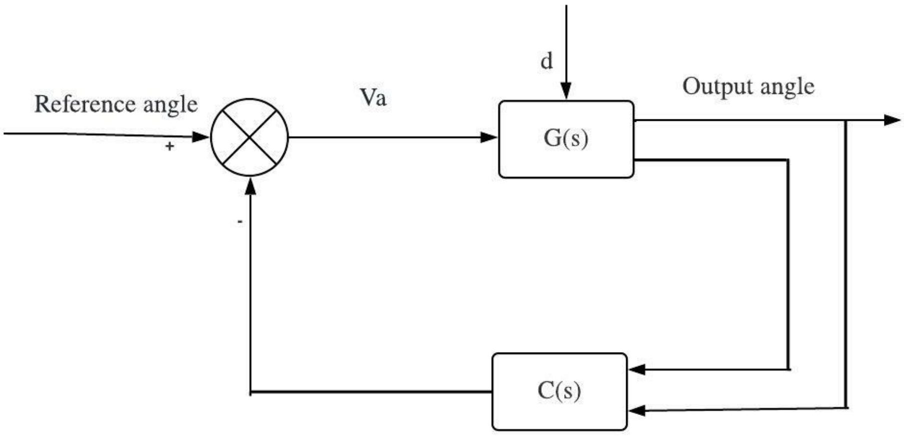

Figure 4.10: A general block diagram of PI regulator.

Representing the model in state-space representation, by considering zero disturbance (d = 0) it becomes:

$$r_1 \dddot{\alpha} + r_2\ddot{\alpha} + r_3\dot{\alpha} = V_a \tag{4.31}$$

Let $\dot{\alpha} = \dot{x_1} = x_2$, for $\alpha = x_1$ then, $\ddot{\alpha} = \ddot{x_1} = \dot{x_2} = x_3$

$$\dddot{\alpha} = \frac{1}{r_1}V_a - \frac{r_3}{r_1}x_2 - \frac{r_2}{r_1}x_3 \tag{4.32}$$

$$\dot{x} = \begin{bmatrix} 0 & 1 & 0 \\ 0 & 0 & 1 \\ 0 & -\frac{r_3}{r_1} & -\frac{r_2}{r_1} \end{bmatrix} \begin{bmatrix} x_1 \\ x_2 \\ x_3 \end{bmatrix} + \begin{bmatrix} 0 \\ 0 \\ \frac{1}{r_1} \end{bmatrix} V_a \tag{4.33}$$

$$= Ax + BV_a$$

$$\alpha = \begin{bmatrix} 1 & 0 & 0 \end{bmatrix} \begin{bmatrix} x_1 \\ x_2 \\ x_3 \end{bmatrix} + 0V_a \tag{4.34}$$

$$= Cx + DV_a$$

The PI Regulator can be realized as state feedback, as seen below:

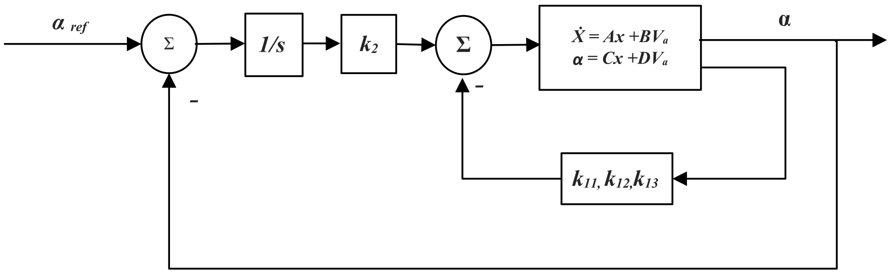

Figure 4.11: Block diagram of PI regulator as a state feedback.

Now, introducing a new state variable, z, to design a PI-Regulator,

$$z = \int \alpha dt$$

$$\dot{z} = \alpha = x_1 \tag{4.35}$$

Equation (4.34) describes a state-variable which determines the mathematical state of a general dynamical system and it is used to summarize the system in order to predict the future values or outputs. Therefore, it is used to get the state-space of the system, which is a set of possible combinations of state-variable values.

Combining Equations (4.33), (4.34), and (4.35), the augmented state equation is:

$$\dot{\tilde{x}} = \begin{bmatrix} \dot{x} \\ \dot{z} \end{bmatrix} = \left[\begin{array}{ccc|c} 0 & 1 & 0 & 0 \\ 0 & 0 & 1 & 0 \\ 0 & -\frac{r_3}{r_1} & -\frac{r_2}{r_1} & 0 \\ \hline 1 & 0 & 0 & 0 \end{array}\right] \begin{bmatrix} x_1 \\ x_2 \\ x_3 \\ z \end{bmatrix} + \left[\begin{array}{c} 0 \\ 0 \\ \frac{1}{r_1} \\ \hline 0 \end{array}\right] V_a \tag{4.36}$$

$$\dot{\tilde{x}} = \begin{bmatrix} A & 0 \\ C & 0 \end{bmatrix} \begin{bmatrix} x \\ z \end{bmatrix} + \begin{bmatrix} B \\ D \end{bmatrix} V_a$$

$$\dot{\tilde{x}} \cong \tilde{A}\tilde{x} + BV_a$$

$$\text{Where, } \tilde{A} = \left[\begin{array}{c|c} A & 0 \\ \hline C & 0 \end{array}\right],$$

$$\tilde{B} = \begin{bmatrix} B \\ \hline D \end{bmatrix} \text{ and}$$

$$\tilde{x} = [x \;\; z]^T = \begin{bmatrix} x \\ z \end{bmatrix}$$

And the output equation becomes:

$$\alpha = [C \quad 0] \begin{bmatrix} x \\ z \end{bmatrix} + DV_a \tag{4.37}$$

Now, from the control theory, the state $x(t)$ will be controllable at $t = t_0$ when there exists a piecewise continuous input$u(t)$ which will drive the state to any final state x(t) for a finite interval $(t - t_0) \geq 0$. And the system is called controllable if every state of the system is controllable in a finite interval (SmarajitGhosh, n.d.). Therefore, the original system's pair (A, B) is controllable and hence, $(\tilde{A}, \tilde{B})$ is also controllable. Therefore, the proportional-integral (PI) type Regulator takes the form:-

$$V_\alpha = -\tilde{k}\tilde{x} = -[k_1 \quad k_2] \begin{bmatrix} x \\ z \end{bmatrix}$$

$$V_\alpha = -k_{11}x_1 - k_{12}x_2 - k_{13}x_3 - k_2 \int \alpha dt \tag{4.38}$$

The gain matrix $\tilde{k} = [k_{11} \quad k_{12} \quad k_{13} \quad k_2]$ is to be computed at a specified closed-loop transfer function stable pole's location.

From pole placement or pole-assignment theory, assuming that all state variables are measurable and available for feedback and the system considered is completely state controllable, the poles of the closed-loop system may be placed at any desired locations by means of state feedback through an appropriate state feedback gain (Ogata et al., 2010). In this case, the open-loop system has three poles, and the PI-Controller contributes one pole. Hence the poles of the closed-loop system become four. Let, -1, -2, $-(2 \pm j2)$ Therefore, the equivalent augmented system characteristic equation is obtained as:

$$\Delta(s) = |SI - \tilde{a} + \tilde{B}\tilde{k}| \tag{4.39}$$

$$\Delta(s) \quad = \quad (s+1)(s+2)(s+2+j2)(s+2-j2) \tag{4.40}$$

$$\Delta(s) = s^4 + 7s^3 + 22s^2 32s + 16 \tag{4.41}$$

Where,

$$|SI - \tilde{A} + \tilde{B}\tilde{k}| \equiv \left| \begin{bmatrix} s & 0 & 0 & 0 \\ 0 & s & 0 & 0 \\ 0 & 0 & s & 0 \\ 0 & 0 & 0 & s \end{bmatrix} - \begin{bmatrix} 0 & 1 & 0 & 0 \\ 0 & 0 & 1 & 0 \\ 0 & -\frac{r_3}{r_1} & -\frac{r_2}{r_1} & 0 \\ 1 & 0 & 0 & 0 \end{bmatrix} + \begin{bmatrix} 0 \\ 0 \\ \frac{1}{r_1} \\ 0 \end{bmatrix} [k_{11} \ k_{12} \ k_{13} \ k_2] \right|$$

$$|SI - \tilde{A} + \tilde{B}\tilde{k}| \equiv \begin{vmatrix} s & -1 & 0 & 0 \\ 0 & s & -1 & 0 \\ \frac{1}{r_1}k_{11} & \frac{r_3}{r_1} + \frac{1}{r_1}k_{12} & s + \frac{r_2}{r_1} + \frac{1}{r_1}k_{13} & \frac{1}{r_1}k_2 \\ -1 & 0 & 0 & s \end{vmatrix}$$

$$|SI - \tilde{A} + \tilde{B}\tilde{k}| \equiv s^4 + (\frac{r_2 + k_{13}}{r_1})s^3 + (\frac{r_3 + k_{12}}{r_1})s^2 + (\frac{k_{11}}{r_1})s + \frac{1}{r_1}k_2 \tag{4.42}$$

Equating Equations (4.40) and (4.41) to prove Equation (4.39), and to get the constants value:-

$$\Delta(s) = |SI - \tilde{A} + \tilde{B}\tilde{k}| \tag{4.43}$$

$$s^4 + 7s^3 + 22s^2 + 32s + 16 = s^4 + (\frac{r_2 + k_{13}}{r_1})s^3 + (\frac{r_3 + k_{12}}{r_1})s^2 + (\frac{k_{11}}{r_1})s + \frac{1}{r_1}k_2$$

Therefore, equating similar coefficients, the constants values are obtained.

$$\frac{r_2 + k_{13}}{r_1} = 7 \tag{4.44a}$$
$$\frac{r_3 + k_{12}}{r_1} = 22 \tag{4.44b}$$
$$\frac{k_{11}}{r_1} = 32 \tag{4.44c}$$
$$\frac{k_2}{r_1} = 16 \tag{4.44d}$$

By substituting the values of constants $r_1,\ r_2\ and\ r_3$ from Equation (4.29a) to (4.29c), the values of k constants obtained are:

$$k_{11} = -1.072 \tag{4.45a}$$
$$k_{12} = 3.1944 \tag{4.45b}$$
$$k_{13} = 73.4655 \tag{4.45c}$$
$$k_2 = -0.536 \tag{4.45d}$$

Now, it is noted that, by substituting the values of constants, $r_1,\ r_2\ and\ r_3$ the feedback gains, $k_{11},\ k_{12},\ k_{13},\ and\ k_2$ of PI-Regulator are computed. Realizing the function C(s) in PI – Controller and by simulating the system, the overall response is checked and it is regulated to zero.

The numerical values of constants in Equation (4.29a) to (4.29c) are obtained by substituting Equation (3.26) and referring to the Table 3.2 as:

$$r_1 = -0.0335 \tag{4.46a}$$
$$r_2 = -73.7 \tag{4.46b}$$
$$r_3 = -3.9314 \tag{4.46c}$$
$$-\frac{r_3}{r_1} = -117.3552 \tag{4.46d}$$
$$-\frac{r_2}{r_1} = -2200 \tag{4.46e}$$
$$\frac{1}{r_1} = -29.8507 \tag{4.46f}$$

Therefore, by substituting the values of constants from Equation (4.45a) to (4.45d), the augmented state equation becomes:

$$\dot{\hat{x}} = \begin{bmatrix} 0 & 1 & 0 & 0 \\ 0 & 0 & 1 & 0 \\ 1 & -117.3552 & -2200 & 0 \\ 1 & 0 & 0 & 0 \end{bmatrix} x + \begin{bmatrix} 0 \\ 0 \\ -29.8507 \\ 0 \end{bmatrix} V_a \tag{4.47}$$

Therefore, the overall block diagram of state feedback as PI Regulator is shown in the Figure 4.12. Where,

$$A = \begin{bmatrix} 0 & 1 & 0 \\ 0 & 0 & 1 \\ 0 & -\frac{r_3}{r_1} & -\frac{r_2}{r_1} \end{bmatrix} = \begin{bmatrix} 0 & 1 & 0 \\ 0 & 0 & 1 \\ 0 & -117.3552 & -2200 \end{bmatrix} \tag{4.48}$$

$$B = \begin{bmatrix} 0 \\ 0 \\ \frac{1}{r_1} \\ 0 \end{bmatrix} = \begin{bmatrix} 0 \\ 0 \\ -29.8507 \\ 0 \end{bmatrix} \tag{4.49}$$

$$C = [1 \quad 0 \quad 0] \quad And, \tag{4.50}$$

$$D = 0 \tag{4.51}$$

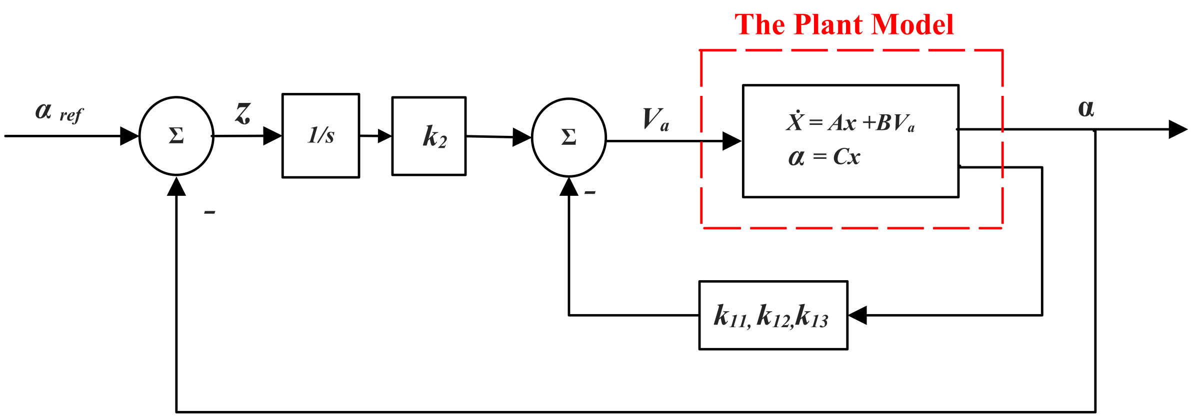

Figure 4.12: The overall block diagram of PI Regulator as a state feedback.

4.4.1 Initial Parameter Uncertainty

As the overhead crane system is designed to lift and transport different amount of mass, it is desired to the robustness of the designed controllers by varying the amount of payload. In this thesis, the nominal value of the payload is considered as 6 kg and the robustness of the designed controllers is tested by varying the amount of payload to 10 kg and 12 kg keeping all other parameters. Therefore, there are two cases:

- ***Case 1***: When the load mass is 10 kg:

At 10 kg value of the load mass swing angle to input armature voltage open-loop transfer function (OLTF) of the system becomes:

$$\frac{\alpha(s)}{V_a(s)} = \frac{-1}{0.0335s^3 + 73.7005s^2 + 3.004s} \tag{4.52}$$

The gains of PI-Regulator for this case are:

$$\begin{aligned} k_{11} &= -1.072 \\ k_{12} &= 2.2634 \\ k_{13} &= 73.466 \\ k_2 &= -0.536 \\ -\frac{r_3}{r_1} &= -89.5642 \\ -\frac{r_2}{r_1} &= -2200.02 \\ \frac{1}{r_1} &= -2985075 \end{aligned}$$

- ***Case 2***: When the load mass is 12 kg:

At 12 kg of the payload, the swing angle to input armature voltage open-loop transfer function (OLTF) of the system becomes:

$$\frac{\alpha(s)}{V_a(s)} = \frac{-1}{0.033501s^3 + 73.7005s^2 + 3.00424s} \tag{4.53}$$

The gains of PI-Regulator for this case are:

$$
\begin{aligned}
k_{11} &= -1.072032 \\
k_{12} &= 2.2634 \\
k_{13} &= 73.466 \\
k_{2} &= -0.53602 \\
-\frac{r_3}{r_1} &= -89.5622 \\
-\frac{r_2}{r_1} &= -2199.9493 \\
\frac{1}{r_1} &= -29.8499
\end{aligned}
$$

Therefore, using the Simulink model, the performance and robustness of designed controller is tested with different cases. First, the performance of controllers is checked by adding disturbance to the system. Then, the robustness of designed controllers is tested by initial parameter variation, the payload mass in this case. Finally, by changing the desired maximum swing angle, the response of controllers is checked and evaluated in each case. The reader can see the Simulink models of each case in the appendix-3. The result of each response is compared and their respective discussions are held in the next chapter.

CHAPTER FIVE

RESULT AND ANALYSIS

5.1 Introduction

In this chapter, the results of each of the designed controllers and discussions on each of the obtained responses are presented. The validity and stabilization of the controllers for overhead crane system dynamics are simulated using MATLAB/Simulink environment. The performance of the controllers is tested for an anti-swing angle angle and the trolley position in the presence of disturbances and the given controller performance is evaluated and analyzed using MATLAB/Simulink. MATLAB/Simulink is used as a simulation platform and all the exercises were conducted with Intel Core i5 Processor, 2.7 GHz and 8 GB RAM system specifications; with Windows 11 computer.

The overhead crane system starts to move from zero degree, or zero radian, relative to the vertical axis, and then lift up and drop down vertically or moves the load from one place to the other, horizontally, with some swing of the load mass relative to the trolley position, either until it reaches again zero degree on the air or until the load reaches the desired place. The overhead crane system in this thesis is expected to operate and maintain the load mass without any swing angle, and in some special cases, with a small swing relative to the trolley position, up to a maximum displacement of 0.35 m from rest. The position of trolley with respect to the maintained swing angle is obtained from the relation between the swing angle and trolley position in the system modelling (The reader can refer to Equation (3.22)). Therefore, the controller performance and robustness is tested for both the load swing angle and the trolley position respectively.

Disturbance added to the plant is considered as non-smooth input voltage value. Assuming the overhead crane system is under the variation of voltage value, which can result from the fluctuation of the supply, or any reasons, which may affect the smooth flow of voltage.

The amount of disturbance is considered as 0.1 V, 1 V, 2.5 V, and 5 V in increasing amount of the voltage. Where, each of considered distrubance amount is taken as 1 V, 10 V, 25 V, and 50 V in MATLAB/Simulink considering with a factor of 10^{-1}. The varying amount of voltage is added as a disturbance to test the robustness of designed controllers for overhead crane system. And the parameter uncertainty is taken as the payload mass variation at 6 kg (nominal value), 10 kg, and 12 kg respectively.

5.2 System Performance with PID Controller

The PID Controller parameters from Figure 4.2 is as shown in the Simulink block diagram of Figure 5.1. Then, the system performance with PID controller with analytically tuned PID parameters is shown in the Figure 5.1, and Figure 5.2 for swing angle and in the Figure 5.3 for the trolley position with the different mount of desired swing angle respectively.

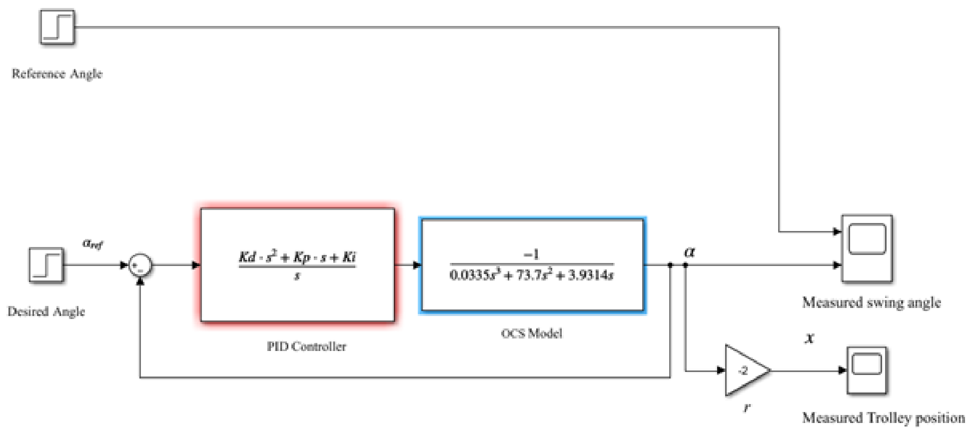

Figure 5.1: The Simulink diagram of overhead crane system with PID controller.

For the Figure above, the PID parameters are the obtained gains in pole placement method and the plant transfer function is the system model obtained, which is done in the chapter three. The Simulink output response for the two cases is shown in Figure 5.2 and Figure 5.3, for swing angle in two cases. Where, the former is when the desired swing angle is 10 degree (0.175 radian) at maximum and Figure 5.3 is when there is no swing at all. Figure 5.4 shows the response of system trolley position when the required amount of swing is 10 degree and 0 degree.

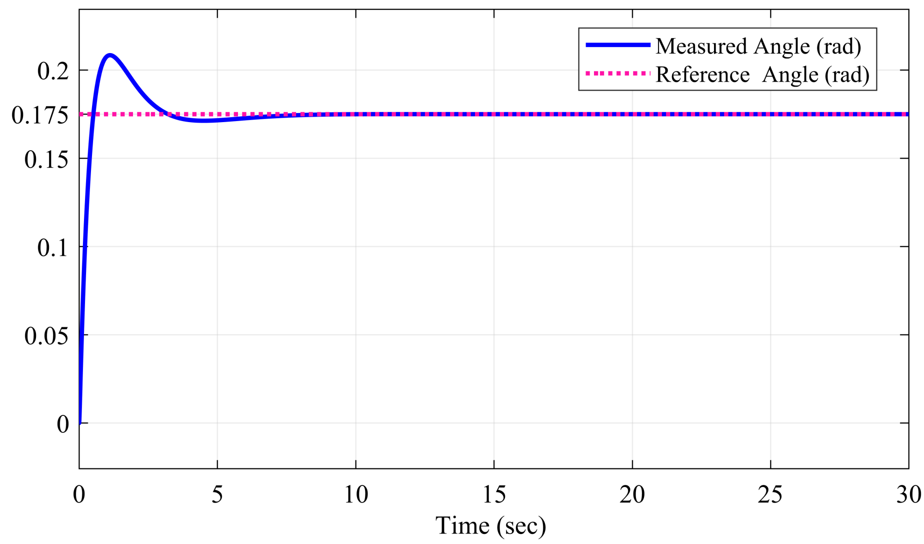

Figure 5.2: System performance of swing angle with PID controller at maximum swing of 10 degree

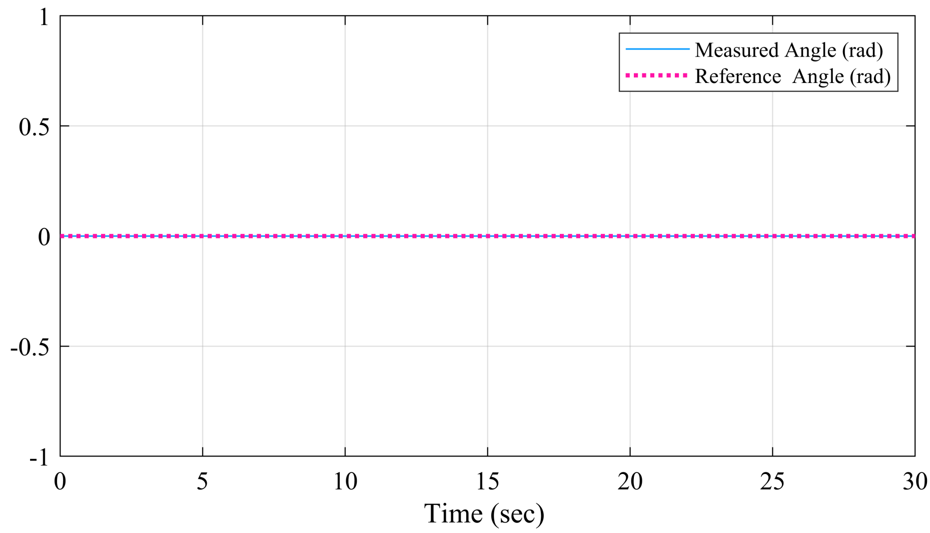

Figure 5.3: System performance of trolley position with PID controller at maximum swing of 10 degree

As seen from the output response, the stability is maintained by keeping the bounds of the gains value in the CLTF. Similarly, the response of trolley position obtained in similar two cases is described in Figure 5.4.

Note that, the position of trolley represents the maximum distance of the trolley from the start of the movement until the required amount of angle swing is reached. And the relation between the swing angle and trolley position is obtained in Equation (3.22).

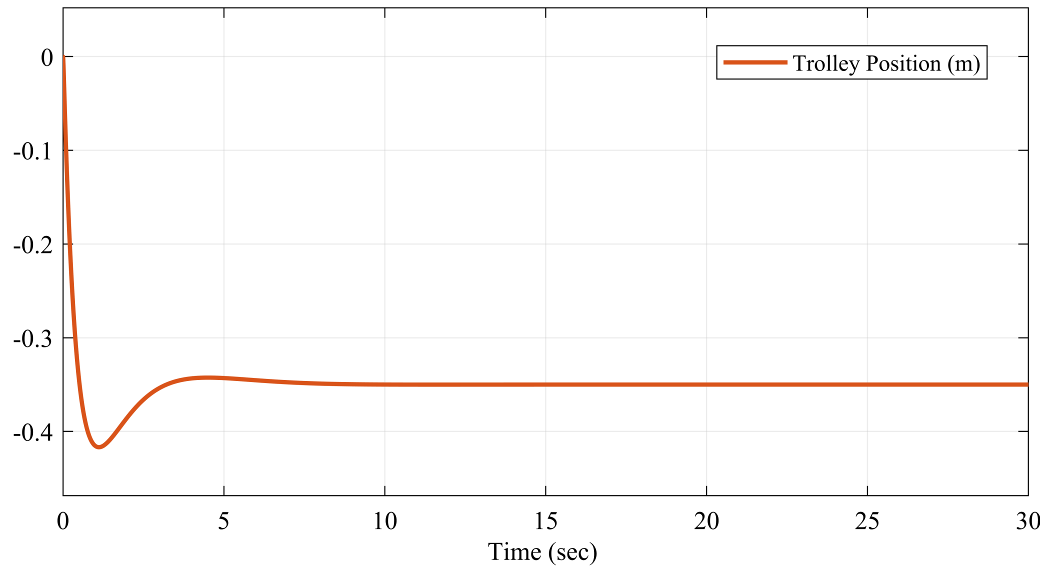

(*a*) *When the desired swing angle is* 0.175 *radian at maximum.*

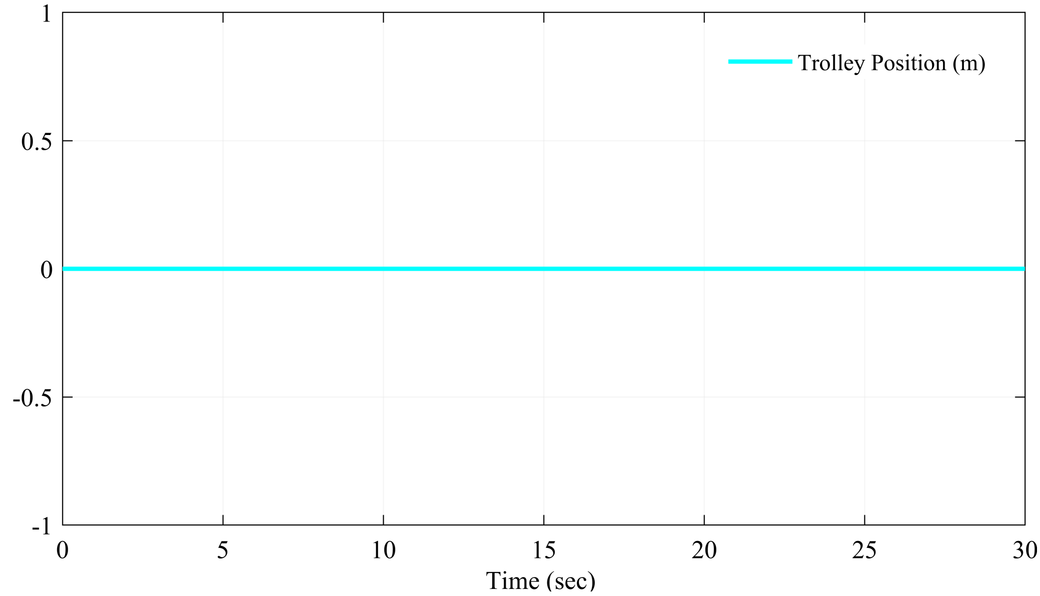

(*b*) *When the desired swing angle is* 0 *radian*

Figure 5.4: The trolley position response of a system for PID controller under different desired swing.

Also, by considering disturbances the system response is described in Figure 5.5, where different amount of disturbances are added to test the performance of the PID controller. As seen from the responses of each case, either above or below the desired values, the designed controller performed well and the desired set values are reached before 7 sec for both the swing angle and trolley position cases.

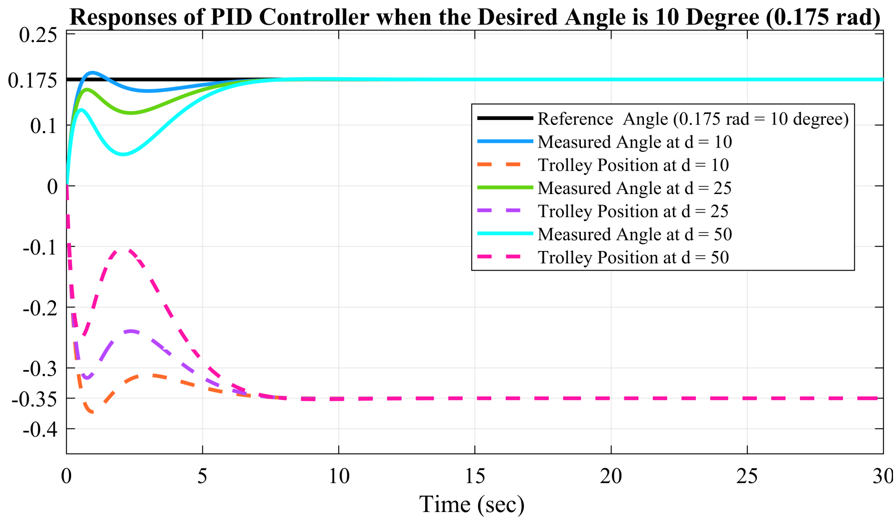

(a) *When the desired swing angle is* 0.175 *radian at maximum.*

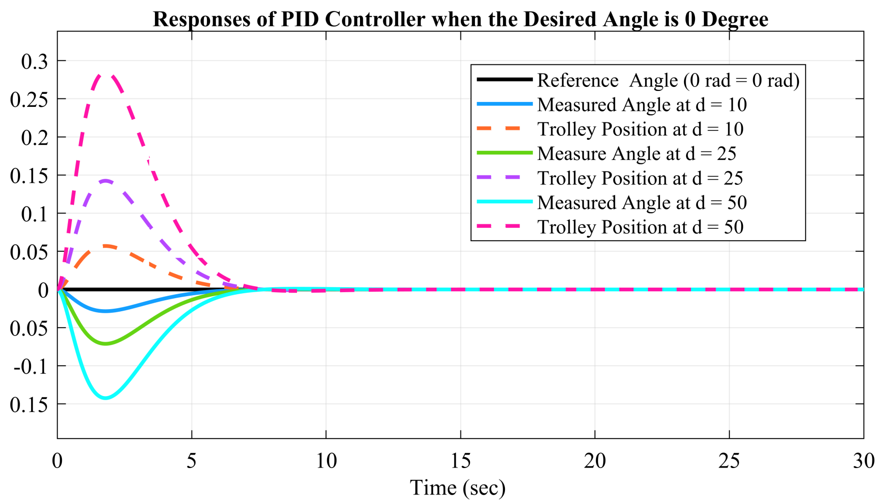

(b) *When the desired swing angle is* 0 *radian, ornoswingatall.*

Figure 5.5: PID controller performance for swing angle and trolley position with different amount of disturbances.

5.3 System Performance with Fuzzy-PID Controller

The performance of a system with PID controller is shown with and without disturbance to the plant. Now, in FPID responses it is expected to get better responses than conventional PID controller. Figure 5.6 shows the responses of FPID for the swing angle and trolley position when the desired angle is 10 degree at maximum and Figure 5.7 shows the response of FPID when there is no swing at all.

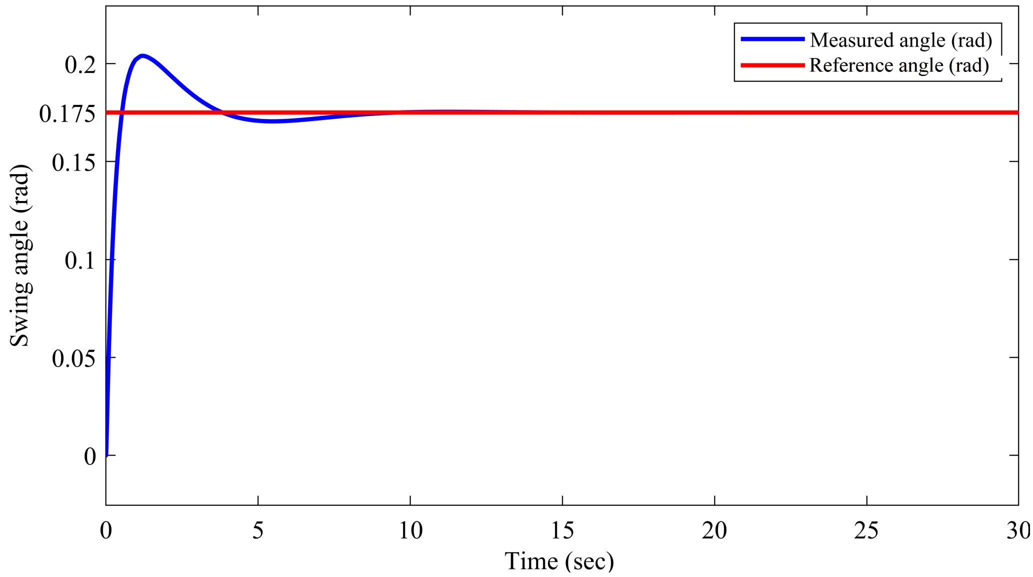

(a) *Swing angle.*

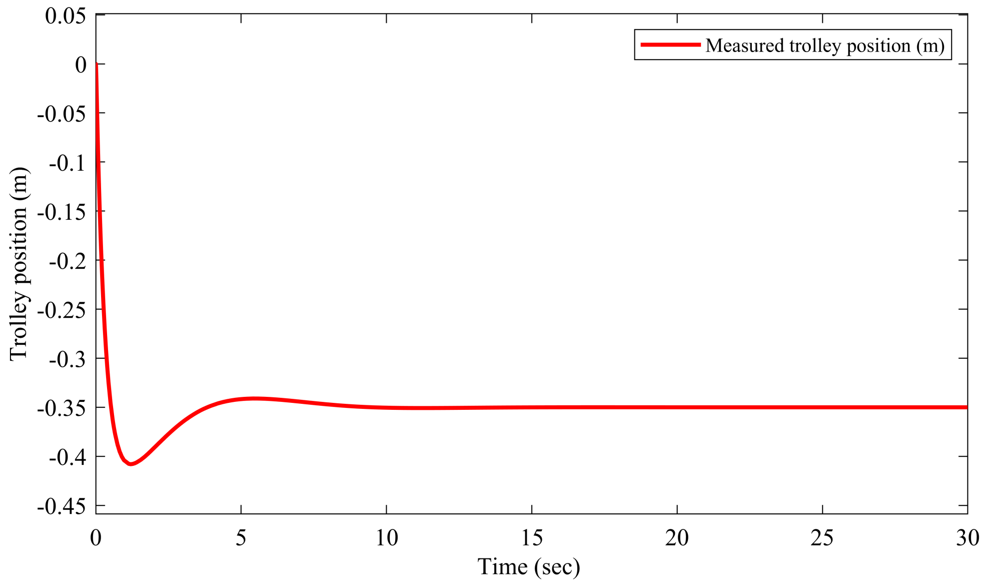

(b) *The trolley position.*

Figure 5.6: FPID controller performance at maximum of 10degree swing.

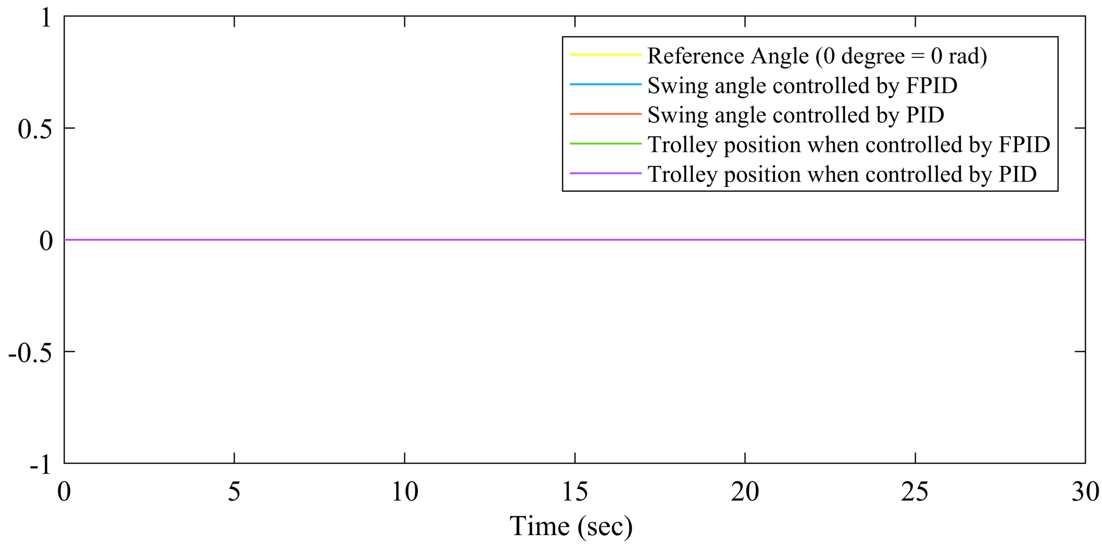

Figure 5.7: FPID controller performance for both swing angle and trolley position.

Similarly, FPID angle responses and trolley position responses with different amount of disturbances when the swing angle is 10 degree at maximum is shown in Figure 5.8 and Figure 5.9.

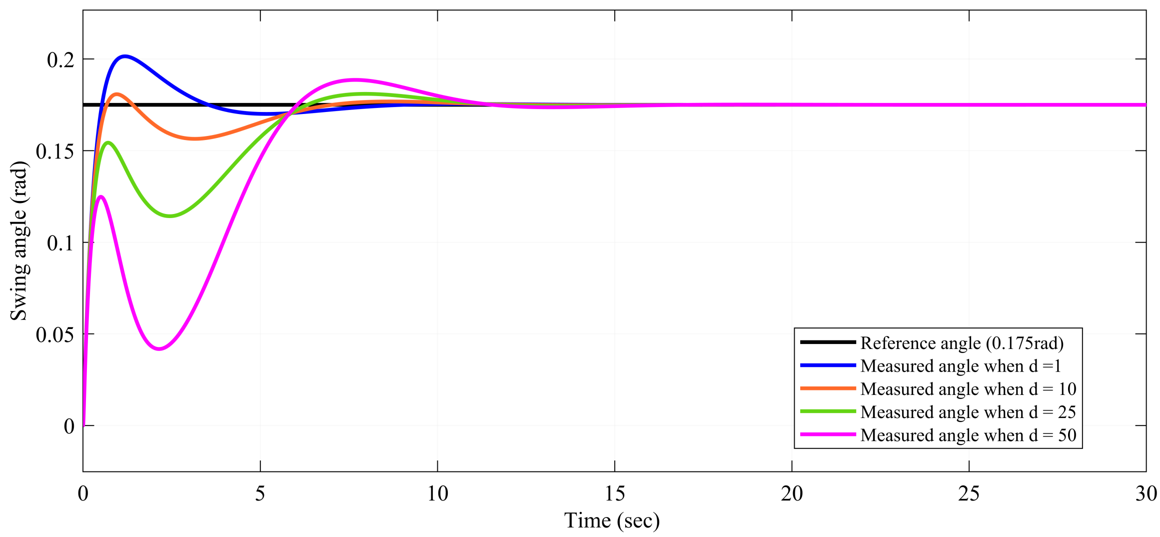

Figure 5.8: System performance of swing angle with FPID controller at maximum of 10 degree swing and different amount of disturbances.

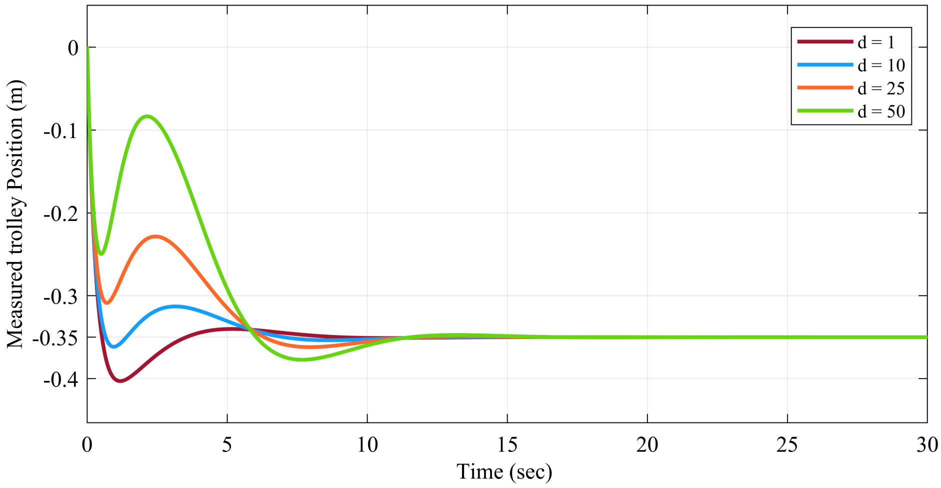

Figure 5.9: System performance of trolley position with FPID controller at maximum of 10 degree swing and different amount of disturbances.

FPID Angle and Position Responses with different disturbance values when there is no swing at all (0-degree of swing angle) is shown in Figure 5.10. where, as seen from the responses, when the amount of disturbance increases, overshoot for the trolley position increases. However, both the swing angle and trolley position attained their desired value with in less than 1 seconds. This validates the robustness of controller.

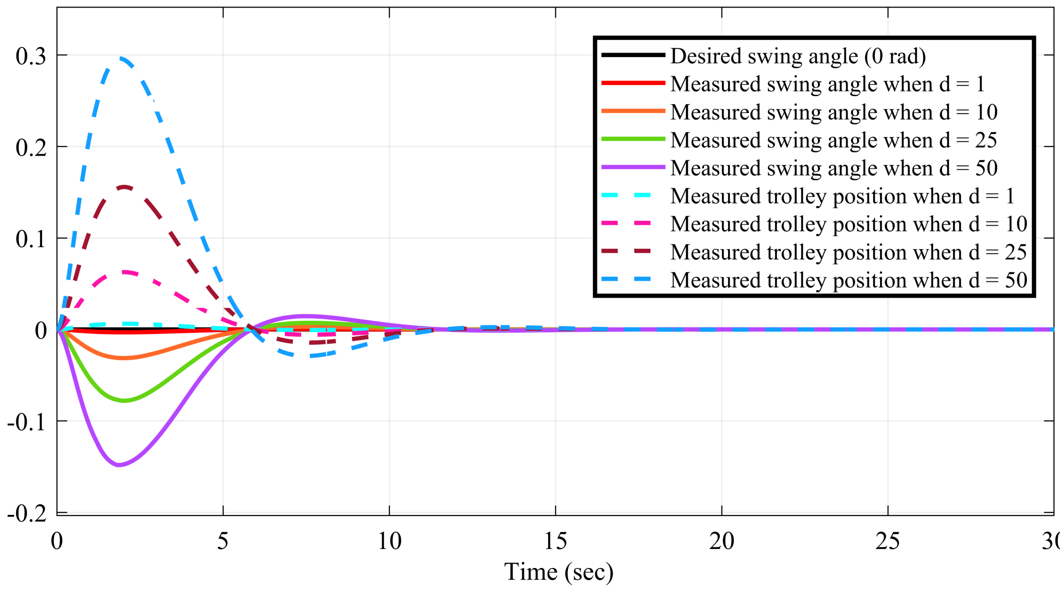

Figure 5.10: FPID controller performance for both swing angle and trolley position at 0 degree desired angle

The performance comparison of FPID and PID at maximum of 10 degree load swing without disturbance:

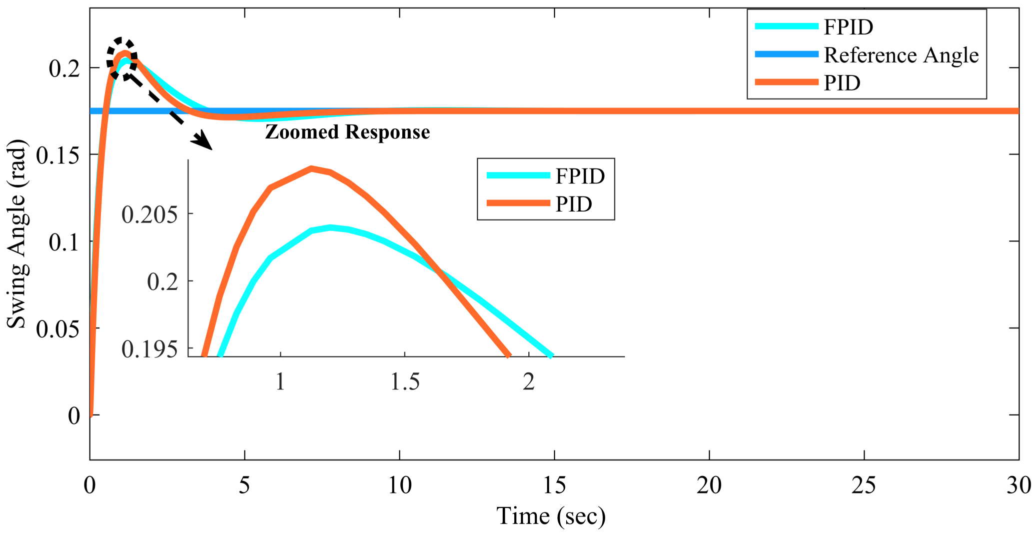

Figure 5.11: Performance comparison of PID and FPID controller for maximum swing angleof 10 degree

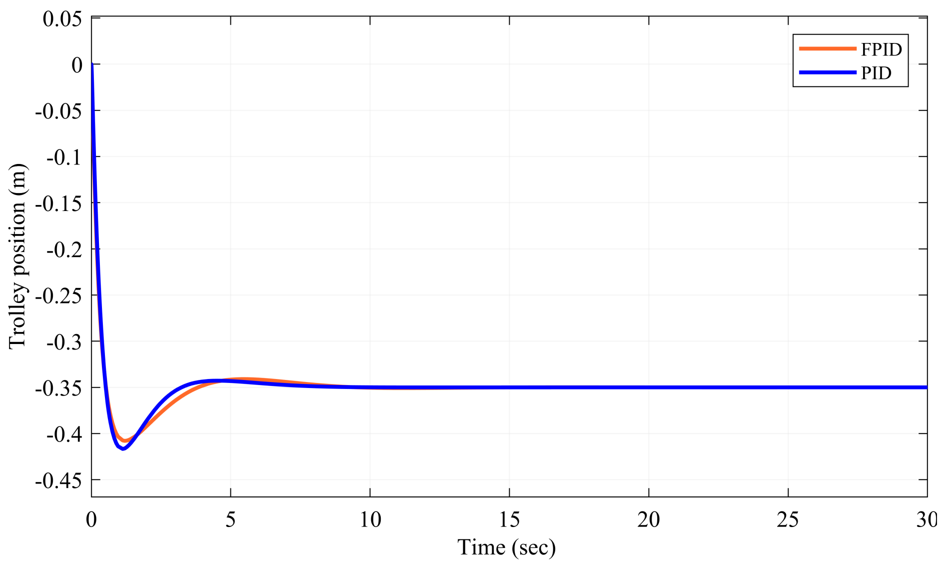

Figure 5.12: Performance comparison of PID and FPID controller for maximum swing angle of 10 degree.

As seen from the Figure 5.11 and Figure 5.12, the responses of the desired maximum swing angle and trolley position is attained with a better performance for fuzzy PID controller.

The performance comparison of FPID and PID at maximum of 10 degree load swing with disturbance:

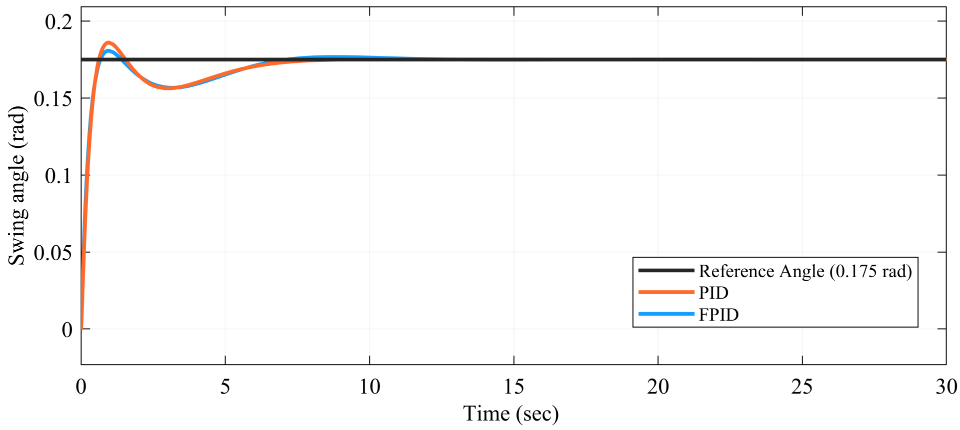

Figure 5.13: System performance of swing angle with FPID and PID controller at maximum of 10 degree swing and with disturbance.

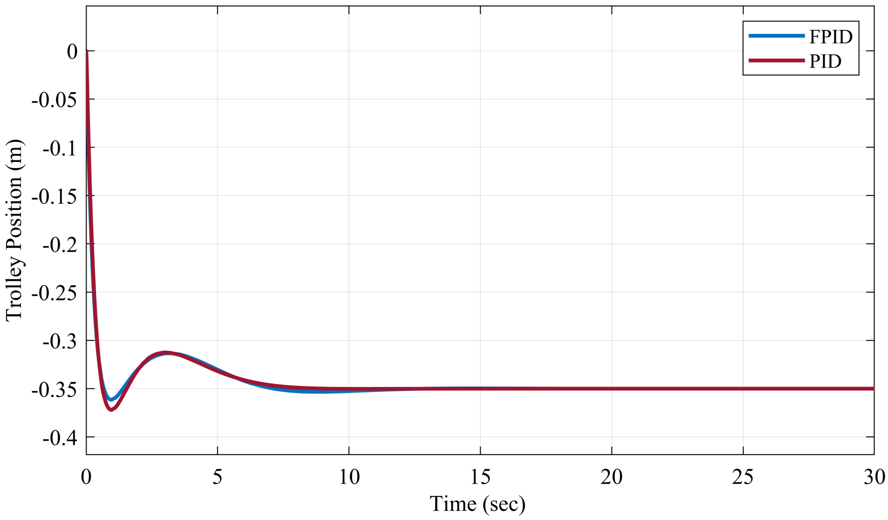

Figure 5.14: System performance of trolley position with FPID and PID controller at maximum of 10 degree swing and with disturbance.

Similarly, the swing angle and position of trolley is maintained at the desired positions with a better performance with FPID controller even with disturbance added to system as seen in the figures above.

5.4 System Performance with PSO-PID Controller

Based on the PSO tunning technique and the parameters for PSO presented in chapter four, the tunned gains are shown in the Table 5.1.

The responses obtained based on the PSO optimized PID gains is shown in the Figure 5.16 and Figure 5.16 for maximum of 10 degree case and Figure 5.17 and Figure 5.18

shows the responses with the desired angle of 0 degree (no swing at all) for each of the swing angle and trolley position cases.

Table 5.1: PID domains based on PSO optimization

PID Gains	Parameters
K_p	-280
K_i	-30
K_d	-498

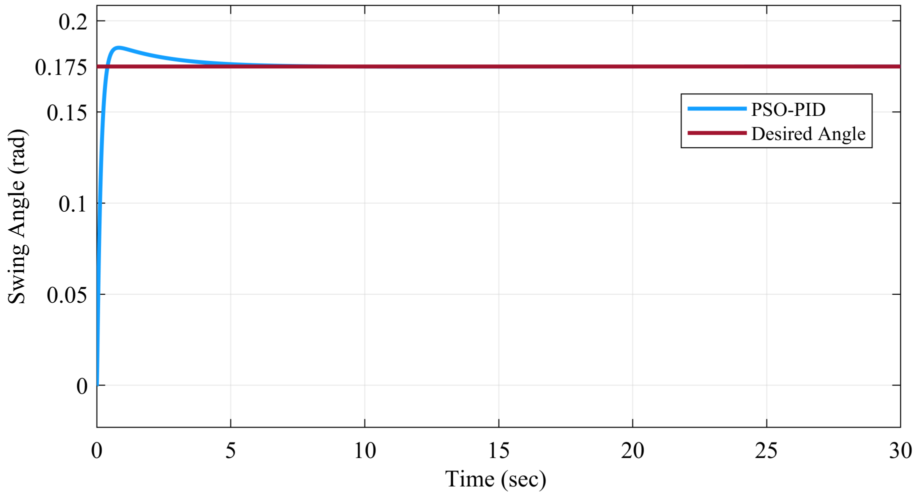

Figure 5.15: System performance of swing angle with PSO-PID controller at maximum of 10 degree swing.

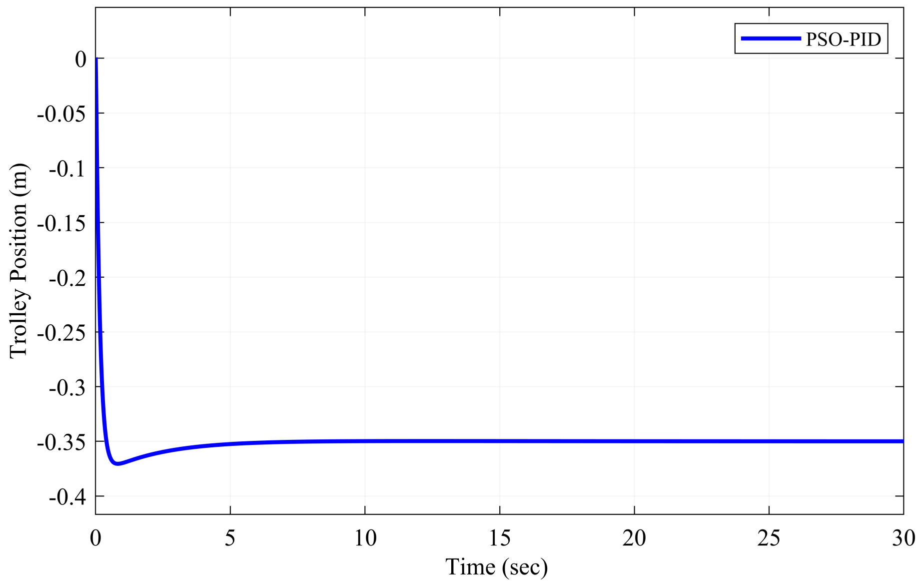

Figure 5.16: System performance of the trolley position with PSO-PID controller at maximum of 10 degree swing.

The PSO optimized PID domains are valid with improved rising time and settling time for the performance of the system at maximum swing of 10 degree with the optimized PID domains as seen in the Figure 5.15 and Figure 5.16. Similarly, the trolley position is also attained with in very few seconds. The performance of controller for the desired 0 degree swing is shown in the Figure 5.17 and Figure 5.18 accordingly.

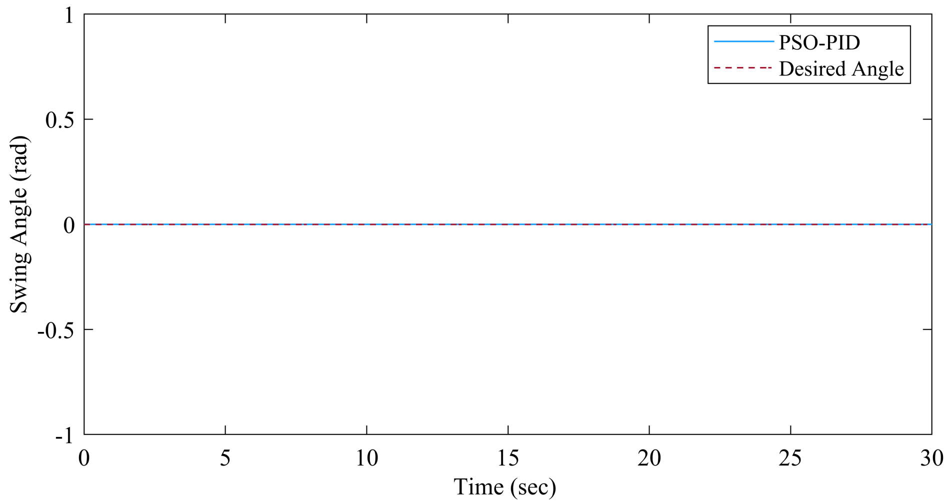

Figure 5.17: System performance of swing angle with PSO-PID controller at no desired swing.

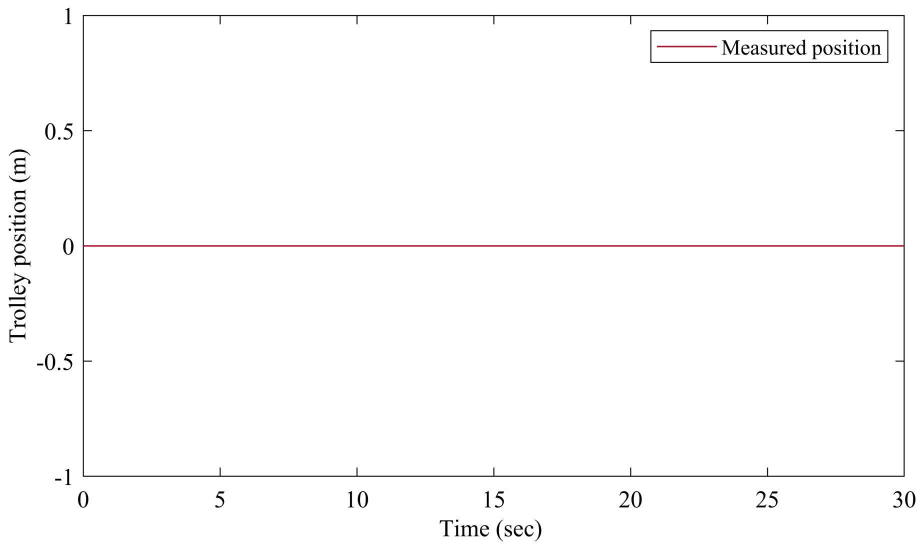

Figure 5.18: System performance of the trolley position with PSO-PID controller at no desired swing.

Figure 5.15 and Figure 5.17 shows the response of the system with PSO-PID controller in two cases. Where, the first case is when the desired swing is 10 degree (0.175 radian) and next case is when the desired swing 0 degree. As seen from Figure 5.15 and Figure 5.16, the swing angle maintained the required value within some seconds and the position of trolley maintained the required position with in few seconds relative to the swing angle response. Which is defined as the swing angle maintained its desired amount and also the trolley attained the expected maximum movement, which is 35 cm in this study.

For PSO-PID, the Performance Index (PI) is:

$$P(k) = \frac{1}{J(k)}, for\ minJ(k) = min((1 - e^{-\beta})(M_p + e_{ss}) + e_{-\beta}(T_s - t_r) + IAE)$$

$$Where,\ IAE = \int_0^\infty |e(t)|dt$$

$$IAE = 0.9994$$

Taking $\beta =$ 0.8, Min(J) = 2.3255 and P(k) = 0.43.

PSO-PID Controller Performance for Swing Angle and Trolley Position with Disturbance and at maximum desired swing of 10 degree:

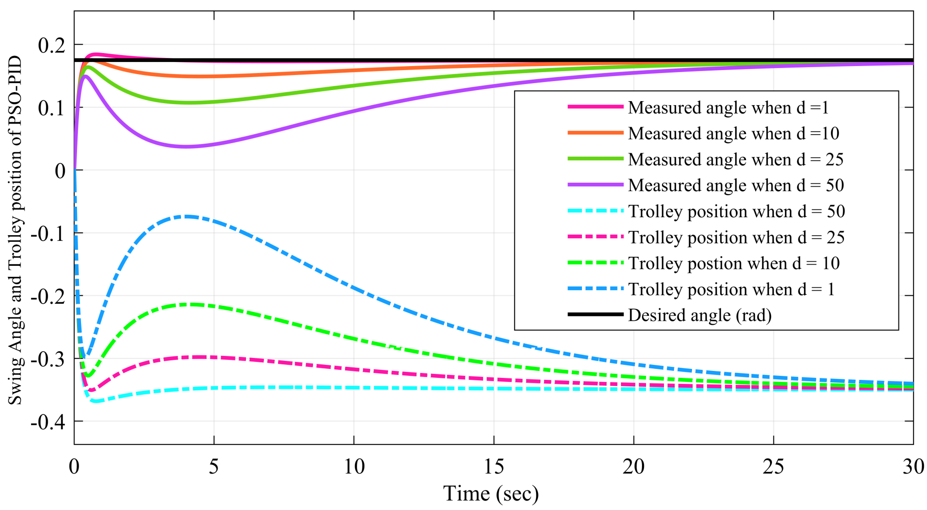

Figure 5.19: Performance of PSO-PID controller for maximum swing angle of 10 degree and at different amount of disturbances.

PSO-PID Controller Performance for Swing Angle and Trolley Position with Disturbance and at desired swing of 0 degree:

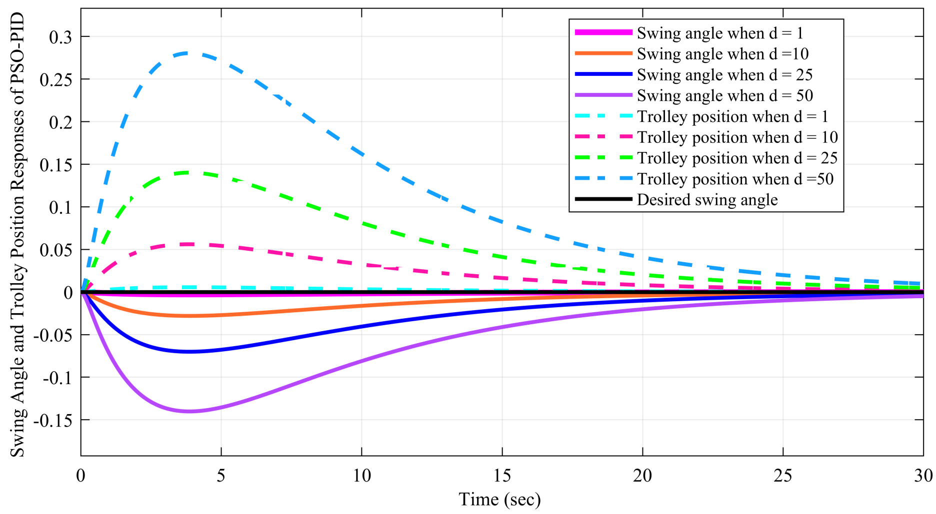

Figure 5.20: Performance of PSO-PID controller for desired swing 0 degree and at different amount of disturbances.

As seen from the Figures above, the designed controller performance is tested by increasing the amount of disturbance to the system. And the system attains the required amount after some seconds even at the worst cases.

A comparison of the performance between PID and PSO-PID at maximum of 10 degree load swing with disturbance:

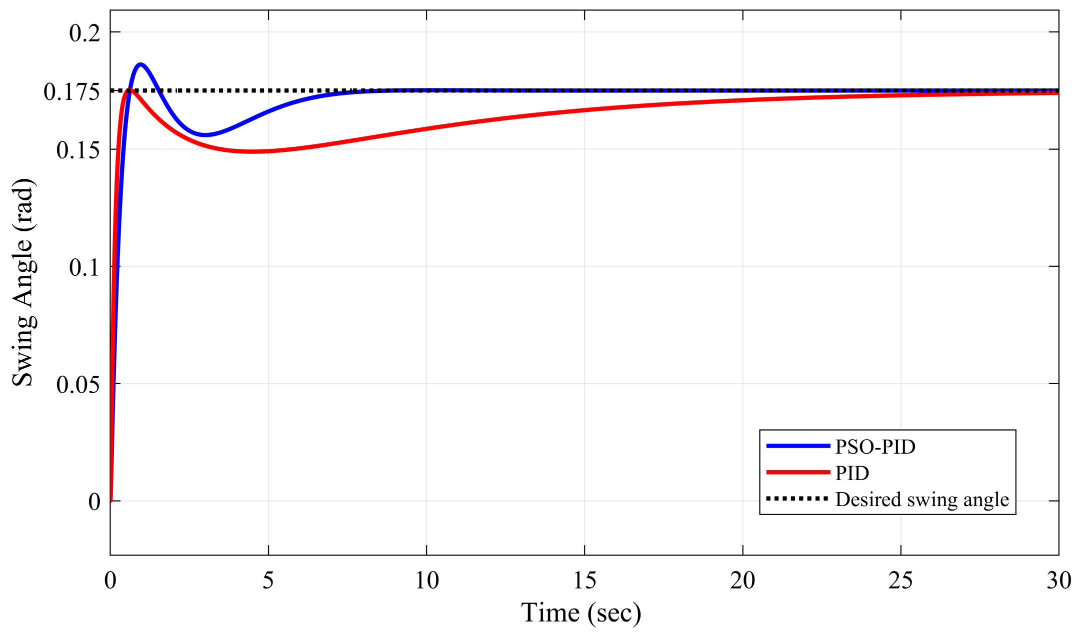

Figure 5.21: The performance comparison of swing angle with PID and PSO-PID controllers at maximum desired swing angle 10 degree (0.175 rad).

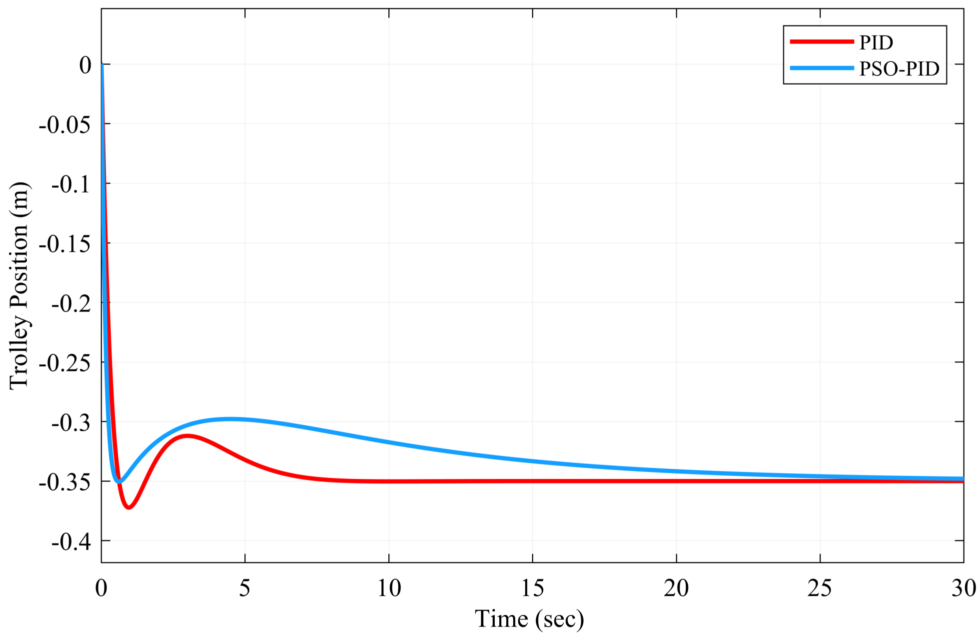

Figure 5.22: The performance comparison of trolley position with PID and PSO-PID controllers at maximum desired swing angle 10 degree (0.175 rad).

As seen from the Figures above, PSO-PID is better to control the swing angle at 10 degree of maximum required swing and PID performed well for all other cases.

5.5 System Performance with PI-Regulator

In PI-regulator case, the responses are analyzed by changing the desired angle, as well as by checking the performance of the controller in the presence of disturbance to the system. Therefore, before getting into the responses, two things are considered:

- First, the disturbance for the overhead crane system in this study is assumed as any disturbance in the overall system that may cause non-smooth input voltage flow. The wind disturbance is not considered as a disturbance for the overhead crane system. Because, the overhead crane system works with heavy loads and wind has no effect on it. Therefore, the wind disturbance neglected.
- Second, the amount of swing angle to test the validity of controller is either 10 degree = 0.175 rad or 0 degree = 0 rad. The reference angle of the step input represents a maximum angle of swing (10 degree = 0.175 rad) and the reference angle of 0 represents no swing at all, that is the core aim of this thesis.

  Therefore, a total of four cases are shown with their respective Simulink models and their responses. Their summary is listed in a simple tabular form next to the responses.

- **Case - 1:** When there is disturbance to the plant and the desired angle is 10 degree = 0.175 rad

In this case, the reference angle is a small swing angle ($10^\circ = 0.175$radian) and the performance of controller is tested by assuming disturbances and uncertain initial values. The Simulink model is shown in Appendix - 3.

In this case, when the magnitude of disturbance increases, the overshoot also increases. That means for higher magnitude of disturbance, there is overshoot and for lower magnitude of disturbance, undershoot exists. Note that, in both cases, the controller regulated the system to the desired value with in some seconds.

Swing Angle responses with different disturbance values:

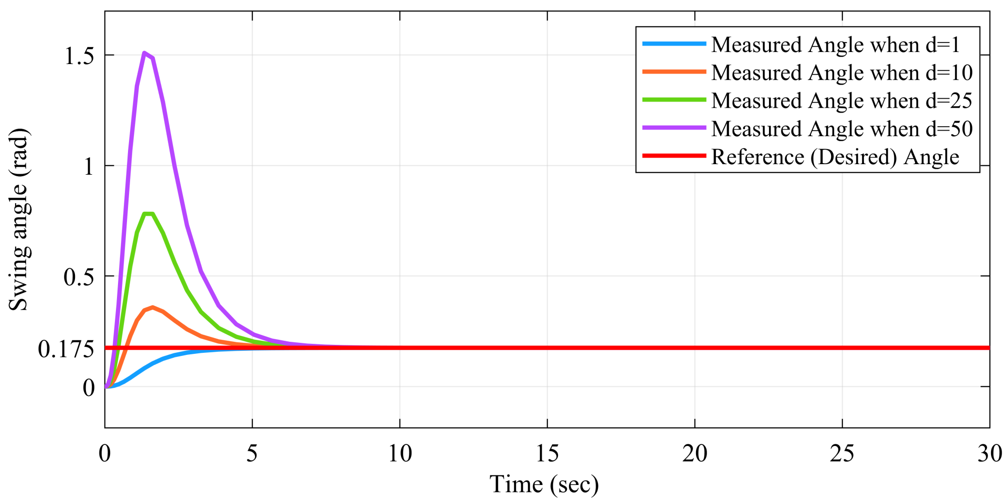

Figure 5.23: Response for the system swing angle considering small swing angle and disturbances

As seen from the Figure 5.23, even though there is a disturbance while in the operation of the overhead crane system, the controller made the swing angle to not exceed above than the setpoint value, which is a small swing angle. For the trolley position also the required amount is attained with in some seconds, as seen from the Figure 5.24.

Position responses with different disturbance values:

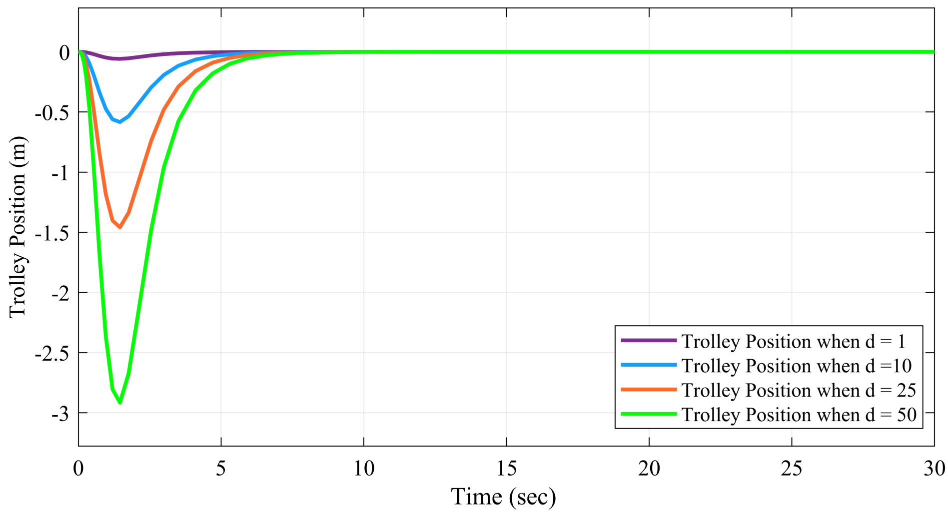

Figure 5.24: Response for the trolley position considering small swing angle and disturbances

Similarly, as seen in the Figure 5.24, the position of trolley is also attained the required position even for the high amount of disturbance added to the system.

- **Case - 2:** When there is no disturbance on the plant and the maximum amunt of swing angle is 10 degree = 0.175 rad

In this case also, the reference angle is a small swing angle ($10° = 0.175$radian) without considering disturbance and uncertain initial values. The Simulink model is shown in Appendix - 3 and its response is shown in Figure 5.25.

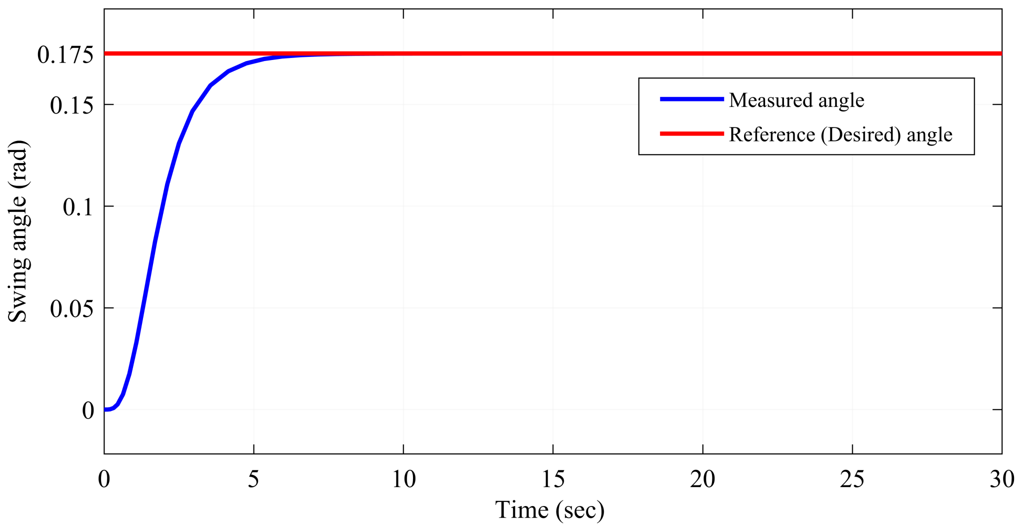

Figure 5.25: Swing angle response for the system considering small swing angle without system uncertainty disturbances.

As seen from Figure 5.25, the controller performed well relative to the given set point. The response of this case has improved time responses than the previous, case - 1. It maintained the set swing angle with improved settling time. Here, even though it maintained the required value, the response is sluggish and it has high rise time.

Trolley position response with swing angle, without any disturbance:

Figure 5.26 shows that the trolley position is maintained. Which means, the swing angle of the load become zero after the trolley displacement of 35 cm = 0.35 m from the rest.

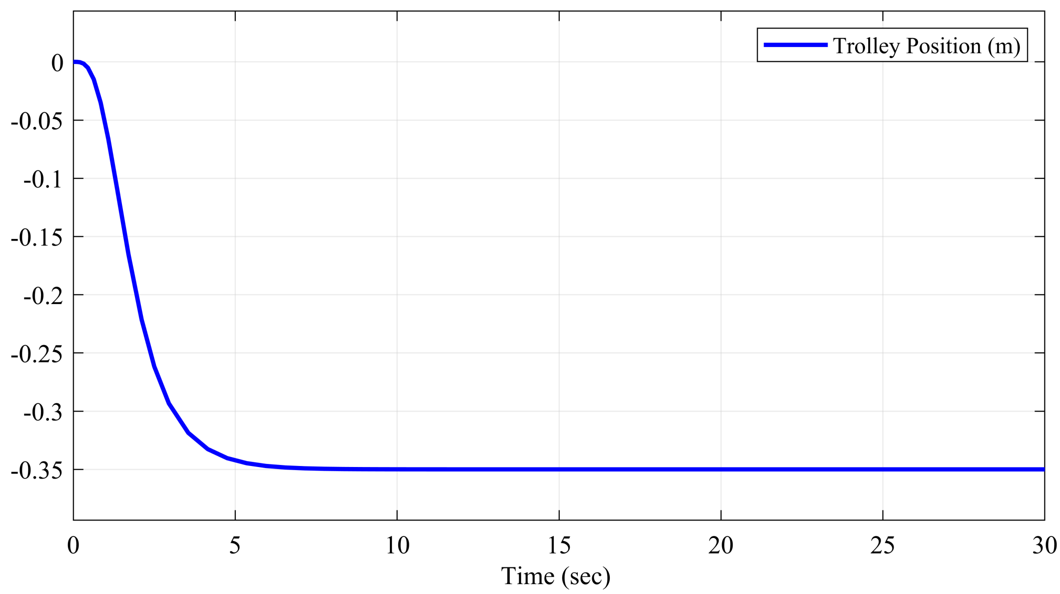

Figure 5.26: The trolley position response for the system considering no swing angle and considering system uncertainty disturbances

- **Case - 3:** When there is disturbance to the plant and the desired angle is 0 degree = 0 rad

In this case, the reference angle is zero and considering disturbance. Which means, while there is a disturbance but referring with no swing angle at all. As seen from the response in the Figure 5.27, the response converges to zero angle even though there is a disturbance in the system. And the validity of the controller is proved well even though there is disturbance when operating with the overhead crane system.

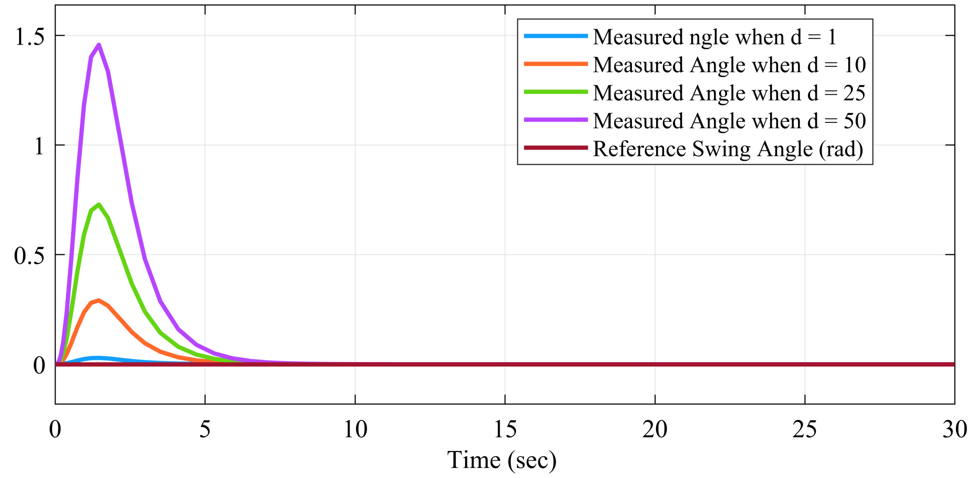

Figure 5.27: Swing angle response for the system considering no swing angle and considering and disturbances

Trolley position response with no swing angle, with added disturbances:

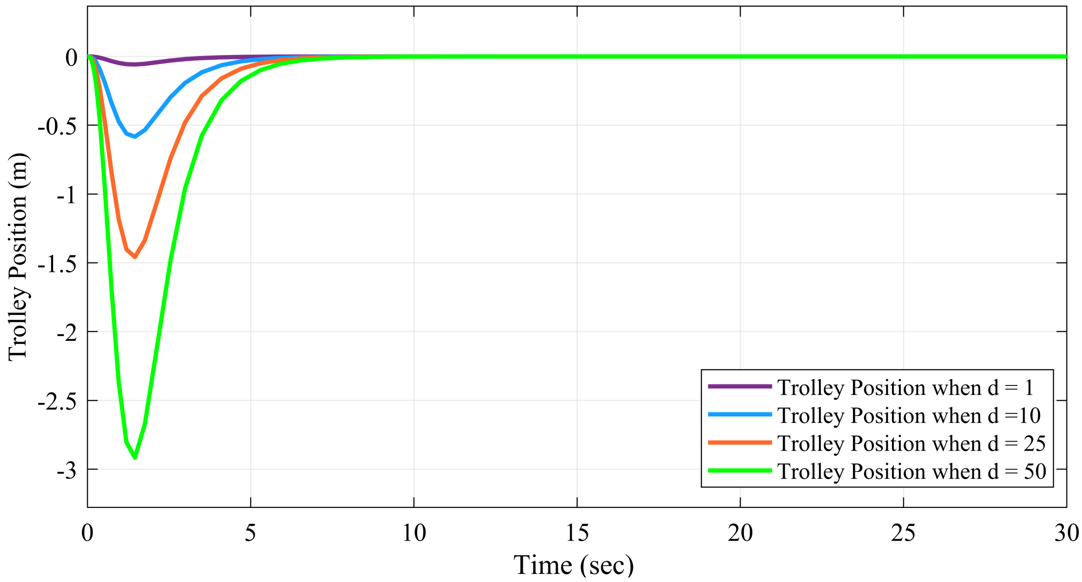

Figure 5.28: Swing angle response for the system considering no swing angle and without considering system uncertainty disturbances.

- **Case - 4:** When there is no disturbance to the plant and the desired angle is 0 degree = 0 rad

This is the last case where, without any disturbance and the reference angle is zero or with no swing angle at all while the operation of the overhead crane system. The Simulink model is shown in the Appendix - 1 and the performance of the controller is proved as seen from the response in the Figure 5.29 and Figure 5.30.

The controller attaind the required setpoint at all the given times. It attained the basic aim of the thesis. And all the cases in simple tabular form is shown in the table 5.2.

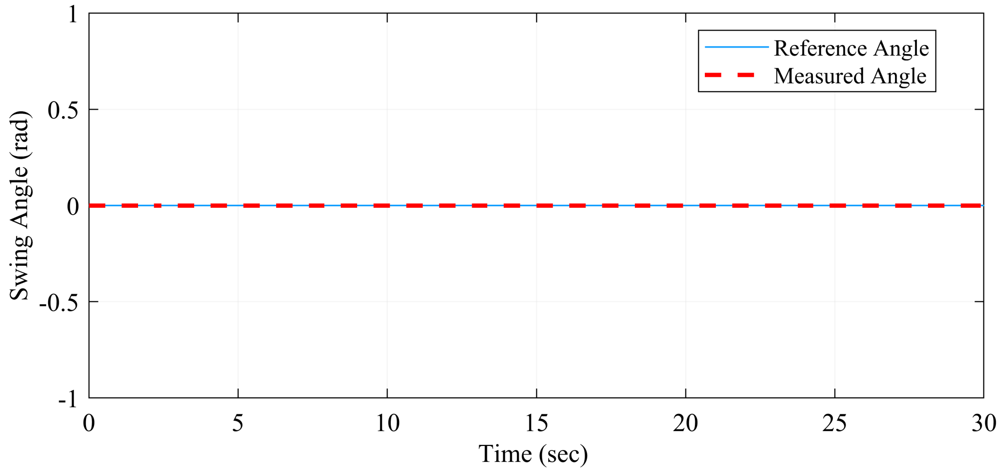

Figure 5.29: Trolley position response for the system considering no swing angle and without considering system uncertainty disturbances.

Trolley position response with no swing angle, and without disturbance:

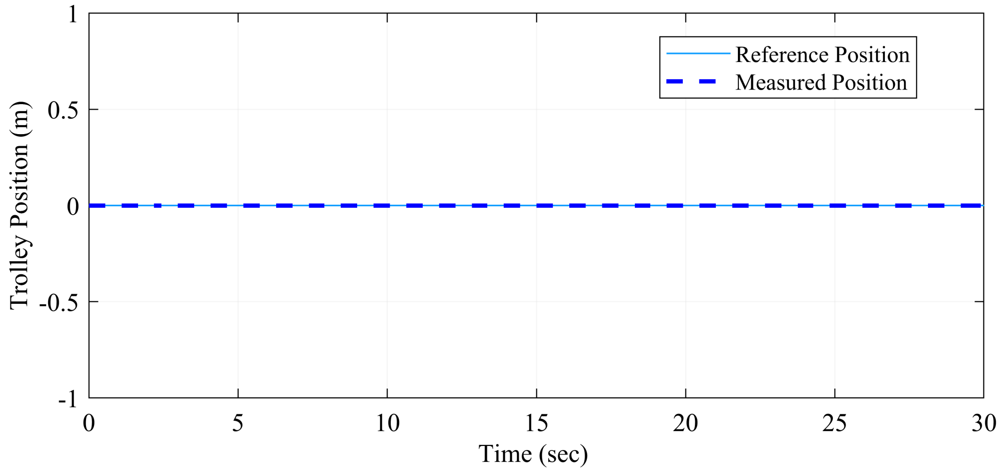

Figure 5.30: The Swing angle response for the system considering no swing angle and without considering system uncertainty disturbances.

These all cases are summarized in the Table 5.2

Table 5.2: Summary of a performance of the system by using PI-Regulator and varying the reference angle and disturbance amount.

Cases	Reference Angle (α_{ref})	Disturbance (d)	Measured Angle (α)	Measured Position (x)
Case-1	10° or 0.175 rad	1 V	Approaches to 10° or 0.175 rad	Approaches 35 cm
		10 V	”	”
		25 V	”	”
		50 V	”	”
Case-2	10° or 0.175 rad	0 V	10° or 0.175 rad	Approaches 35 cm
Case-3	0° or 0 rad	1 V	Approaches to 0° or 0 rad	Approaches 35 cm in less than 7 sec
		10 V	”	”
		25 V	”	”
		50 V	”	”
Case-4	0° or 0 rad	0 V	0° or 0 rad	0

- When both the desired angle is 10° = 0.175 radian and there is a disturbance, the output approaches also to 10° = 0.175 radian.

  i.e., when the reference angle (or) the set point is small swing angle, then the response also has a swing angle as the desired value.
- When the reference angle is 10° = 0.175 radian and there is no disturbance, the output still approaches 10° = 0.175 radian with but with improved time responses.

  i.e., when the desired operation has some swing angle, but there is no disturbance added to the system, the response approaches to the required angle value.
- When the desired angle is 0° = 0 radian and there is the disturbance, the output angle approaches to zero. Even though there is disturbance added to the system, the controller performed well to get the desired value.

  i.e., now, when there is no swing in the required angle and there is disturbance in the system, the output response approaches to the desired value, after time response errors. And,
- Lastly, when the reference angle is 0° = 0 radian and there is no disturbance, the output angle meets the reference with no error at all.

This is the aimed desired angle. Where, when with zero swing angle reference and no disturbance, the response also has no swing angle. This study is based on the performance improvement of overhead crane system, using PI-Regulator as the load swing angle regulator. Because of the robustness of the controller, the swing angle is regulated to zero, the desired value of the study and it dynamically adjusted the capability of the overhead crane system.

It ensures no overshoot, swift response and fine precision of both the swing angle and the position of the trolley. In addition to this, PI-Regulator enhances the performance of the whole system and provides a new scheme in developing an overhead crane system with high performance.

5.6 Comparison of the Performance of System

5.6.1 Comparison of the Performance of Designed Controllers

The performance of controllers is tested by adding disturbance to the system. Therefore, the comparison of swing angle reduction performance based on PID, Fuzzy-PID, PSO-PID and PI-Regulator responses is shown in the Figure 5.31 at the desired maximum swing angle of 10 degree (0.175 radian) and added disturbance (At the worst case in this study) with their respective time domain performance measures is shown in the Table 5.3.

Table 5.3: Performance of designed controllers with disturbances in the system.

Controllers	Rise time (sec)	Settling time (sec)	Maximum Overshoot (%)
PID	0.3822	5.3449	17.7099
FPID	0.3800	6.64918	15.1083
PSO-PID	0.2527	2.1372	5.2499
PI-Regulator	2.4134	4.6637	0

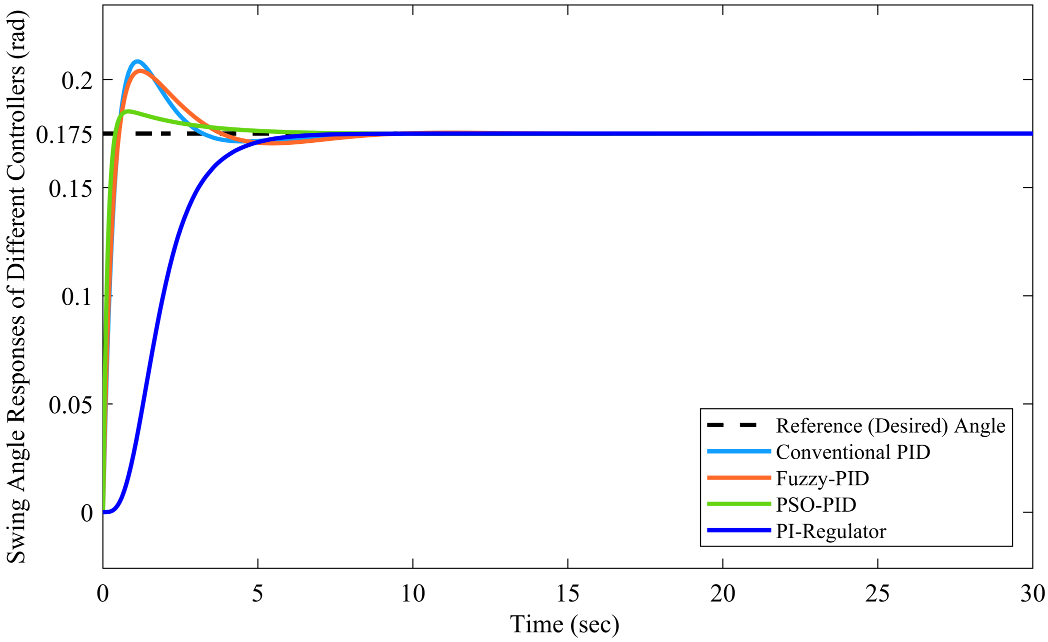

(a) *SwingAngle.*

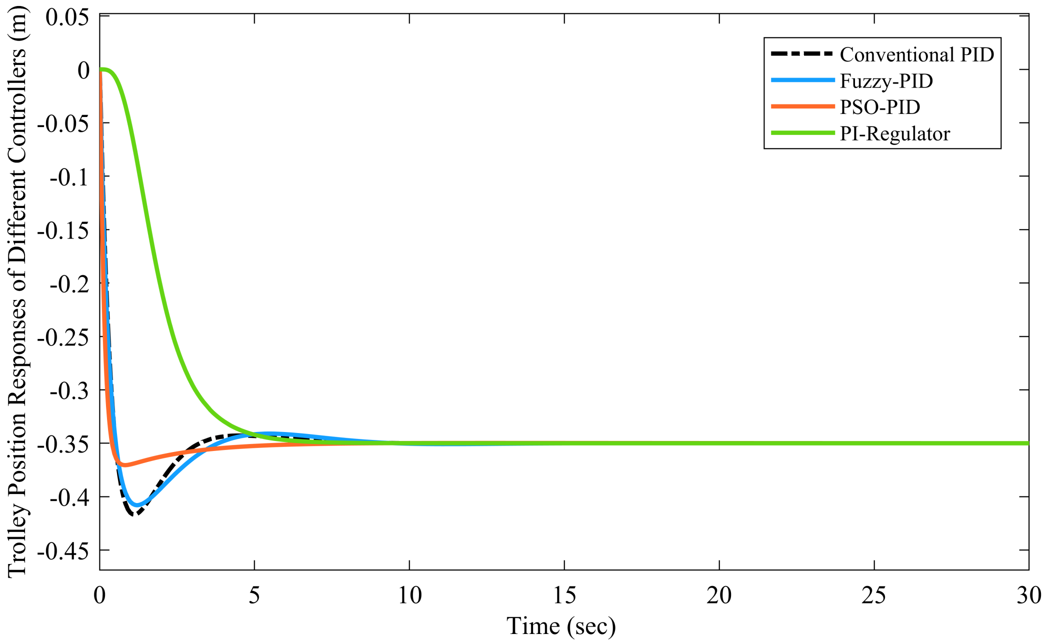

(b) *Trolley Position.*

Figure 5.31: Performance of controllers

5.6.2 Comparison of the Robustness of Designed Controllers

When the parameter uncertainty in three cases, where when the load mass is 6 kg, 10 kg, and 12 kg.

- **Case - 1:** When the load mass is 6 kg (at nominal value).

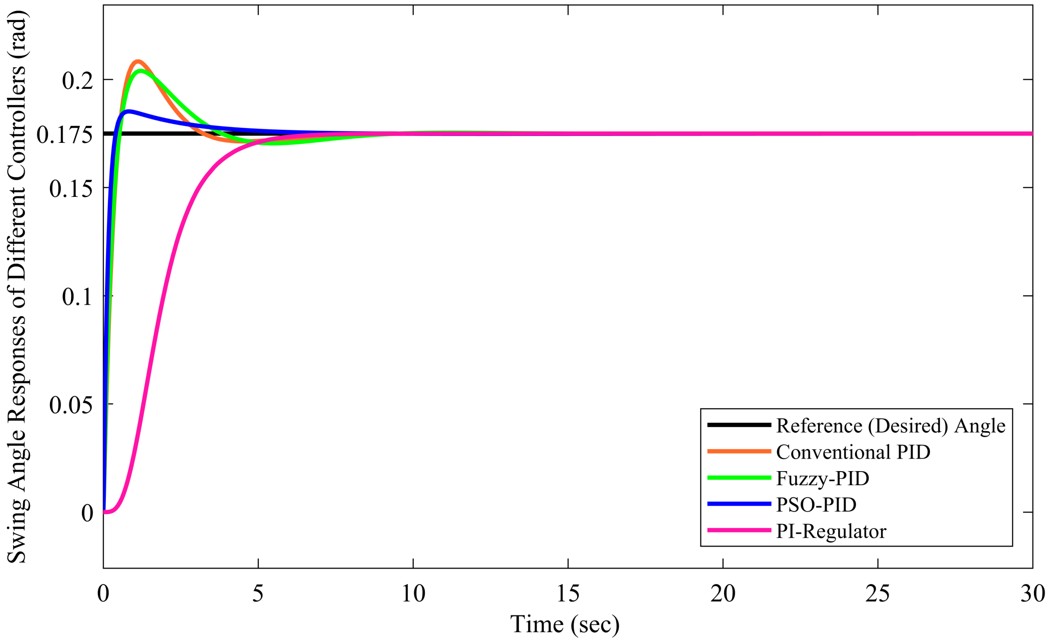

Figure 5.32: The swing angle responses of all controllers at maximum swing of 10-degree.

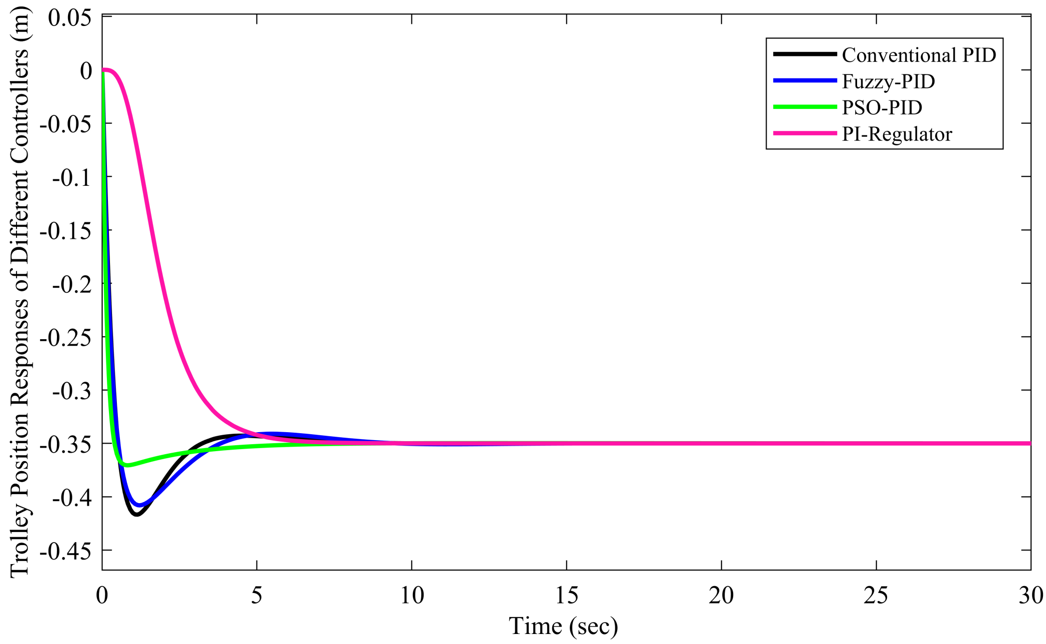

Figure 5.33: The trolley position responses of controllers at maximum swing of 10-degree.

- **Case - 2:** When the load mass is 10 kg.

For the varied load mass of 10 kg at maximum allowable swing angle of 10-degree, the response for the measured swing angle and relative trolley position is shown in the Figure below. And the respective time domain responses are listed in the Table5.4 for this case.

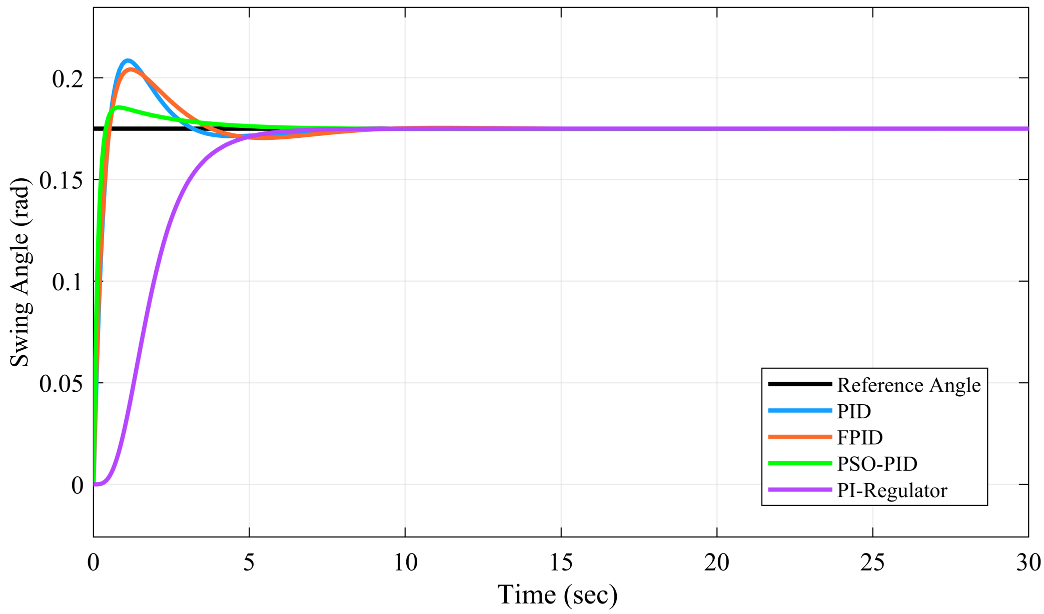

(a) *SwingAngle.*

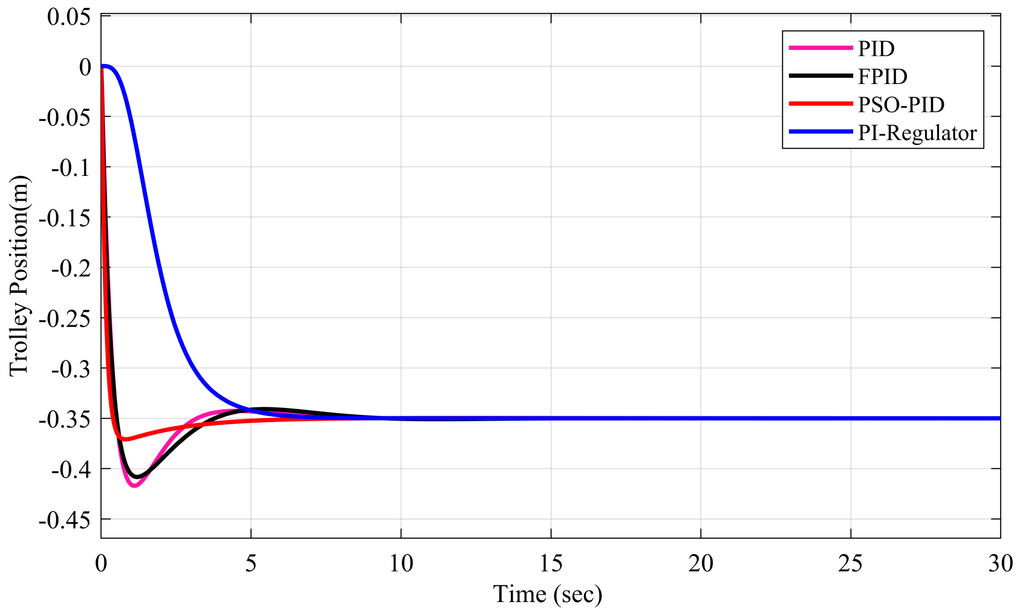

(b) *Trolley Position.*

Figure 5.34: Controller performance at load mass of 10kg

- **Case - 3:** When the load mass is 12 kg.

Similarly, taking the uncertain parameter of payload at 12 kg, which is considered as the maximum amount, the response of controllers is compared and their robustness is verified as shown in the Figures below and the corresponding time domain performance parameters are shown in the Table 5.4.

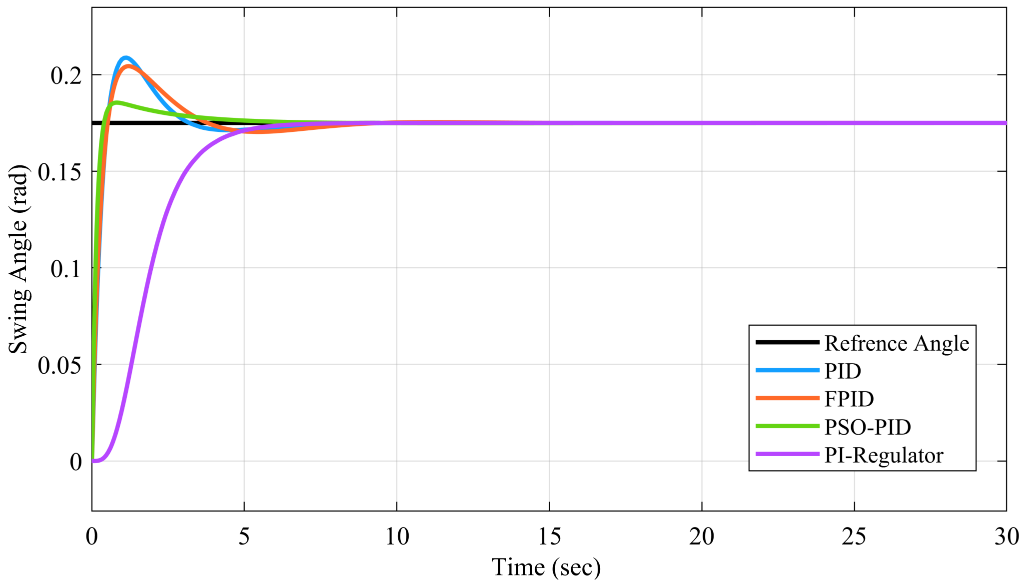

(a) *SwingAngle.*

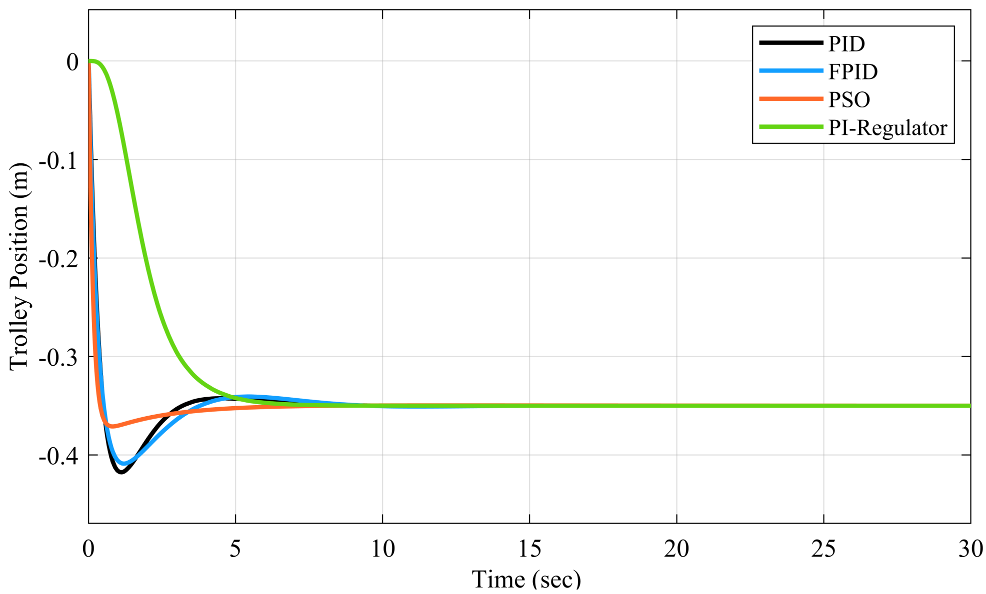

(b) *Trolley Position.*

Figure 5.35: Controller performance at load mass of 12kg.

Table 5.4: The robustness of designed controllers with Parameter uncertainty.

Controllers	Performance of Controllers with mass variation/ Parameter Uncertainty								
	6 kg			10 kg			12 kg		
	$t_r(sec)$	$t_s(sec)$	$M_p(\%)$	$t_r(sec)$	$t_s(sec)$	$M_p(\%)$	$t_r(sec)$	$t_s(sec)$	$M_p(\%)$
PID	0.3780	4.8693	19.0588	0.3749	4.9411	19.1566	0.3766	5.0241	19.3041
FPID	0.3758	6.6151	16.5736	0.3722	6.6017	16.6573	0.3742	6.6338	16.7984
PSO-PID	0.2515	3.1352	5.8677	0.2490	3.13025	5.9636	0.2507	3.1517	6.0193
PI- Regulator	2.6173	5.1356	0	2.6023	5.1248	0	2.6153	5.1149	0

5.6.3 Performance of Controllers at any Desired Swing Angle

- For 10-degree swing: The designed controllers performance when the desired maximum swing of the load is $10° = 0.175$ rad, PID has a settling time (t_s) of 4.8693 sec and with a maximum overshoot (M_p) of 19.0588%; FPID with t_s of 6.6151 sec and M_p of 16.5736%; PSO-based PID with t_s of 3.1352 sec and M_p of 5.8677%; And finally, the designed PI-Regulator has t_s of 5.1356 sec and M_p 0% respectively, as summarized in the Table 5.5.

  The responses for the swing angle case, at maximum of 10-degree is shown in the Figure 5.36. And the corresponding trolley position where the swing angle is eliminated is also shown in the Figure 5.37.

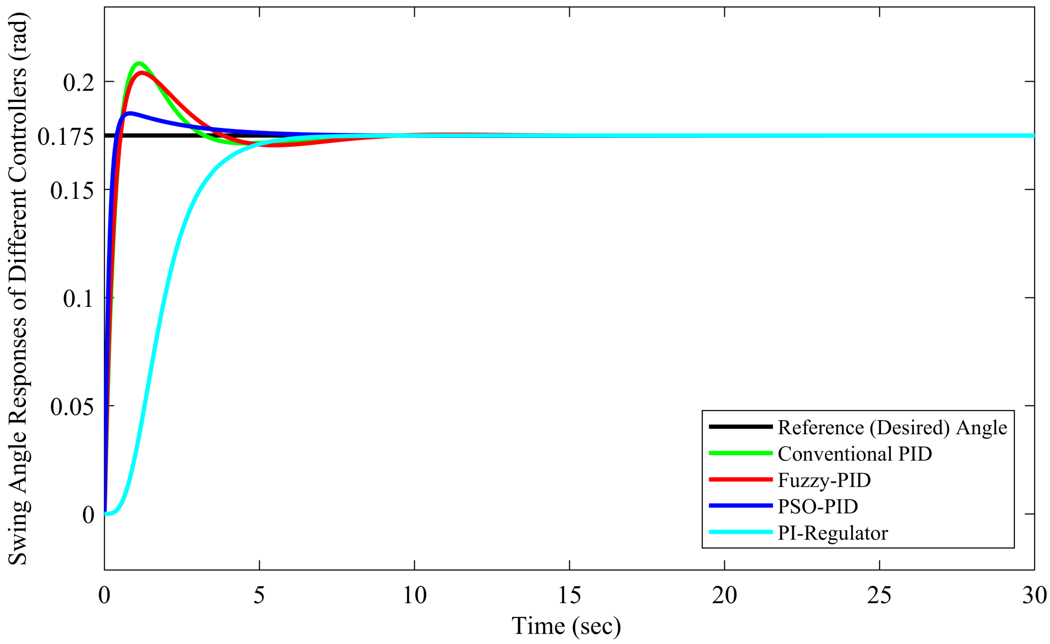

Figure 5.36: The swing angle responses of all controllers at the maximum swing of 10-degree.

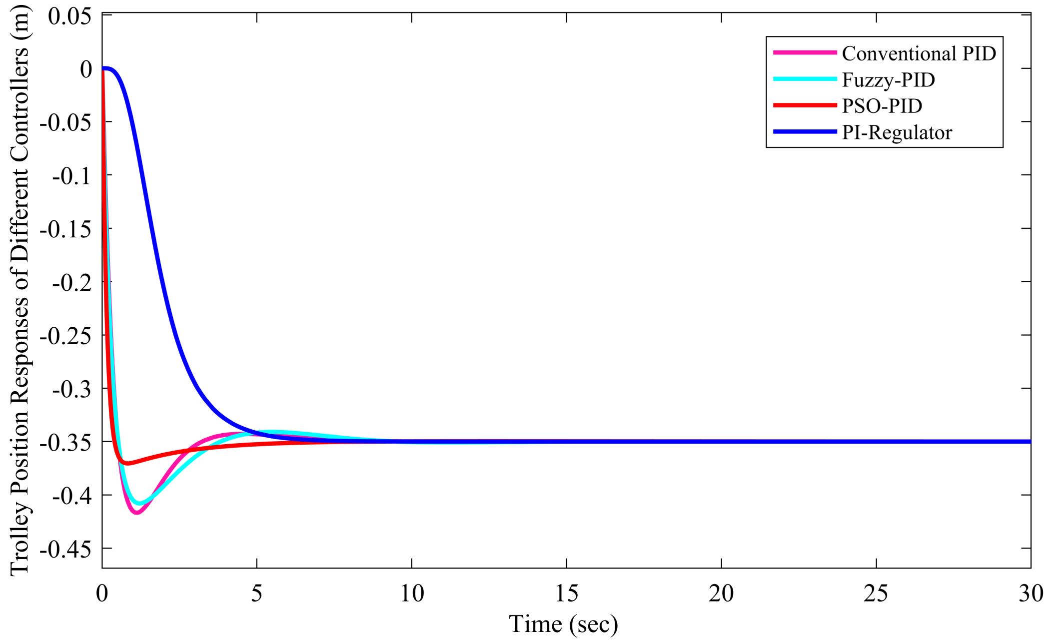

Figure 5.37: The trolley position responses of controllers at the maximum swing of 10-degree.

- For 5-degree swing: In this case, when the maximum permissible swing angle of the payload is 5 degree and the maximum position of the trolley from the initial point to the point where the payload is downward with no swing angle at all (0-degree of swing) is 0.175 m (17.5 cm) accordingly.

  For both the swing angle and trolley position, the performance of controllers is shown in Figure 5.39 and Figure 5.39, and corresponding time domain parameters are shown in the Table 5.5. From the responses, it is noted that even though the amount of swing increases, the performance of controllers is valid for whatever the desired swing is.

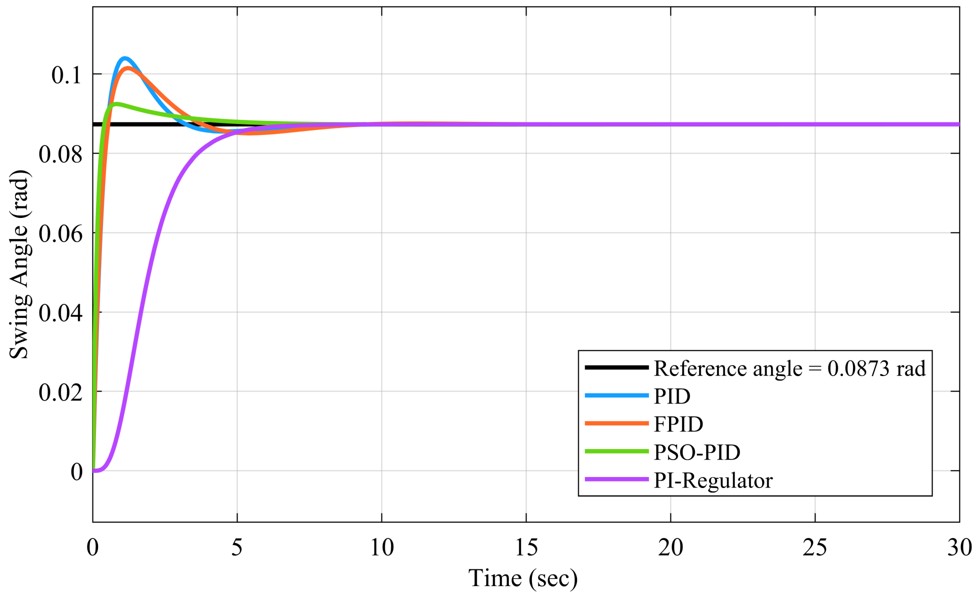

Figure 5.38: System performance of swing angle with all designed controllers at maximum swing of 5-degree.

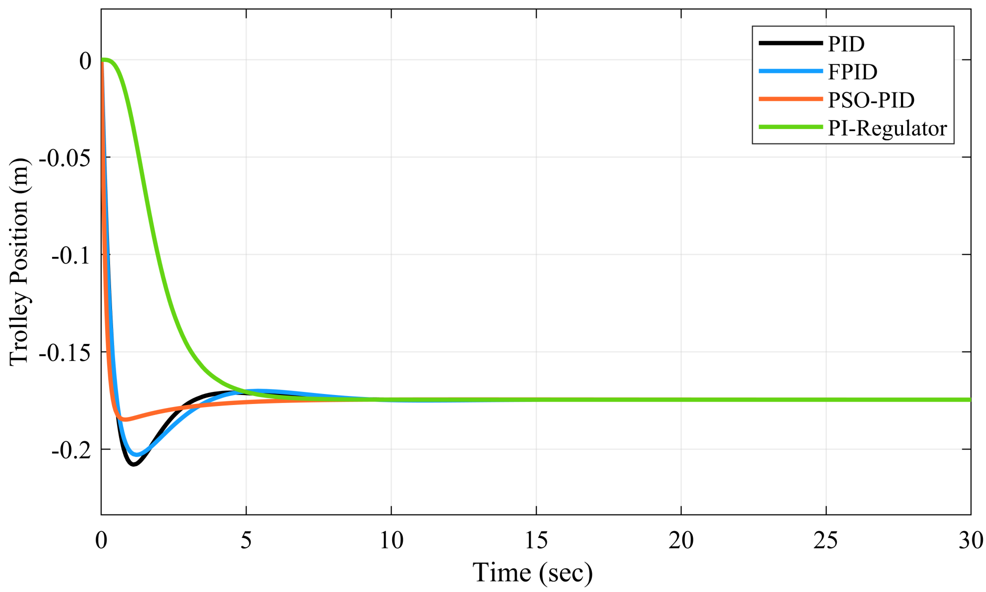

Figure 5.39: System performance of trolley position with all designed controllers at maximum swing of 5-degree.

Table 5.5: The validity of controllers with different amount of maximum swing.

Controllers	Validity of controllers with different amount of maximum swing					
	10-Degree = 0.175 rad			5-Degree = 0.0875 rad		
	$t_r(sec)$	$t_s(sec)$	$M_p(\%)$	$t_r(sec)$	$t_s(sec)$	$M_p(\%)$
PID	0.3780	4.8693	19.0588	0.3787	4.8827	19.0765
FPID	0.3758	6.6151	16.5736	0.3844	6.5810	16.2087
PSO-PID	0.2515	3.1352	5.8677	0.2527	3.1359	5.8575
PI- Regulator	2.6173	5.1356	0	2.6119	5.1322	0

CONCLUSIONS AND RECOMMENDATIONS

CONCLUSIONS

The main aim of this thesis was to control an overhead crane system efficiently under different conditions. To achieve the required aim, the system background is studied, and the existing literature is reviewed and the limitations are seen. Then, a system model is derived based on the performance characteristics of overall system and various control techniques for overhead crane are designed and implemented in MATLAB/Simulink. Therefore, based on the designed system model, the conventional PID, Fuzzy PID, PSO-Based PID, and PI-Regulator algorithms are discussed with the swing angle constraints for 2-Dimensional overhead crane system and their respective responses with time domain performance measures are presented with desired swing angle and corresponding trolley position.

First, by using the pole placement approach, the PID controller parameters were successfully obtained. Second, a fuzzy logic based PID (FPID) controller is designed with a minimum number of rules and with improved performance. Then, the PSO optimized PID (PSO-PID) controller design is successful by attaining the range of PID controller gains. Finally, the PI-Regulator design is done, and the performance of the system with each of the designed controllers is tested and proved. Therefore, the performance of designed controllers is verified with disturbances, and the robustness of controllers is tested by varying the mass of payload. Similarly, the performance improvement of the system with the designed controllers is validated by adjusting the maximum amount of reference (desired) swinging angle. As a result, the validity of proposed controllers is checked for the effects of load oscillation, including juggling torque.

In general, an overhead crane system performance improvement with each of the developed controllers against various levels of disturbances, and payload mass variation is evaluated, discussed, and compared. The simulation results show that the developed strategies perform satisfactorily in terms of precise and reliable trolley placement as well as efficient payload swing reduction without steady state error. Therefore, the system performance is improved with the designed controllers that meet the load anti-sway and trolley trajectory tracking requirements under different mentioned conditions. And finally, of the designed controllers in this thesis, PSO-PID had the best performance compared to others.

RECOMMENDATIONS

This research work makes the following recommendations for future researchers:

- Extending self-adaptive PID technique and PI-Regulator approach to a 3-Dimensional (3-D) overhead crane system.
- Hardware implementation of the designed techniques.
- Investigating the performance by using AC motor as an actuator of the system.

Research Fund Acknowledgment

This research thesis was funded by Adama Science and Technology University under the grant number of ASTU/SM-R/531/22, Adama, Ethiopia.

REFERENCES

7 TYPES OF CRANES USED IN CONSTRUCTION WORKS. (2017, 11). Retrieved from https://cranenetworknews.com-7-types-of-cranes-used-in-construction-works

Ahmad, M., Ismail, R. R., Ramli, M., & Hambali, N. (2010). Analysis of iir filter with nctf-pi control for sway and trajectory motion of a dptoc system. In *2010 international conference on electronic devices, systems and applications* (pp. 54–58).

Åström, K. J., & Wittenmark, B. (2013). *Adaptive control.* Courier Corporation.

Azmi, N. I. M., Yahya, N. M., Fu, H. J., & Yusoff, W. A. W. (2019). Optimization of the pid-pd parameters of the overhead crane control system by using pso algorithm. In *Matec web of conferences* (Vol. 255, p. 04001).

Chandran, P., Vivek, A., & Amritha, S. (2017). Optimisation of overhead crane. In *2017 international conference on circuit, power and computing technologies (iccpct)* (pp. 1–8).

Chaudhary, H., Khatoon, S., & Singh, R. (2016). Anfis based speed control of dc motor. In *2016 second international innovative applications of computational intelligence on power, energy and controls with their impact on humanity (cipech)* (pp. 63–67).

Chen, H., Fang, Y., & Sun, N. (2017). A swing constrained time-optimal trajectory planning strategy for double pendulum crane systems. *Nonlinear Dynamics*, *89*(2), 1513–1524.

Chiou, J.-S., Tsai, S.-H., & Liu, M.-T. (2012). A pso-based adaptive fuzzy pid-controllers. *Simulation Modelling Practice and Theory*, *26*, 49–59.

Cranes — Monitoring for crane design working period. (2014, 06). Retrieved from https://www.iso.org/obp/ui/#iso:std:iso:12482:ed-1:v1:en

Dostál, P., Kubalčík, M., Bobál, V., & Vojtěšek, J. (2011). Nonlinear adaptive control of a chemical reactor. In *2011 19th mediterranean conference on control & automation (med)* (pp. 600–605).

D P Kothari, I. J. N. (2010). *Electric machines.* Tata McGraw Hill Education Private Limited.

Engineering Design Process. (2022, 06). Retrieved from https://www.sciencebuddies.org/science-fair-projects/engineering-design-process/engineering-design-compare-scientific-method

Fang, Y., Dixon, W. E., Dawson, D. M., & Zergeroglu, E. (2003). Nonlinear coupling control laws for an underactuated overhead crane system. *IEEE/ASME transactions on mechatronics*, *8*(3), 418–423.

Fang, Y., Ma, B., Wang, P., & Zhang, X. (2011). A motion planning-based adaptive control method for an underactuated crane system. *IEEE Transactions on control systems technology*, *20*(1), 241–248.

FEM classification. (2016, 05). Retrieved from https://www.huchez.com/en/fem-classification

FEM/DIN Double Girder Overhead Crane. (2022, 06). Retrieved from https://www.weihuacraneglobal.com/product/FEMDIN-Double-Girder-Overhead-Crane.htmll

FEM/DIN standard double girder overhead crane. (2016, 10). Retrieved from https://www.overheadcraneskit.com/femdin-standard-double-girder-overhead-crane.html

Gao, X., Yang, Y., & Wu, Z. (2016). Genetic algorithm for scheduling double different size crane system with different truck ready times. In *2016 ieee international conference on industrial engineering and engineering management (ieem)* (pp. 447–451).

Garrido, R., & Soria, A. (2005). Control of a servomechanism using non-linear damping. *Proceedings of the Institution of Mechanical Engineers, Part I: Journal of Systems and Control Engineering*, *219*(4), 295–299.

Garrido, S., Abderrahim, M., Gimenez, A., Diez, R., & Balaguer, C. (2008). Anti-swinging input shaping control of an automatic construction crane. *IEEE Transactions on Automation Science and Engineering*, *5*(3), 549–557.

Gopal, A., Sultani, M. M., & Bansal, J. C. (2020). On stability analysis of particle swarm optimization algorithm. *Arabian Journal for Science and Engineering*, *45*(4), 2385–2394.

Guo, H., Feng, Z.-Y., & She, J. (2020). Discrete-time multivariable pid controller design with application to an overhead crane. *International Journal of Systems Science*, *51*(14), 2733–2745.

Haq, H., & Okumus, H. I. (2016). A simple approach to dc motor modeling and comparative implementation of pi and flc for its speed controlling. *Int J Innov Res Sci Eng Technol*, *5*, 98–105.

Hu, Y., Postolache, O., Yang, Y., & Xu, W. (2021). Microwave radar based estimation of the sway angle of payload in overhead crane system. In *2021 telecoms conference (conftele)* (pp. 1–6).

Huang, J., Maleki, E., & Singhose, W. (2013). Dynamics and swing control of mobile boom cranes subject to wind disturbances. *IET Control Theory & Applications*, *7*(9), 1187–1195.

Jaafar, H., Mohamed, Z., Ramli, L., & Abdullahi, A. (2018). Vibration control of a nonlinear double-pendulum overhead crane using feedforward command shaping. In *2018 ieee conference on systems, process and control (icspc)* (pp. 118–122).

Jaafar, H. I., & Mohamed, Z. (2017). Pso-tuned pid controller for a nonlinear double-pendulum crane system. In *Asian simulation conference* (pp. 203–215).

Khan, A., Chatterjee, B., & Dey, C. (2016). Real time performance evaluation of a self-tuning fuzzy pid controller on an inverted pendulum in crane mode operation. In *2016 international conference on intelligent control power and instrumentation (icicpi)* (pp. 22–26).

Kothari, C. R. (2004). *Research methodology: Methods and techniques*. New Age International.

Lee*, H.-H. (2005). Motion planning for three-dimensional overhead cranes with high-speed load hoisting. *International Journal of Control*, *78*(12), 875–886.

Li, S.-j., Xu, Z.-y., Wu, H., Hu, S.-h., & Xu, J.-x. (2005). Intelligent anti-swing control for horizontal moving process of bridge crane. In *2005 international conference on control and automation* (Vol. 2, pp. 1091–1096).

Liu, D., et al. (2019). Research on anti-swing of bridge crane based on fuzzy self-adaptive pid controller. In *2019 international conference on intelligent informatics and biomedical sciences (iciibms)* (pp. 245–249).

Lu, B., Fang, Y., & Sun, N. (2015). Adaptive trajectory tracking control for a four-rope crane. In *2015 ieee international conference on advanced intelligent mechatronics (aim)* (pp. 488–493).

Lu, B., Fang, Y., & Sun, N. (2018). Modeling and nonlinear coordination control for an underactuated dual overhead crane system. *Automatica*, *91*, 244–255.

Ma, X., & Bao, H. (2018). An anti-swing closed-loop control strategy for overhead cranes. *Applied Sciences*, *8*(9), 1463.

Mahfouf, M., Kee, C., Abbod, M. F., & Linkens, D. A. (2000). Fuzzy logic-based anti-sway control design for overhead cranes. *Neural Computing & Applications*, *9*(1), 38–43.

Masoud, Z. N., & Nayfeh, A. H. (2003). Sway reduction on container cranes using delayed feedback controller. *Nonlinear dynamics*, *34*(3), 347–358.

Moon, M. S., VanLandingham, H. F., & Beliveau, Y. J. (1996). Fuzzy time optimal control of crane load. In *Proceedings of 35th ieee conference on decision and control* (Vol. 2, pp. 1127–1132).

Ngo, Q. H., & Hong, K.-S. (2010). Sliding-mode antisway control of an offshore container crane. *IEEE/ASME transactions on mechatronics*, *17*(2), 201–209.

Ogata, K., et al. (2010). *Modern control engineering* (Vol. 5). Prentice hall Upper Saddle River, NJ.

Önen, Ü., & Çakan, A. (2017). Anti-swing control of an overhead crane by using genetic algorithm based lqr. *International Journal of Engineering And Computer Science*, *6*(6).

Overhead crane. (2022, 05). Retrieved from https://en.wikipedia.org/wiki/Overhead_crane

OVERHEAD CRANE TYPES - Different types of overhead cranes. (2022, 06). Retrieved from https://gruasyaparejos.com/en/cranes-and-rigging/

Park, M.-S., Chwa, D., & Eom, M. (2014). Adaptive sliding-mode antisway control of uncertain overhead cranes with high-speed hoisting motion. *IEEE Transactions on Fuzzy Systems*, *22*(5), 1262–1271.

Park, M.-S., Chwa, D., & Hong, S.-K. (2008). Antisway tracking control of overhead cranes with system uncertainty and actuator nonlinearity using an adaptive fuzzy sliding-mode control. *IEEE Transactions on Industrial Electronics*, *55*(11), 3972–3984.

Piazzi, A., & Visioli, A. (2002). Optimal dynamic-inversion-based control of an overhead crane. *IEE Proceedings-Control Theory and Applications*, *149*(5), 405–411.

Ramli, L., Mohamed, Z., Abdullahi, A. M., Jaafar, H. I., & Lazim, I. M. (2017). Control strategies for crane systems: A comprehensive review. *Mechanical Systems and Signal Processing*, *95*, 1–23.

Ramli, L., Mohamed, Z., Efe, M., Lazim, I. M., & Jaafar, H. (2020). Efficient swing control of an overhead crane with simultaneous payload hoisting and external disturbances. *Mechanical systems and signal processing*, *135*, 106326.

Ross, T. J. (2005). *Fuzzy logic with engineering applications.* John Wiley & Sons.

Shao, X., Zhang, J., & Zhang, X. (2019). Takagi-sugeno fuzzy modeling and pso-based robust lqr anti-swing control for overhead crane. *Mathematical Problems in Engineering*, *2019*.

Shyu, K.-K., Jen, C.-L., & Shang, L.-J. (2005). Design of sliding-mode controller for anti-swing control of overhead cranes. In *31st annual conference of ieee industrial electronics society, 2005. iecon 2005.* (pp. 6–pp).

Singh, A., & Agrawal, H. (2018). A fractional model predictive control design for 2-d gantry crane system. *Journal of Engineering Science and Technology*, *13*(7), 2224–2235.

Singh, A. P., Srivastava, T., Agrawal, H., & Srivastava, P. (2017). Fractional order controller design and analysis for crane system. *Progress in Fractional Differentiation and Applications*, *3*(2), 155–162.

Singhose, W., Porter, L., Kenison, M., & Kriikku, E. (2000). Effects of hoisting on the input shaping control of gantry cranes. *Control engineering practice*, *8*(10), 1159–1165.

SmarajitGhosh. (n.d.). *Control systems-theory and applications*. Pearson Education.

Solihin, M. I., et al. (2007). Fuzzy-tuned pid control design for automatic gantry crane. In *2007 international conference on intelligent and advanced systems* (pp. 1092–1097).

Sun, N., & Fang, Y. (2012). New energy analytical results for the regulation of underactuated overhead cranes: An end-effector motion-based approach. *IEEE Transactions on Industrial Electronics*, *59*(12), 4723–4734.

Sun, N., Fang, Y., Chen, H., & Lu, B. (2016). Amplitude-saturated nonlinear output feedback antiswing control for underactuated cranes with double-pendulum cargo dynamics. *IEEE transactions on Industrial Electronics*, *64*(3), 2135–2146.

Sun, N., Fang, Y., Zhang, X., & Yuan, Y. (2012). Transportation task-oriented trajectory planning for underactuated overhead cranes using geometric analysis. *IET Control Theory & Applications*, *6*(10), 1410–1423.

Sun, Z., Ling, Y., Qu, H., Xiang, F., Sun, Z., & Wu, F. (2020). An adaptive de algorithm based fuzzy logic anti-swing controller for overhead crane systems. *International Journal of Fuzzy Systems*, *22*(6), 1905–1921.

Sun, Z., Ling, Y., Sun, Z., Bi, Y., Tan, S., & Ding, L. (2019). Designing and application of fuzzy pid control for overhead crane systems. In *2019 2nd international conference on information systems and computer aided education (iciscae)* (pp. 411–414).

Sun, Z., Ling, Y., Tan, X., Zhou, Y., & Sun, Z. (2021). Designing and application of type-2 fuzzy pid control for overhead crane systems. *International Journal of Intelligent Robotics and Applications*, *5*(1), 10–22.

Sun, Z., Wang, N., Bi, Y., & Zhao, J. (2015). A de based pid controller for two dimensional overhead crane. In *2015 34th chinese control conference (ccc)* (pp. 2546–2550).

Tao, G. (2003). *Adaptive control design and analysis* (Vol. 37). John Wiley & Sons.

Tuan, L. A., Lee, S.-G., Dang, V.-H., Moon, S., & Kim, B. (2013). Partial feedback linearization control of a three-dimensional overhead crane. *International Journal of Control, Automation and Systems*, *11*(4), 718–727.

Tuan, L. A., Moon, S.-C., Lee, W. G., & Lee, S.-G. (2013). Adaptive sliding mode control of overhead cranes with varying cable length. *Journal of Mechanical Science and Technology*, *27*(3), 885–893.

Types of cranes and classifications. (2016, 04). Retrieved from `https://www.craneskit.com/types-of-cranes-andclassification.htmll`

Waikoonvet, J., Suksabai, N., & Chuckpaiwong, I. (2021). Collision-free path planning for overhead crane system using modified ant colony algorithm. In *2021 9th international electrical engineering congress (ieecon)* (pp. 325–328).

Wang, X., Liu, H., Lai, X., Xu, Z., & Jiang, R. (2017). A new approach of anti-swing control system based on run-to-run control and fuzzy control for overhead crane. In *2017 13th international conference on natural computation, fuzzy systems and knowledge discovery (icnc-fskd)* (pp. 1264–1270).

Wang, Z., Chen, Z., & Zhang, J. (2011). On pso based fuzzy neural network sliding mode control for overhead crane. In *Practical applications of intelligent systems* (pp. 563–572). Springer.

Wang, Z., Shi, Y., & Li, S. (2018). Research on anti-swaying of crane based on ts type adaptive neural fuzzy control. In *2018 chinese control and decision conference (ccdc)* (pp. 5503–5508).

Wei-feng, X., & Shan, L. (2019). Synchronized optimal control of intelligent crane car based on multilevel fuzzy-pid control. In *2019 chinese automation congress (cac)* (pp. 4402–4406).

What is Overhead Bridge Crane — Dongqi overhead crane. (2016, 05). Retrieved from https://www.craneskit.com/overhead-bridge-crane.html

Wu, Z., Xia, X., & Zhu, B. (2015). Model predictive control for improving operational efficiency of overhead cranes. *Nonlinear Dynamics*, *79*(4), 2639–2657.

Xie, X., Yue, D., Park, J. H., & Li, H. (2018). Relaxed fuzzy observer design of discrete-time nonlinear systems via two effective technical measures. *IEEE Transactions on Fuzzy Systems*, *26*(5), 2833–2845.

Yang, J. H., & Yang, K. S. (2007). Adaptive coupling control for overhead crane systems. *Mechatronics*, *17*(2-3), 143–152.

Yusoff, W. A. W., Yahya, N. M., & Senawi, A. (2006). Tuning of optimum pid controller parameter using particle swarm optimization algorithm approach. *Fakulti Kejuruteraan Mekanikal Universiti Malaysia Pahang*.

Zhai, D., An, L., Dong, J., & Zhang, Q. (2017). Switched adaptive fuzzy tracking control for a class of switched nonlinear systems under arbitrary switching. *IEEE Transactions on Fuzzy Systems*, *26*(2), 585–597.

Zhang, M., Ma, X., Rong, X., Tian, X., & Li, Y. (2016). Adaptive tracking control for double-pendulum overhead cranes subject to tracking error limitation, parametric uncertainties and external disturbances. *Mechanical Systems and Signal Processing*, *76*, 15–32.

Zhang, M., Ma, X., Song, R., Rong, X., Tian, G., Tian, X., & Li, Y. (2018). Adaptive proportional-derivative sliding mode control law with improved transient performance for underactuated overhead crane systems. *IEEE/CAA Journal of Automatica Sinica*, *5*(3), 683–690.

Zhang, X., Liu, H., & Tu, L. (2020). A modified particle swarm optimization for multimodal multi-objective optimization. *Engineering Applications of Artificial Intelligence*, *95*, 14-15.

APPENDICES

Appendix 1: The Root Locus Plot of CLTF of PID Controller

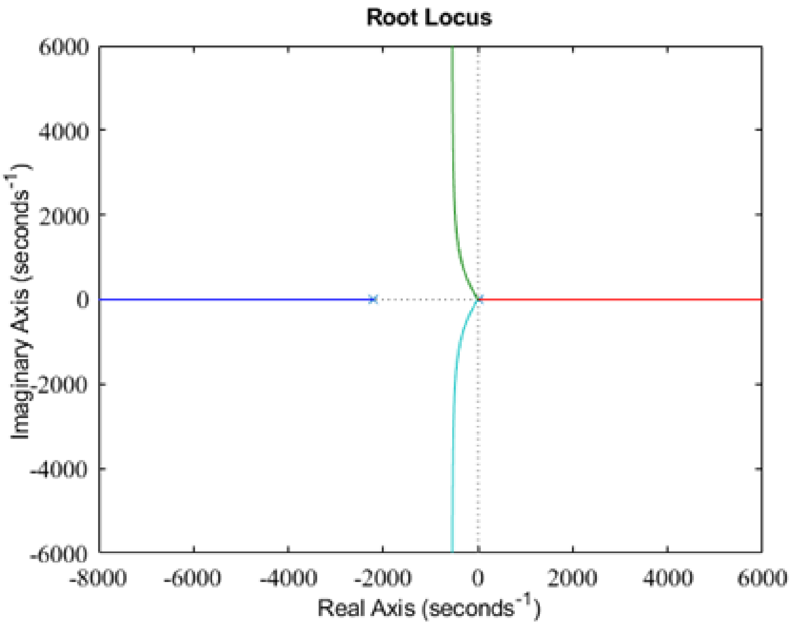

Figure 1: The root-locus of CLTF of PID controller.

Appendix 2: Surface View of FLC (PID Gains)

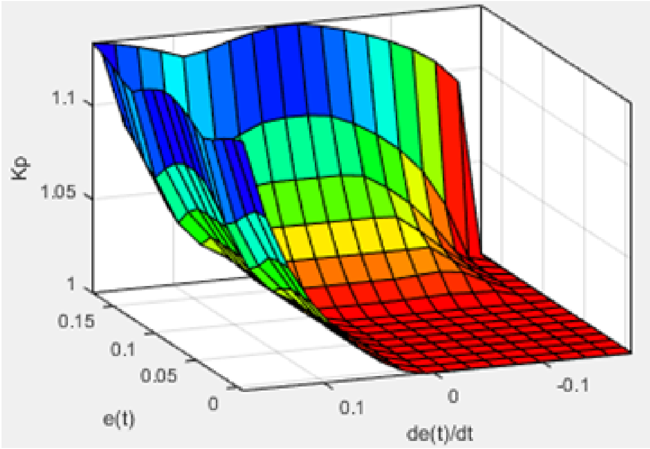

(a) Kp

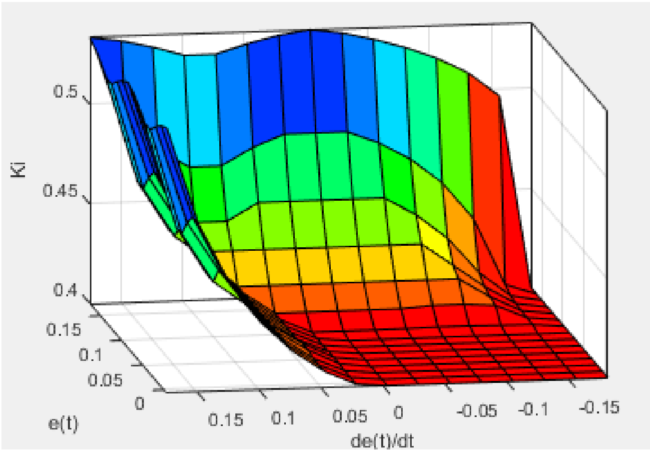

(b) Ki

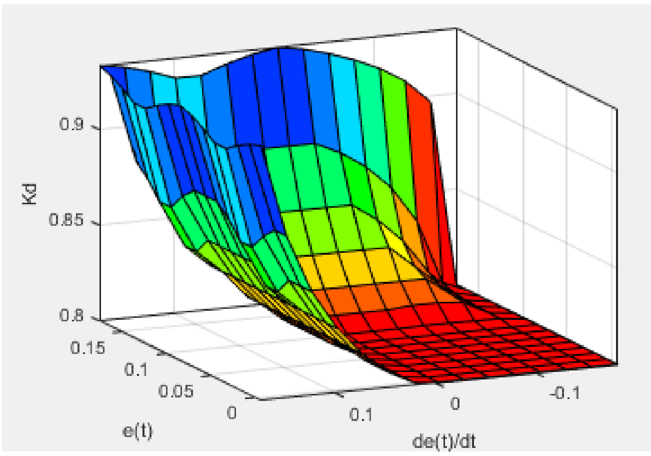

(c) Kd

Figure 2: Fuzzy surface viewer of FLC Controller.

Appendix 3: Simulink Models of PI-Regulator Design

Case 1: When there is disturbance to the plant and the desired angle is 10 degree (0.175radian).

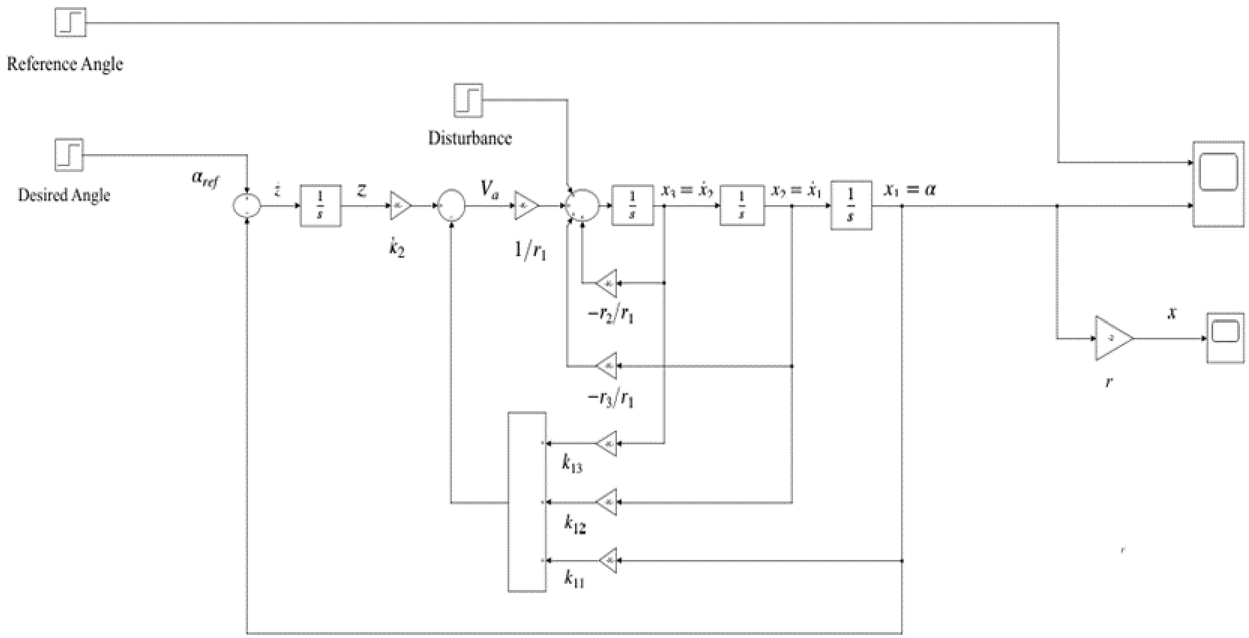

Figure 3: Simulink model of PI-Regulator for case-1.

Note: The amount of disturbance is changed as required for all cases.

Case 2: When there is no disturbance and the reference (desired) angle is less than or equal to 10 degree (0.175radian).

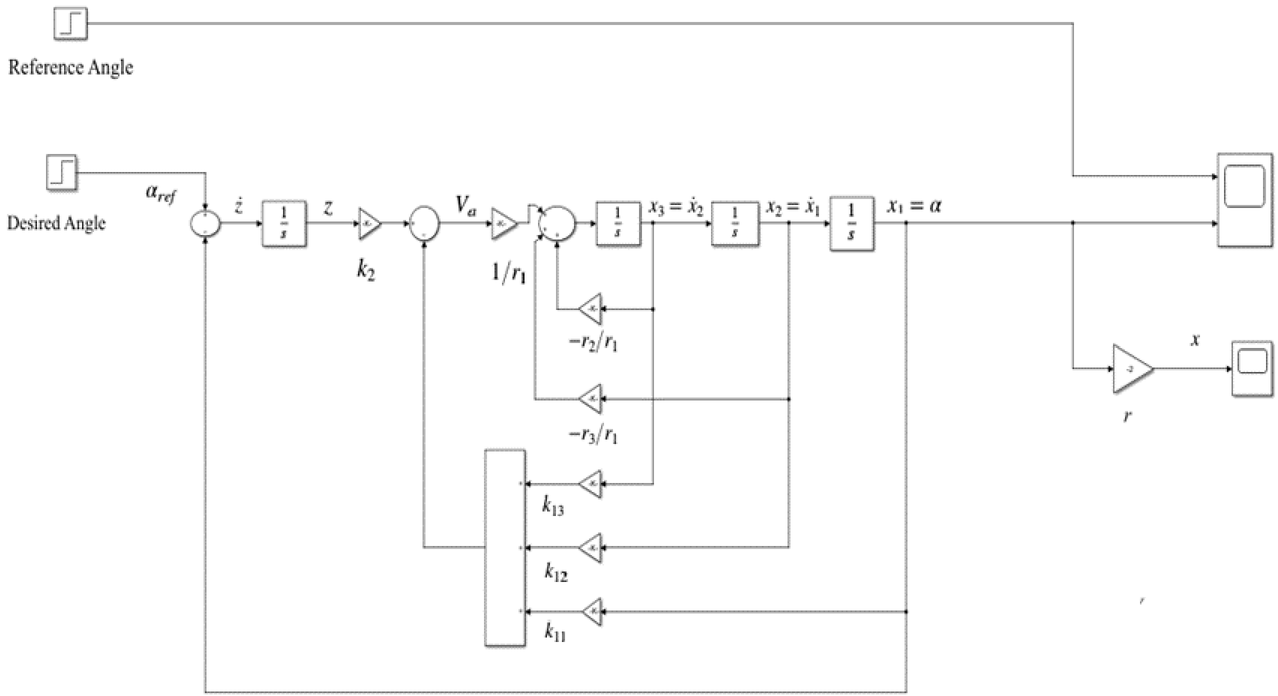

Figure 4: Simulink model of PI-Regulator for case-2.

Case 3: When there is disturbance and the required angle is 0 degree (0 radian).

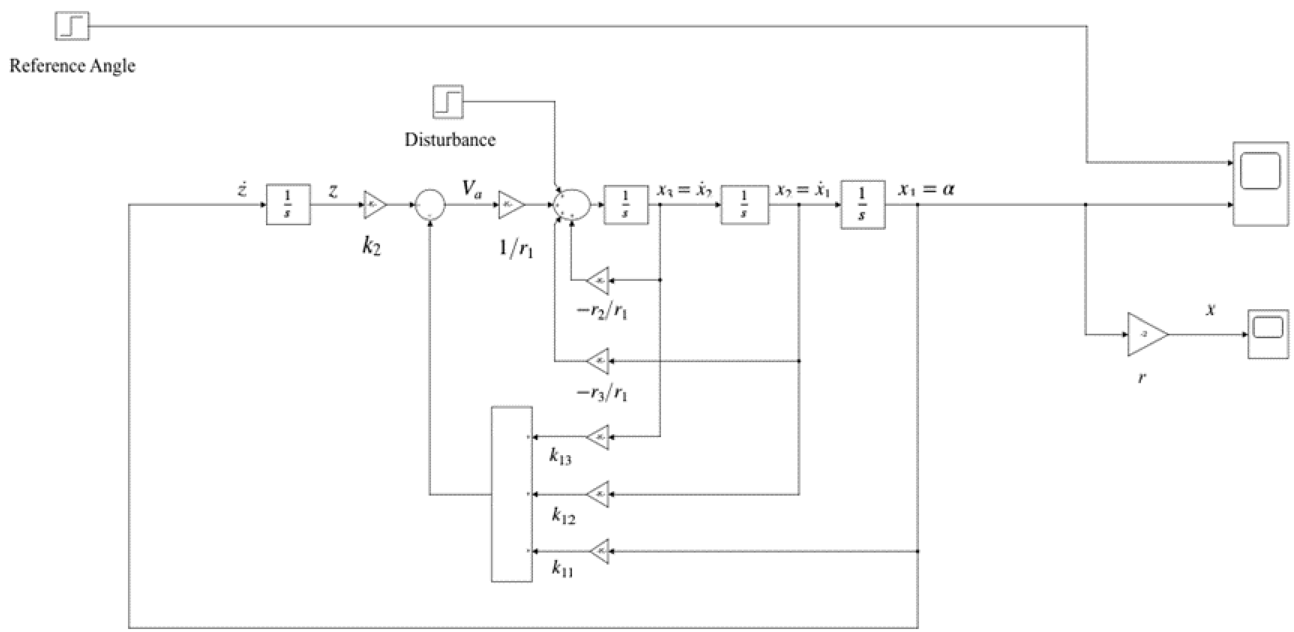

Figure 5: Simulink model of PI-Regulator for case-3.

Case 4: When there is no disturbance and the reference (desired) angle is 0 degree (0 radian).

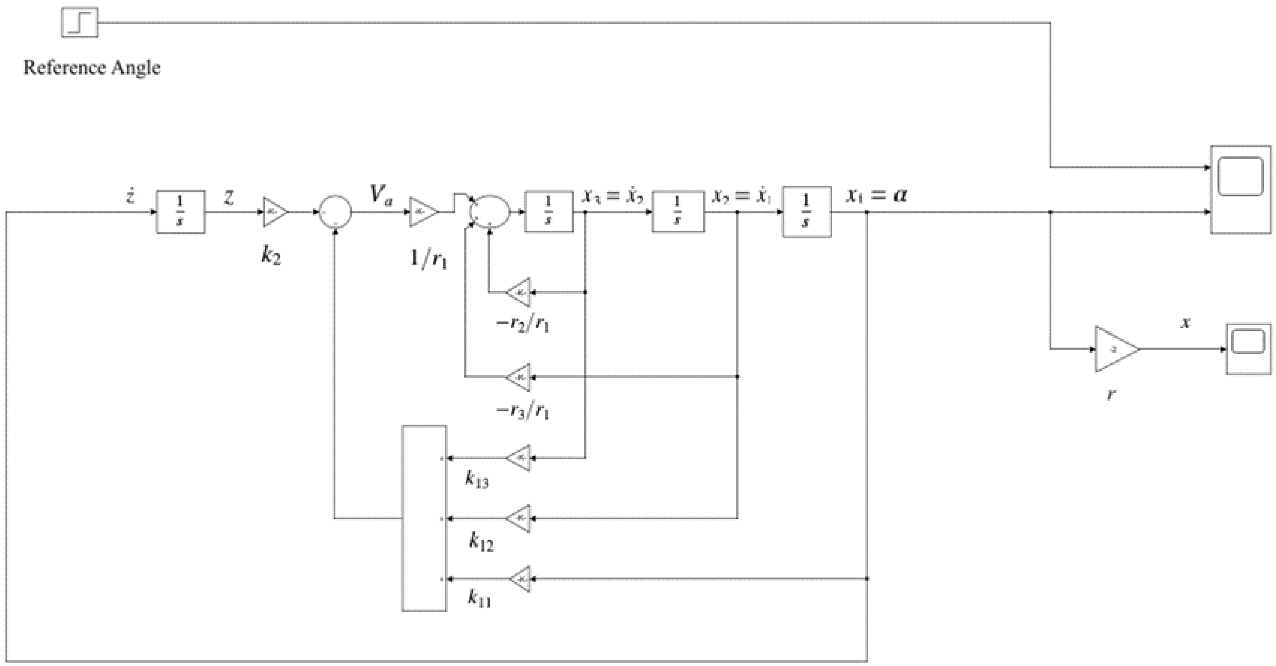

Figure 6: Simulink model of PI-Regulator for case-4.